

Computing Optimal Control of Cascading Failure in DC Networks

Qin Ba Ketan Savla

Abstract

We consider discrete-time dynamics, for cascading failure in DC networks, whose map is composition of failure rule with control actions. Supply-demand at the nodes is monotonically non-increasing under admissible control. Under the failure rule, a link is removed permanently if its flow exceeds capacity constraints. We consider finite horizon optimal control to steer the network from an arbitrary initial state, defined in terms of active link set and supply-demand at the nodes, to a feasible state, i.e., a state which is invariant under the failure rule. There is no running cost and the reward associated with a feasible terminal state is the associated cumulative supply-demand. We propose two approaches for computing optimal control, and provide time complexity analysis for these approaches. The first approach, geared towards tree reducible networks, decomposes the global problem into a system of coupled local problems, which can be solved to optimality in two iterations. In the first iteration, optimal solutions to the local problems are computed, from leaf nodes to the root node, in terms of the coupling variables. In the second iteration, in the reverse order, the local optimal solutions are instantiated with specific values of the coupling variables. When restricted to the class of constant control actions, the optimal solutions to the local problems possess a piecewise linear property, which facilitates analytical solution. The second approach computes optimal control by searching over the reachable set, which is shown to admit an equivalent finite representation by aggregation of control actions leading to the same reachable active link set. An algorithmic procedure to construct this representation is provided by leveraging and extending tools for arrangement of hyperplanes and convex polytopes. Illustrative simulations, including showing the effectiveness of a projection-based approximation algorithm, are also presented.

I. INTRODUCTION

Cascading failure in physical networks can be modeled via discrete-time dynamics, where the time epochs correspond to component failures. The map of the dynamical system is described in terms of composition of a failure rule with a control policy. A common failure rule is permanent removal of a link from the network if its physical flow exceeds capacity. Analysis of such dynamics under a given control policy has attracted considerable attention, primarily through simulations, e.g., see [1]–[5]. However, control *design* is relatively less well understood, e.g., see [6] and our previous work in [7] for few such examples. In this paper, we consider such an optimal control problem for power networks.

The network state is described in terms of active links, i.e., links which have not been removed so far, and the external power withdrawal/injection, also referred to as *supply-demand*, at the nodes. Under the failure rule, at a given network state, links are permanently removed if their power flow, as determined by the DC model, exceeds

The authors are with the Sonny Astani Department of Civil and Environmental Engineering at the University of Southern California, Los Angeles, CA. {qba, ksavla}@usc.edu. They were supported in part by NSF CAREER ECCS Project No. 1454729.

thermal capacity constraint. The control actions correspond to changing supply-demand at the nodes. A network state is called *feasible* if it is invariant under the failure rule, and is called *infeasible* otherwise. We are interested in designing control actions to steer the network from an arbitrary initial state to a terminal feasible state within a given finite time horizon. In this paper, admissible control actions are those under which the supply-demand at the nodes is non-increasing, and we consider the setting in which there is no running cost and the cost associated with a terminal feasible state is equal to the negative of cumulative supply-demand associated with that state.

The optimal control problem studied in this paper was formulated in [6], [8], where the focus was primarily on low-complexity control policies. To the best of our knowledge, a formal framework for computing optimal control beyond these low-complexity policies is lacking in the literature. The objective of this paper is to develop rigorous approaches to address this shortcoming. Specifically, we provide two distinct approaches.

The first approach is geared towards tree reducible networks, i.e., networks which can be reduced to a tree by recursively replacing subnetworks between two nodes, and containing no supply or demand nodes in the interior, with single links. For such networks, we decompose the (global) optimal control problem into a system of coupled local problems associated with nodes in the tree corresponding to the reduced network. This system of coupled problems can be solved to optimality in two iterations. In the first iteration, from leaf nodes to the root, every node computes an optimal solution to the associated local problem as a function of the local coupling variable. This coupling variable corresponds to the sequence of outflows from the node. In the second iteration, in the reverse order from the root to the leaf nodes, the local optimal solutions are instantiated with specific values of the coupling variables. When restricted to constant control actions, i.e., when the supply-demand at the nodes are decided at $t = 0$ and remain constant thereafter, the local problems, in spite of non-convexity, possess a piecewise linear property with respect to the coupling variables, which facilitates analytical solution.

The second approach computes optimal control by *searching* for an optimal feasible terminal state among the states reachable from the initial condition. This search is made possible by showing that the reachable set admits an equivalent finite representation. The key is that the one-step reachable set from any network state can be partitioned into a finite number of aggregated states, with each partition corresponding to the same reachable active link set. These partitions are determined by admissibility constraints for control actions (to maintain monotonicity of supply-demand at the nodes), and the link failure rules. Taking into account the linearity of these constraints, we leverage and extend tools from the domain of *arrangement of hyperplanes* e.g., see [9] [10, Chapter 24], and *convex polytopes*, e.g., see [11] [12], to construct these partitions. Each element of the partition, at every network state appearing in the search, is a polytope. We use the notion of *incidence graph* to represent these partitions, and provide an incremental algorithm to compute the incidence graph of the previous transformation of a polytope. The latter depends on a novel transformation between polytopes.

Among the key determinants of the time complexity for constructing arrangement are (i) the dimension of the control action space, which is one less than the number of non-transmission nodes in a connected network, and (ii) the computation of flow in DC model as a function of supply-demands at nodes under different active link sets. We address (i) by developing a projection-based approximation. An extreme case is projection on to a one dimensional

space, to which belongs the scaling-based, or proportional, control policies in [8, Section 6.1.1]. Note that these are the only control policies reported in the literature, to the best of our knowledge, for the problem considered in this paper. We address (ii) by developing an analytical approach to incrementally compute pseudo-inverse of the graph Laplacian. While this has attracted interest recently on its own, e.g., see [13], [14], our contribution is in extending the analysis to the case where link failures could cause loss of connectivity, and in providing an interesting interpretation of the analytical results.

In summary, the paper makes several important contributions in computing optimal control of cascading failure in DC networks. First, it provides a formal description of the control problem and a general search-based solution strategy that could be implemented using, e.g., a variety of sampling or other approximation techniques. Second, the network decomposition approach illustrates how certain properties of the network and the admissible control action set translate into tractable computational complexity. Third, the algorithmic procedure for constructing equivalent finite representation of the reachable set is, to the best of our knowledge, the first instance of the application of the elegant computational geometric tools related to arrangement of hyperplanes to an engineering application, beyond path planning and related topics in robotics, e.g., see [15]. Overall, these contributions bring a much needed formalism to the domain of resilient operation of power networks faced with the prospect of cascading failures.

The rest of the paper is organized as follows. A formal description of the cascading failure dynamics and the optimal control problem, as well as an outline of the search based approach for computing optimal control, are provided in Section II. The decomposition based approach for computing optimal control for tree reducible networks is provided in Section III. The equivalent finite representation of the reachable set to enable the search based approach is described in Section IV. Section V contains an algorithmic procedure based on arrangement of hyperplanes to efficiently construct the finite representation of the reachable set. Discussions on time complexity of the algorithmic procedure is in Section VI. Section VII contains the projection-based approximation and illustrative simulations on the benchmark IEEE 39 network, and concluding remarks are provided in Section VIII. The appendix contains analytical results on incremental computation of pseudo-inverse of the graph Laplacian and proofs omitted in other sections.

We conclude this section by defining a few notations. \mathbf{R} , $\mathbf{R}_{\geq 0}$ and $\mathbf{R}_{>0}$ respectively denote the set of real, non-negative real, and positive real numbers. $\mathbf{0}_n$ and $\mathbf{1}_n$ denote vectors of size n , of all zeros and ones respectively; we shall often drop the subscript when the size of the vector is clear from the context. \mathbf{e}_i is the unit vector with 1 on the i -th component and 0 on others. For an integer n , $[n] := \{1, 2, \dots, n\}$. $|S|$ denotes the cardinality of S . We use the shorthand notation $\mathbf{R}^{S_1 \times S_2} := \mathbf{R}^{|S_1| \times |S_2|}$ for index sets S_1 and S_2 . For a matrix $M \in \mathbf{R}^{S_1 \times S_2}$ and two subsets $S'_1 \subseteq S_1$ and $S'_2 \subseteq S_2$, $M_{S'_1 S'_2} \in \mathbf{R}^{S'_1 \times S'_2}$ is the submatrix of M that contains entries in the i th row and the j th column for all $i \in S'_1$ and $j \in S'_2$. In addition, $M_{S'_2} := M_{S_1 S'_2}$. Similarly, given sets S and $S' \subseteq S$, $x_{S'}$ denotes the appropriate sub-vector of vector $x \in \mathbf{R}^S$. Given x_i for all $i \in S$, let $x_S := \{x_i\}_{i \in S}$. The range of a matrix M is denoted by $\mathcal{R}(M)$. For a vector $x \in \mathbf{R}^d$, $\text{diag}(x) \in \mathbf{R}^{d \times d}$ denotes the diagonal matrix whose (diagonal) entries are those of x . The same notation extends to a block diagonal matrix. For two vectors x and y

with the same size, $x \leq y$ means $x_i \leq y_i$ for all i . The same convention is adopted for \geq , $<$ and $>$. Given sets $S_1 \subset \mathbf{R}^n$ and $S_2 \subset \mathbf{R}^n$, $S_1 + S_2$ denotes the Minkowski sum of S_1 and S_2 .

II. PROBLEM SETUP

The problem is formulated within the same simplifications as in [8] on modeling of power system failures, that is, link failures and slow-moving cascade processes are considered; and short-term dynamics is not considered and the standard linearized (DC) approximation to power flow is used. We start by recalling the DC power flow approximation.

A. DC Power Flow Approximation

In this model, it is assumed that the transmission lines are lossless and the voltage magnitudes are constant at 1.0 unit. The graph topology of the power network is described by an *undirected multigraph* $\mathcal{G} = (\mathcal{V}, \mathcal{E})$, that is, multiple parallel links can connect the same two nodes in \mathcal{G} . For convenience, every link in \mathcal{E} is arbitrarily assigned a direction – the results in the paper do not depend on the direction convention. Let $\mathcal{V}_+ \subset \mathcal{V}$ and $\mathcal{V}_- \subset \mathcal{V}$ be the set of supply and demand nodes respectively. A node is called a *transmission node* if it is neither a supply nor a demand node. Let $\mathcal{V}_l := \mathcal{V}_+ \cup \mathcal{V}_-$ denote the set of non-transmission nodes. Since the network can loose connectivity under cascading dynamics, we let $(\mathcal{V}, \mathcal{E}) = (\mathcal{V}^{(1)}, \mathcal{E}^{(1)}) \cup \dots \cup (\mathcal{V}^{(r)}, \mathcal{E}^{(r)})$ denote the partition of the original graph (i.e., the graph at $t = 0$) into its r connected components. The partition will evolve with the dynamics.

The graph \mathcal{G} is associated with a node-link incidence matrix $A \in \mathbf{R}^{\mathcal{V} \times \mathcal{E}}$, where $A_i \in \mathbf{R}^{\mathcal{V}}$ corresponds to link $i \in \mathcal{E}$ and has +1 and -1 respectively on the tail and head node of link i , and 0 on other nodes. The links are associated with a flow vector $f \in \mathbf{R}^{\mathcal{E}}$; The signs of elements of f are to be interpreted as being consistent with the directional convention chosen for links in \mathcal{E} . We also associate \mathcal{G} with a diagonal matrix $W \in \mathbf{R}^{\mathcal{E} \times \mathcal{E}}$ whose diagonal elements give the negative of susceptances, or weights, of the corresponding links. For brevity, w_i shall denote the i -th diagonal element of W . The nodes are associated with phase angles $\phi \in \mathbf{R}^{\mathcal{V}}$, and the supply and demand nodes are associated with a supply-demand vector $p \in \mathbf{R}^{\mathcal{V}}$; $p_i > 0$ for $i \in \mathcal{V}_+$ and $p_i < 0$ for $i \in \mathcal{V}_-$.

The quantities defined above are related by Kirchhoff's law and Ohm's law in DC approximation as follows:

$$\begin{aligned} Af &= p \\ f &= WA^T \phi \end{aligned} \tag{1}$$

In order for (1) to be feasible, the supply-demand vector p needs to be balanced over $\mathcal{G}^{(i)}$ for all $i \in [r]$, that is,

$$p \in \mathcal{B}_{\mathcal{E}} := \left\{ u \in \mathbf{R}^{\mathcal{V}} \mid \sum_{v \in \mathcal{V}^{(i)}} p_v = 0, i \in [r] \right\} \tag{2}$$

For a given network $\mathcal{G} = (\mathcal{V}, \mathcal{E})$ with balanced supply and demand p , there exists a unique flow f satisfying (1), and it is given by [16]:

$$f = WA^T L^\dagger(\mathcal{E})p =: f(\mathcal{E}, p) \tag{3}$$

where $\text{diag}\{L_1, L_2, \dots, L_r\} = L = AWA^T \in \mathbf{R}^{\nu \times \nu}$ is the weighted Laplacian matrix of \mathcal{G} , with L_i being the laplacian matrix of $\mathcal{G}^{(i)}$ for all $i \in [r]$, and $L^\dagger = \text{diag}\{L_1^\dagger, L_2^\dagger, \dots, L_r^\dagger\}$ is its pseudo-inverse. (3) implies that, for a given \mathcal{E} , $f(\mathcal{E}, p)$ is linear in p .

B. Cascading Failure Dynamics

Let \mathcal{E}^0 be the initial link set and let p^0 be the initial supply-demand vector satisfying the balance condition in (2). The corresponding link flow f is uniquely determined by (1) or (3). We associate with each link $i \in \mathcal{E}^0$ a thermal capacity $c_i > 0$. If the magnitude of flow on a link $i \in \mathcal{E}^0$ exceeds its thermal capacity, i.e., $|f_i| > c_i$, then link i fails and is removed from the network irreversibly. This changes the topology of the network, causing flow redistribution, which might lead to more link failures, and so on. Such continuing link failures constitute the *uncontrolled* cascading failure dynamics. Note that we consider a link failure rule which is deterministic and which depends solely on the instantaneous flow. This is to be contrasted with other deterministic outage rules based on moving average of successive flows, or stochastic line outage rules, e.g., see [6], [17].

Our objective in this paper is to stop cascading failure through appropriate control actions. While shedding all load at $t = 0$ achieves this objective trivially, we desire to take control actions that are optimal in a certain sense. Consider the following description of controlled cascading failure dynamics in discrete-time. Each time epoch corresponds to failure of some links. The node set remain the same. Let (\mathcal{E}^t, p^t) be the state of the network at time t , with $\mathcal{E}^t \subset 2^{\mathcal{E}^0}$ and $p^t \in \mathbf{R}^\nu$ denoting the *active link set* and supply-demand vector at time t , respectively. We consider load shedding as the control and, for convenience, employ control variable $u \in \mathbf{R}^\nu$ to be supply-demand vector after load shedding. The controlled cascading failure dynamics, for $t = 0, 1, \dots$, and starting from the initial state (\mathcal{E}^0, p^0) , is given by:

$$(\mathcal{E}^{t+1}, p^{t+1}) = \mathcal{F}(\mathcal{E}^t, p^t, u^t), \quad u^t \in U(\mathcal{E}^t, p^t) \quad (4)$$

where

$$\begin{aligned} \mathcal{F}_{\mathcal{E}}(\mathcal{E}, p, u) &\equiv \mathcal{F}_{\mathcal{E}}(\mathcal{E}, u) := \{i \in \mathcal{E} \mid -c_i \leq f_i(\mathcal{E}, u) \leq c_i\} \\ \mathcal{F}_p(\mathcal{E}, p, u) &\equiv \mathcal{F}_p(u) := u \end{aligned} \quad (5)$$

where the functions $\mathcal{F}_{\mathcal{E}}$ and \mathcal{F}_p are for the maps for \mathcal{E}^{t+1} and p^{t+1} , respectively. As defined in (5), $\mathcal{F}_{\mathcal{E}}$ is the set of feasible links in \mathcal{E} under supply-demand vector u ; and the control input u^t at time t becomes the next state supply-demand vector p^{t+1} .

Remark 1:

- 1) The number of connected network components may increase in (4). When this happens at a network state (\mathcal{E}, p) , it is possible that $p \notin \mathcal{B}_{\mathcal{E}}$. The definition of $U(\mathcal{E}, p)$ in (6) ensures the the balance condition is satisfied by the controls over all components.
- 2) Before the system reaches a steady state, the time epoch corresponds to link failure in (4). After that, the time epoch is chosen arbitrarily, for example, to be the uniform unit time. This is without loss of generality.

3) Even though its form appears to be specific to DC power networks, (4)-(5) can be readily extended to other large scale dynamical systems in the following situations: (i) each single constituent component of systems is allowed to fail while other components remains in operation; and (ii) the underlying physical dynamics are on a considerable faster time scale compared with the cascade of components failure. In that case, the system is assumed to reach an physical equilibrium at each time epoch in (5) and u is used to denote the controllable settings that is capable of choosing the physical equilibrium state in the way described by function \mathcal{F}_p .

In order for $\mathcal{F}_\mathcal{E}(\mathcal{E}, u)$ in (5) to be well-defined, u must be balanced with respect to the active link set \mathcal{E} . This is ensured by the following definition of state-dependent control space $U(\mathcal{E}, p)$:

$$U(\mathcal{E}, p) = \text{cube}(p) \cap \mathcal{B}_\mathcal{E} \quad (6)$$

where $\text{cube}(p)$ characterizes the load shedding property, and is defined as:

$$\text{cube}(p) := \{u \in \mathbf{R}^\nu \mid 0 \leq u_v \leq p_v \text{ for } p_v \geq 0; p_v \leq u_v \leq 0 \text{ for } p_v < 0\} \quad (7)$$

$U(\mathcal{E}, p)$ includes all *admissible* load shedding controls at state (\mathcal{E}, p) . In particular, if all the supply and demand nodes are disconnected from each other at state (\mathcal{E}, p) , then $\mathcal{B}_\mathcal{E} = \{\mathbf{0}\}$, and in this case $U(\mathcal{E}, p) = \{\mathbf{0}\}$.

Figure 1 illustrates repeating sequence of flow redistribution, control action, and link failures, under the cascading dynamics proposed in (4)-(5). If the initial flow $f(\mathcal{E}^0, p^0)$ is infeasible, and if the control action is $u^0 \in U(\mathcal{E}^0, p^0)$, then the next state supply-demand vector is $p^1 = u^0$. If the resulting flow is within the capacity, i.e., $|f(\mathcal{E}^0, p^1)| \leq c$, then there are no link failures, and hence $\mathcal{F}(\mathcal{E}^0, p^0, u^0) = (\mathcal{E}^1, p^1) = (\mathcal{E}^0, p^1)$. In order to maintain the network state, one would choose subsequent control actions as $u^t = p^1$ for all $t \geq 1$.

On the other hand, if $|f_i(\mathcal{E}^0, p^0)| > c_i$ for some links i , then those links will fail, and hence $\mathcal{E}^1 = \mathcal{F}_\mathcal{E}(\mathcal{E}^0, u^0) \neq \mathcal{E}^0$ and $p^1 = u^0$. Therefore, the new link flows are $f(\mathcal{E}^1, p^1)$. Thereafter, control action u^1 is chosen, possibly equal to p^1 if $|f(\mathcal{E}^1, p^1)| \leq c_{\mathcal{E}^1}$, and the process repeats.

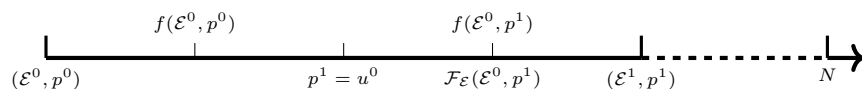


Fig. 1: The sequence of flow redistribution, control action, and link failures, under the proposed cascading dynamics.

C. Problem Formulation

Let

$$\mathcal{S} := \{(\mathcal{E}, p) \mid p \in \mathcal{B}_\mathcal{E}, -c_i \leq f_i(\mathcal{E}, p) \leq c_i, \forall i \in \mathcal{E}\} \quad (8)$$

denote the set of *feasible states*. Set \mathcal{S} is invariant under the uncontrolled cascading dynamics. Note that $(\mathcal{E}, \mathbf{0}) \in \mathcal{S}$ for every $\mathcal{E} \in 2^{\mathcal{E}^0}$. Since $\mathcal{E}^t, t \geq 0$, is non-increasing sequence, and \mathcal{E}^0 is finite, the dynamics converges to a steady state within $2^{\mathcal{E}^0}$ time epochs.

Our objective is to choose control actions to steer the network from an arbitrary given initial state (\mathcal{E}^0, p^0) to a feasible state $(\mathcal{E}^N, p^N) \in \mathcal{S}$ within a given finite horizon N , while optimizing a certain performance criterion. The control horizon N is typically much smaller than $2^{\mathcal{E}^0}$. Let a generic sequence of control actions over the control horizon be denoted by $u := (u^0, \dots, u^{N-1})$. In this paper, we wish to solve the following optimal control problem:

$$\sup_{u^{[N]} \in \mathcal{D}(N, \mathcal{E}^0, p^0)} s^T p^N \quad (9)$$

where $s \in \{1, 0, -1\}^{\mathcal{V}}$ is a constant defined as: $s_v := 1$ for $v \in \mathcal{V}_+$, $s_v := -1$ for $v \in \mathcal{V}_-$, and $s_v := 0$ otherwise, and the set of feasible control actions is defined as:

$$\begin{aligned} \mathcal{D}(\mathcal{E}^0, p^0, N) := \\ \{(u^0, \dots, u^{N-1}) \mid u^t \in U(\mathcal{E}^t, p^t) \text{ for } t = 0, \dots, N-1; (\mathcal{E}^{N-1}, u^{N-1}) \in \mathcal{S}; (\mathcal{E}^t, p^t)_{t \in [N]} \text{ satisfies (4) - (5)}\} \end{aligned} \quad (10)$$

For brevity, we shall not show the dependence of \mathcal{D} on \mathcal{E}^0, p^0 and N when clear from the context.

Remark 2: 1) (10) implies that when checking feasibility of a given u , one has to check an additional condition for u^{N-1} in comparison to that for u^t for $t = 0, \dots, N-2$. In addition to checking $u^{N-1} \in U(\mathcal{E}^{N-1}, p^{N-1})$, one also to check if the resulting (\mathcal{E}^N, p^N) belongs to \mathcal{S} .

2) In (9), we use supremum rather than maximum because \mathcal{D} is not closed in general, as illustrated in Example 1 below. This matter is addressed in Section IV-B and it could be ignored before that. The computational complexity of characterizing \mathcal{D} , and hence of solving (9) is attributed to the cascading dynamics in (4).

Example 1: Consider the optimal control problem in (9) for the network shown in Fig. 2a, for $N = 3$. Node 1 is the supply node and node 2 and 3 are the demand nodes. The initial supply-demand vector is $p^0 = [30, -10, -20]^T$. The link weights are $w = [2, 1, 1, 1]^T$ and the link capacities are $c = [6, 7, 14, 5]^T$. Consider $u^0 = [21 + 2/k, -7 - 1/k, -14 - 1/k]^T$ for some $k \geq 1$. The resulting flow is $f(\mathcal{E}^0, u^0) = [8 + 6/(7k), 4 + 3/(7k), 9 + 5/(7k), 5 + 2/(7k)]^T$. Consequently, links e_1 and e_4 fail due to flow exceeding capacity, and the resulting \mathcal{E}^1 is shown in Fig. 2b. For $u^1 = [21, -7, -14]^T$, $f_2(\mathcal{E}^1, u^1) = 7 \leq c_2$, $f_3(\mathcal{E}^1, u^1) = 14 \leq c_3$, and therefore there are no more link failures. This implies that $u^{[N]}(k) := (u^0(k), u^1(k), u^2(k)) = ([21 + 2/k, -7 - 1/k, -14 - 1/k]^T, [21, -7, -14]^T, [21, -7, -14]^T) \in \mathcal{D}$ for every $k \geq 1$. However, $\hat{u} = (\hat{u}^0, \hat{u}^1, \hat{u}^2) = \lim_{k \rightarrow \infty} u(k) = ([21, -7, -14]^T, [21, -7, -14]^T, [21, -7, -14]^T) \notin \mathcal{D}$. This is because $f(\mathcal{E}^0, \hat{u}^0)$ is such that only link e_1 fails, and the resulting $\hat{\mathcal{E}}^1$ is shown in Fig. 2c. Furthermore, $f(\hat{\mathcal{E}}^1, \hat{u}^1) = [\text{null}, 28/3, 35/3, 7/3]^T$, which implies that e_2 fails. Thereafter, $\hat{\mathcal{E}}^2 = \{e_3, e_4\}$, $f_3(\hat{\mathcal{E}}^2, \hat{u}^2) = 21 > c_3$ and $f_4(\hat{\mathcal{E}}^2, \hat{u}^2) = 7 > c_4$. All links fail under \hat{u} and $u \notin \mathcal{D}$. This demonstrates that \mathcal{D} is not closed for the given choice of network parameters.

Remark 3: In writing the optimal control problem in (9), we only consider the terminal cost $s^T p^N$, in addition to imposing feasibility condition on the terminal state. $s^T p^N$ is the remaining cumulative supply and demand once the cascading failure stops, and hence is a natural choice for the objective function in (9). Extension to including running cost is discussed in Remark 15.

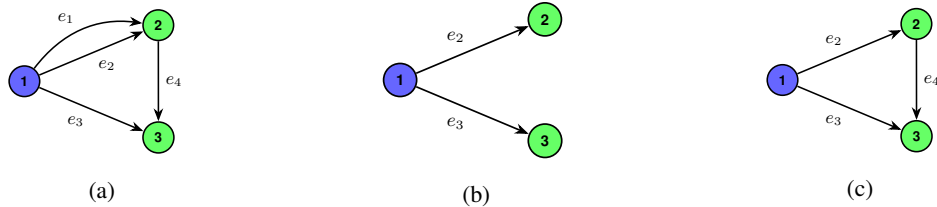


Fig. 2: The graph topology for the network used in Example 1 to illustrate that the feasible control action set \mathcal{D} is not necessarily closed.

D. Solution by Optimal Tree Search

A generic approach to solving (9) is by performing an optimal search on a directed tree composed of the states reachable from the initial state (\mathcal{E}^0, p^0) in at most N time steps, e.g., see [18, Chap 3]. In other words, the tree is rooted at (\mathcal{E}^0, p^0) , and has depth N . Each node of the tree corresponds to a state (\mathcal{E}, p) which is reachable in one time step from its parent node under a control action which is associated with the incoming arc to that node; see Fig. 3 for an illustration. When considering one time step reachable set from a given node (\mathcal{E}, p) , one only considers control actions belonging to $U(\mathcal{E}, p)$. The set of goal states for the search is \mathcal{S} and we associate every state $(\mathcal{E}, p) \in \mathcal{S}$ with a *utility* quantified by $s^T p$. The goal is to search for a feasible state with maximal utility.

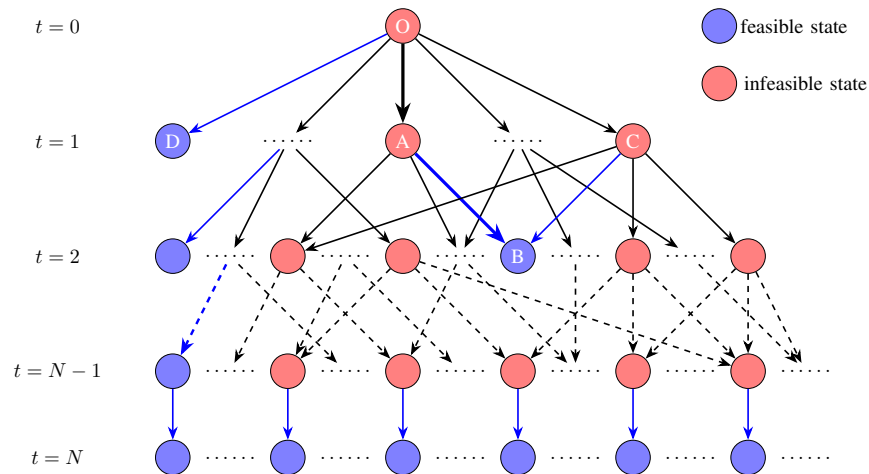


Fig. 3: The tree composed of states reachable from (\mathcal{E}^0, p^0) in at most N time steps.

Let $J_t(\mathcal{E}, p)$ be the maximum among utilities of all the states that can be reached in at most t time steps starting from (\mathcal{E}, p) . Solving (9) is equivalent to computing $J_N(\mathcal{E}^0, p^0)$. This computation can be done as follows:

$$J_1(\mathcal{E}, p) = \max_{u \in U(\mathcal{E}, p)} s^T u \quad \text{s.t.} \quad -c_{\mathcal{E}} \leq f(\mathcal{E}, u) \leq c_{\mathcal{E}} \quad (11a)$$

$$J_t(\mathcal{E}, p) = \sup_{u \in U(\mathcal{E}, p)} J_{t-1}(\mathcal{F}_{\mathcal{E}}(\mathcal{E}, u), u), \quad t = 2, \dots, N \quad (11b)$$

where (11a) uses the flow capacity constraint to account for the additional constraint to be satisfied by u^{N-1} , as commented on in Remark 2. (11a) is a linear program and commonly referred to as *LP power redispatch*, e.g., see [19]. (11b) uses supremum because $\mathcal{F}_{\mathcal{E}}(\mathcal{E}, u)$, and hence $J_{t-1}(\mathcal{F}_{\mathcal{E}}(\mathcal{E}, u), u)$, is not continuous w.r.t. u . It is straightforward to see that $J_1(\mathcal{E}, p) \leq J_t(\mathcal{E}, p) \leq s^T p$ for all (\mathcal{E}, p) and $t \in [N]$.

Remark 4: Though (11) is similar to the value iteration in dynamic programming, we note that in this paper a search algorithm in forward direction over the state tree is preferred over the value iteration in backward direction, because the reachable set can be considerably smaller than the state space. Comparison of time complexity of these two algorithms can be found in Section VI-B. Moreover, we shall be implicitly referring to reachable set by *state space* hereafter, as only the former is relevant for searching.

Executing optimal tree search, or equivalently implementing (11), is not directly amenable to a computational procedure, since the number of one-step reachable states from (\mathcal{E}, p) , or equivalently the set of feasible control actions $U(\mathcal{E}, p)$, is a continuum in general. A natural strategy is to discretize $U(\mathcal{E}, p)$, at the expense of getting less scalable algorithms and approximate solutions. In this paper, we propose the following two approaches for better computational efficiency:

- (I) (semi-)analytic solution for certain class of networks, or for optimal solution within a certain subset of feasible control actions (Section III); and
- (II) an algorithmic procedure to construct an *equivalent* finite abstraction of the set of feasible control actions, such that computing optimal solution over this finite abstraction gives solution to (9) (Section IV-A).

Approach (II) essentially relies on developing a finite abstraction for one time step reachable set from an arbitrary (\mathcal{E}, p) , where the number of abstractions is related to the number of active link sets reachable from (\mathcal{E}, p) . Following (3) and (5), this involves computation of pseudo-inverse of Laplacians associated with several active link sets that are subsets of \mathcal{E} . Doing such a computation from scratch for each subset could overall prove to be a computationally expensive procedure, particularly for large \mathcal{E}^0 or for large N . In Appendix A, we develop an incremental approach for computing pseudo-inverse of the Laplacian to address this challenge.

III. ANALYTICAL SOLUTION

In this section, we present (semi-)analytical solution to (9) in some special cases.

A. Parallel Networks

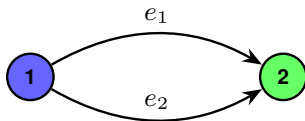


Fig. 4: A parallel network with two links.

A parallel network $(\{1, 2\}, \mathcal{E})$ consists of two nodes that are connected by multiple parallel links, e.g., see Figure 4. We set the convention that the links are directed from node 1 (supply) to node 2 (demand). Since $p_2 = -p_1$, following (1), the link flows are given by:

$$f_i = \frac{w_i}{\sum_{j \in \mathcal{E}} w_j} p_1, \quad i \in \mathcal{E} \quad (12)$$

The following monotonicity result is a straightforward consequence of (12), whose proof is omitted.

Lemma 1: Consider two arbitrary parallel networks $(\{1, 2\}, \mathcal{E})$ and $(\{1, 2\}, \mathcal{E}')$ such that $\mathcal{E} \subseteq \mathcal{E}'$ and two arbitrary supply-demand vectors $p = p_1[1 \ -1]^T$ and $p' = p'_1[1 \ -1]^T$ such that $0 < p_1 \leq p'_1$. Then the followings are true:

(i) $\mathcal{F}_{\mathcal{E}}(\mathcal{E}, p') \subseteq \mathcal{F}_{\mathcal{E}}(\mathcal{E}, p)$; and (ii) $\mathcal{F}_{\mathcal{E}}(\mathcal{E}, p) \subseteq \mathcal{F}_{\mathcal{E}}(\mathcal{E}', p)$.

Remark 5: For a parallel network $(\{1, 2\}, \mathcal{E})$ and a natural number $N \geq 1$, let $u = (u^0, \dots, u^{N-1})$ and $\tilde{u} = (\tilde{u}^0, \dots, \tilde{u}^{N-1})$ be two sequences of control actions and $(\mathcal{E}^0, \dots, \mathcal{E}^N)$ and $(\tilde{\mathcal{E}}^0, \dots, \tilde{\mathcal{E}}^N)$ be the topology sequences under the two controls. Lemma 1 implies that if $u_1^t \geq \tilde{u}_1^t$ for all $0 \leq t \leq N-1$, then $\mathcal{E}^t \subseteq \tilde{\mathcal{E}}^t$ for all $0 \leq t \leq N-1$.

Furthermore, according to (12), $f_i/c_i = (p_1/\sum_{k \in \mathcal{E}} w_k) \cdot (w_i/c_i)$ for all $i \in \mathcal{E}$. Noting the common factor $p_1/\sum_{k \in \mathcal{E}} w_k$ among all links, we label links in the increasing order of w_i/c_i , i.e., $w_i/c_i \leq w_j/c_j$ for $i \leq j$, $i, j \in \mathcal{E}$. The chronological order of link failures according to (4) is expected to be aligned with the reverse labeling of the links and is not affected by different load shedding actions, as implied by the following result.

Lemma 2: Consider the cascading dynamics (4) for a parallel network $(\{1, 2\}, \mathcal{E})$. If $f_j(t) \leq c_j$ for some $j \in \mathcal{E}$ and $t \in [N]$, then $f_i(t) \leq c_i$ for all $i \leq j$.

Proof: Since $f_j(t) = p_1(t)w_j/\sum_{k \in \mathcal{E}} w_k \leq c_j$, then, for $i < j$, we have $f_i(t) = p_1(t)w_i/\sum_{k \in \mathcal{E}} w_k = w_i f_j(t)/w_j \leq w_i c_j/w_j \leq c_i$. The last inequality is due to $w_i/c_i \leq w_j/c_j$ for all $i \leq j$. ■

Remark 6: Lemma 2 implies that for all $t \in [N]$, there exists $j \in \mathcal{E}$ such that $\mathcal{E}^t = [j]$. Because \mathcal{E}^t is non-increasing, at most $|\mathcal{E}| + 1$ number of distinct network topologies can occur in the cascading dynamics.

The monotonicity properties shown in Lemma 1 and the tight characterization of the reachable set of topologies, as implied by Remark 6, allows optimal control synthesis relatively easily. Specifically, we show that a *one-shot control* defined next is optimal within all control policies for parallel networks.

Definition 1: For an initial supply-demand vector $p^0 \in \mathbf{R}^V$, a N stage control sequence (u^0, \dots, u^{N-1}) is called *one-shot control* if there exists $0 \leq t_1 \leq N-1$ such that $u^t = p^0$ for all $t < t_1$, $u^{t_1} \in \text{cube } p^0$, and $u^t = u^{t_1}$ for all $t \geq t_1$. Moreover, if $t_1 = 0$, then it is also called *constant control*.

In order to describe the analytical expression of an optimal one-shot control for a parallel network $(\{1, 2\}, \mathcal{E})$, we first introduce several notations. Let $R_i := (c_i/w_i) \sum_{j=1}^i w_j$ for all $i \in \mathcal{E}$. In general, R_i is neither decreasing nor increasing with respect to i . The following remark is straightforward.

Remark 7: R_i is the maximum supply or demand the network can support when only the first i links are active. $([i], p^0) \in \mathcal{S}$ if and only if $p_1^0 \leq R_i$ for all $i \in \mathcal{E}$.

Let $o_1 := \max \arg \max_{i \in \mathcal{E}} R_i$ and if $o_j < |\mathcal{E}|$, let $o_{j+1} := \max \arg \max_{i > o_j} R_i$. Let o_{end} be the maximum number such that o_{end} is defined. It is straightforward to see that $o_1 < o_2 < \dots < o_{\text{end}} = |\mathcal{E}|$ and $R_{o_1} > R_{o_2} > \dots > R_{o_{\text{end}}} = R_{|\mathcal{E}|}$. For a given initial balanced supply-demand vector $p^0 \in \mathbf{R}^2$, an optimal control depends on the value

of N . A bigger N provides more flexibility for control design. A small N forces to shed big portion of loads to ensure network feasibility at small time instants, for example, at $t = 0$ for $N = 1$. Next we define $N_j(p^0)$ for every balanced $p^0 \in \mathbf{R}^2$ and $j \in [\text{end}]$ which are used in specify optimal controls for p^0 and arbitrary N . First consider $N = |\mathcal{E}|$ and let $(\mathcal{E}_{\text{un}}^0, \dots, \mathcal{E}_{\text{un}}^N)$ be the non-increasing topology sequence of the uncontrolled cascading dynamics (4) (that is, $u^t = p^0$ for all t). Let $R_{o_0} := \infty$, $R_{o_{\text{end}+1}} = 0$ and $\mathcal{E}_{\text{un}}^{-1} \supset \mathcal{E}_{\text{un}}^0$ for convenience. For $0 \leq j \leq \text{end}$, if $R_{o_{j+1}} < p_1^0 \leq R_{o_j}$, then let $N_k(p^0) := 1 + \min \{t \in \{0, \dots, N\} \mid (\mathcal{E}_{\text{un}}^t, p^0) \in \mathcal{S}\}$ for $1 \leq k \leq j$ and N_k be such that $\mathcal{E}_{\text{un}}^{N_k(p^0)-1} \subseteq [o_k] \subset \mathcal{E}_{\text{un}}^{N_k(p^0)-2}$ for all $j+1 \leq k \leq \text{end}$. The above definition implies that $|\mathcal{E}| \geq N_1(p^0) \geq \dots \geq N_{\text{end}}(p^0) = 1$ for all p^0 . In addition, let $N_0(p^0) := \infty$ for all p^0 for convenience.

Proposition 1: Consider a parallel network $(\{1, 2\}, \mathcal{E})$ with link weights $w \in \mathbf{R}_{>0}^{\mathcal{E}}$, flow capacities $c \in \mathbf{R}_{>0}^{\mathcal{E}}$ and initial supply demand vector p^0 and let R_i , $i \in \mathcal{E}$, o_j , $j \in [\text{end}]$, $N_k(p^0)$, $k \in [\text{end}] \cup \{0\}$ be defined as above. If $N_j(p^0) \leq N < N_{j-1}(p^0)$, an optimal control action is as follows: $u^{t,*} = p^0$ for all $0 \leq t < N_j(p^0) - 2$ and $u^{t,*} = \min\{R_{o_j}, p_1^0\}[1 \ -1]$ for all $\max\{N_j(p^0) - 2, 0\} \leq t \leq N - 1$.

Proof: We consider the following cases:

- 1) $p_1^0 \leq R_{|\mathcal{E}|}$. Remark 7 implies that $(\mathcal{E}, p^0) \in \mathcal{S}$. The optimal control for every $N \geq 1$ would be shedding no load. In this case, by definition $N_j(p^0) = 1$ for all $j \in [\text{end}]$. Every $N \geq 1$ satisfies $N_1(p^0) \leq N < N_0(p^0)$. Hence, $u^{*,t} = \min\{R_{o_1}, p_1^0\}[1 \ -1]$ for $t \geq 0$. Followed by the fact that $p_1^0 \leq R_{|\mathcal{E}|} \leq R_1$, u^* is optimal.
- 2) $R_{o_{k+1}} < p_1^0 \leq R_{o_k}$ for some $0 \leq k \leq \text{end} - 1$. By definition, $N_1(p^0) = N_2(p^0) = \dots = N_k(p^0)$ and $N_{k+1}(p^0) \geq \dots \geq N_{\text{end}-1}(p^0) \geq 2 > N_{\text{end}}(p^0) = 1$. We have the following cases.
 - a) $N = 1$. Since $N_{\text{end}}(p^0) \leq 1 \leq N_{\text{end}-1}(p^0)$, $u^* = \min\{R_{o_{\text{end}}}, p_1^0\}[1 \ -1] = R_{|\mathcal{E}|}[1 \ -1]$ is optimal, where the second equality follows from $p_1^0 > R_{o_{k+1}} \geq R_{o_{\text{end}}} = R_{|\mathcal{E}|}$.
 - b) $N \geq N_k$. In this case, $N_1(p^0) \leq N < N_0(p^0)$. Since $p_1^0 \leq R_{o_k} \leq R_{o_1}$, then $u^{t,*} = p^0$ for all t . u^* is optimal if feasible. The latter is a straightforward result from the definition of $N_k(p^0)$.
 - c) $2 \leq N < N_k$. In this case, $N_j(p^0) \leq N < N_{j-1}(p^0)$ for some $k+1 \leq j \leq \text{end} - 1$. Therefore, $p_1^0 > R_{o_{k+1}} \geq R_{o_j}$. $u^{*,t} = p^0$ for $0 \leq t < N_j(p^0) - 2$ and $u^{t,*} = R_{o_j}[1 \ -1]$ for $N_j(p^0) - 2 \leq t \leq N - 1$. We first show that $u^* \in \mathcal{D}(\mathcal{E}, p^0, N)$. Let $(\mathcal{E}^0, \dots, \mathcal{E}^N)$ be the topology sequence under u^* . It is straightforward that $(\mathcal{E}^0, \dots, \mathcal{E}^{N_j(p^0)-2}) = (\mathcal{E}_{\text{un}}^0, \dots, \mathcal{E}_{\text{un}}^{N_j(p^0)-2})$. By definition of $N_j(p^0)$, $[o_j] \subset \mathcal{E}_{\text{un}}^{N_j(p^0)-2} = \mathcal{E}^{N_j(p^0)-2}$. In addition, Remark 7 implies $([o_j], R_{o_j}[1 \ -1]) \in \mathcal{S}$ and, plus the definition of o_j , further implies that $([k], p^0) \notin \mathcal{S}$ for all $k > o_j$. Therefore, $\mathcal{E}^t = [o_j]$ for all $t \geq N_j(p^0) - 1$ and $u^* \in \mathcal{D}(\mathcal{E}, p^0, N)$. We then show optimality of u^* through contradiction. Suppose there exists a control $\tilde{u} \in \mathcal{D}(\mathcal{E}, p^0, N)$ such that $R_{o_j} < \tilde{u}_1^{N-1} \leq p_1^0$. Let $(\tilde{\mathcal{E}}^0, \dots, \tilde{\mathcal{E}}^{N-1})$ be the topology sequence under control \tilde{u} . Remark 5 implies that $\mathcal{E}_{\text{un}}^{N-1} \subseteq \tilde{\mathcal{E}}^{N-1}$. At the same time, since $N < N_{j-1}(p^0)$, $\mathcal{E}_{\text{un}}^{N-1} \supseteq \mathcal{E}_{\text{un}}^{N_{j-1}(p^0)-2} \supset [o_{j-1}]$. Note the inclusion is strict. Therefore, $[o_{j-1}] \subset \tilde{\mathcal{E}}^{N-1}$. Remark 7, combined with the definition of o_j and the assumption that $\tilde{u}_1^{N-1} > R_{o_j}$, implies that $(\tilde{\mathcal{E}}^{N-1}, \tilde{u}^{N-1}) \notin \mathcal{S}$. This contradicts with \tilde{u} being feasible. ■

Remark 8: While Proposition 1 gives the explicit expression of a one-shot control that is optimal for parallel networks, the fact that a one-shot control being optimal is proved in more general settings in [20].

The proof of Proposition 1 implies the following.

Corollary 1: For a parallel network $(\{1, 2\}, \mathcal{E})$ with link weights $w \in \mathbf{R}_{>0}^{\mathcal{E}}$, flow capacities $c \in \mathbf{R}_{>0}^{\mathcal{E}}$ and initial supply demand vector p^0 , for $N \geq |\mathcal{E}| - o_1$, the following constant control u^* is an optimal control: $u^{t,*} = [1 \ -1] \min\{p_1^0, R_{o_1}\}$ for all $0 \leq t \leq N - 1$.

One one hand, Proposition 1 and Corollary 1 justify the study of optimal control within special classes of control policies. On the other hand, while a constant control action can be optimal for non-parallel networks, it is not true in general. This is illustrated in Example 2. In fact, while it is straightforward to see that the set of feasible constant control actions is connected for parallel networks, this is not the case for a general network, even if it admits a one-shot control action that is optimal.

Example 2: Consider the network illustrated in Fig. 5, containing a single supply node 1 and a single demand node 3, having link weights $w = [1, 1, 1, 1, 1]$, and with initial supply-demand vector $p^0 = [3, 0, -3]$. Consider two scenarios corresponding to link capacities $c^1 = [0.8, 0.5, 0.6, 0.25, 1.5]$ and $c^2 = [0.8, 0.5, 0.7, 0.25, 1.5]$, where note that the two scenarios differ only in the capacity of link e_3 . We consider the optimal control problem for $N = 2$. Let $u^t = z_t \times [1, 0, -1]$, $i \in \{0, 1\}$, $0 \leq z_0 \leq z_1$ be the control actions. The flow under u^t for relevant network topologies are: $f([5], u^t) = \frac{1}{4}z_t \times [1, 1, 1, 1, 2]^T$, $f(\{1, 2, 3, 5\}, u^t) = \frac{1}{5}z_t \times [1, 1, 2, \text{null}, 3]^T$, $f(\{1, 3, 5\}, u^t) = \frac{1}{3}z_t \times [1, \text{null}, 1, \text{null}, 2]^T$ and $f_5(\{5\}, u^t) = z^t$. The maximal value of z_t the can be supported by these networks are, respectively, 1, 1.5, 1.8, 1.5 in the first scenario and 1, 1.75, 2.1, 1.5 in the second scenario. It is straightforward to see that the network would get disconnected in both scenarios if no load shedding is implemented. By considering all possible topology sequences that can occur under a control policy, we obtain the following:

- (i) The optimal one-shot control that sheds loads at $t = 1$ is $z_0 = 3$, $z_1 = 1.5$ in both scenarios.
 - (ii) The optimal constant controls are: $z_0 = z_1 = 1.5$ in the first scenario and $z_0 = z_1 = 2.1$ in the second scenario.
 - (iii) An optimal control is $z_0^* = 2.1$ and $z_1^* = 1.8$ in the first scenario and is $z_0^* = z_1^* = 2.1$ in the second scenario.
- We can see in both cases, constant controls perform no worse than one-shot control, and while the best constant control is not optimal over all controls in the first scenario, it is optimal in the second scenario. Furthermore, in the second scenario, a feasible constant control has to satisfy $z_0 = z_1 \in [0, 1] \cap (2, 2.1]$. The set is neither connected nor closed.

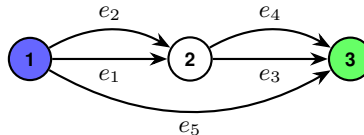


Fig. 5: The graph topology for the network used in Example 2 to illustrate that the set of feasible one-shot control actions is not necessarily connected or closed.

B. A Decomposition Approach for Tree Reducible Networks

In this section, we develop a decomposition approach to compute optimal control for *tree reducible networks*.

Definition 2 (Reducible Network [16]): A network $\mathcal{G} = (\mathcal{V}, \mathcal{E})$ shown in Fig. 6 is called reducible about $v_1 \in \mathcal{V}$ and $v_2 \in \mathcal{V}$ under supply-demand vector $p \in \mathbf{R}^{\mathcal{V}}$ if there exist $\mathcal{G}_1 = (\mathcal{V}_1, \mathcal{E}_1)$ and $\mathcal{G}_2 = (\mathcal{V}_2, \mathcal{E}_2)$ such that all of the following conditions are satisfied:

- 1) $\mathcal{V}_1 \cup \mathcal{V}_2 = \mathcal{V}$, $\mathcal{V}_1 \cap \mathcal{V}_2 = \{v_1, v_2\}$;
- 2) $\mathcal{E}_1 \cup \mathcal{E}_2 = \mathcal{E}$, $\mathcal{E}_1 \cap \mathcal{E}_2 = \emptyset$, $|\mathcal{E}_2| \geq 2$;
- 3) \mathcal{G}_1 and \mathcal{G}_2 are both weakly connected; and
- 4) the supply-demand vector p is supported only on \mathcal{V}_1 .

\mathcal{G}_2 is referred to as the *reducible component*, and $\tilde{\mathcal{G}}_1 = (\mathcal{V}_1, \tilde{\mathcal{E}}_1)$ is referred to as the *reduced network* of \mathcal{G} , where $\tilde{\mathcal{E}}_1 = \mathcal{E}_1 \cup (v_1, v_2)$, and (v_1, v_2) is an additional (virtual) link, not originally present in \mathcal{G} (see Fig. 6). The direction (v_1, v_2) is chosen arbitrarily.

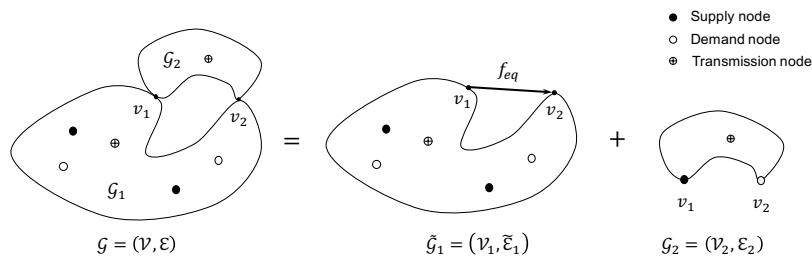


Fig. 6: Illustration of a reducible network.

Definition 3 (Tree Reducible Network [16]): A network $\mathcal{G} = (\mathcal{V}, \mathcal{E})$ with supply-demand vector p is called tree reducible if it is a tree, or it can be reduced to a tree¹ $\mathcal{T} = (\mathcal{V}_T, \mathcal{E}_T)$ by recursively applying network reduction described in Definition 2². In this case, \mathcal{T} is called the reduced tree of \mathcal{G} .

Fig. 7 provides an example of a tree reducible network, where each sub-network (denoted by $\mathcal{G}_1, \dots, \mathcal{G}_8$) in Fig. 7a represents a *reducible component* and corresponds to a link in the *reduced tree* $\mathcal{T} = (\mathcal{V}_T, \mathcal{E}_T)$ shown in Fig. 7b. We assign directions for the links in \mathcal{E}_T as follows³. Pick an arbitrary node in \mathcal{V}_T , and call it the root node. The directions for all the links incident to the root node are chosen to be incoming to the root node. The directions for the remaining links are similarly chosen to be directed towards the root node; see Figure 7b for an example. For

¹A tree is an undirected graph in which any two nodes are connected by at most one path.

² Definition 3 extends the concept of tree reducible network in [16]. The latter only allows for network reduction over parallel and serial subnetworks.

³The results presented in the current Section III do not depend on the particular choice of directions for links in \mathcal{E}_T , as selected here (see also Remark 10(ii)). If some of the virtual links in \mathcal{E}_T coincide with real links in \mathcal{E} , e.g., if $\mathcal{E}_T = \mathcal{E}$, then this is consistent with the remark in Section II that the directions for the links in \mathcal{E} are chosen arbitrarily, and that the results are invariant with respect to the choice of directions.

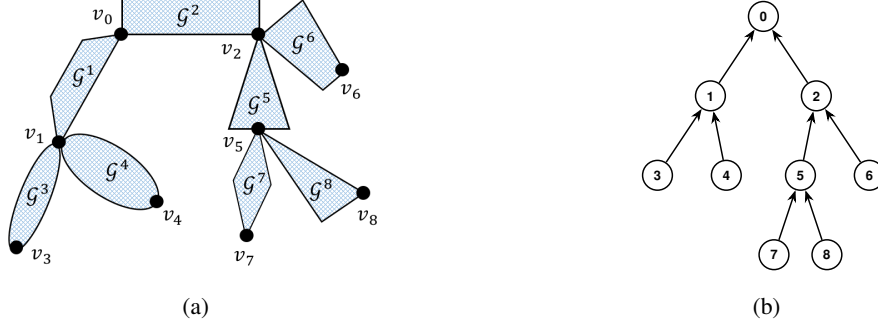


Fig. 7: (a) A tree reducible network \mathcal{G} ; and (b) a reduced tree \mathcal{T} of \mathcal{G} .

the resulting directed tree, we fix a reverse topological ordering⁴ of the nodes $(0, 1, \dots, |\mathcal{V}_T| - 1)$, with 0 being the root node. Figure 7b illustrates such an ordering. In order to minimize notations, we use the same label for a link and its tail node. For example, the link $(5, 2)$ in Figure 7b is labeled as link 5. An in-neighbor (resp., out-neighbor) of a given node is called its child (resp., parent) node. For node $i \in \mathcal{V}_T$, let \mathcal{C}_i denote the set of its children nodes, and let $\bar{\mathcal{C}}_i$ denote the set of nodes consisting of the descendants of i and the node i itself. For example, in Fig. 7b, $\mathcal{C}_2 = \{5, 6\}$ and $\bar{\mathcal{C}}_2 = \{2, 5, 6, 7, 8\}$. With this definition, $\mathcal{V}_T \equiv \bar{\mathcal{C}}_0$. Node i is called a *leaf* if it has no child node, i.e., if $\mathcal{C}_i = \emptyset$.

Let us start with the simple case when the entire network consists of a single reducible component, say \mathcal{G}_i , so that the reduced tree is $\mathcal{T} = (\{0, 1\}, 1)$. Let the nodes 0 and 1 correspond, respectively, to nodes v_0 and v_1 in \mathcal{V}_i . Recall from Definition 2 that v_0 and v_1 are the only supply-demand nodes in \mathcal{G}_i . Let $a_i \in \{1, 0, -1\}^{\mathcal{V}_i}$ be such that a_v is equal to 1 if $v = v_0$, is equal to -1 if $v = v_1$, and is equal to zero otherwise. We do not fix the individual identities of v_0 and v_1 as supply or demand nodes, and the choice of the signs of entries of a_i is merely to set some convention. We let $z_i^t a_i$ with $z_i^t \in \mathbf{R}$ denote the supply-demand vector in \mathcal{G}_i for $t \in [N]$, or equivalently, the control sequence for $t \in \{0, \dots, N - 1\}$. If $\tilde{p}_i a_i$, for $\tilde{p}_i \in \mathbf{R}$, is the initial supply demand vector, then the set of feasible control sequences as per (10) is $\mathcal{D}(N, \mathcal{E}_i^0, \tilde{p}_i a_i)$, where \mathcal{E}_i^0 is the initial active link set in \mathcal{G}_i at $t = 0$. Recall that $\mathcal{D}(N, \mathcal{E}_i^0, \tilde{p}_i a_i)$ captures the constraint that the terminal state at $t = N$ is feasible, as well as the monotonicity constraint implied by (6). We split these two constraints as $\mathcal{D}(\mathcal{E}_i^0, \tilde{p}_i a_i, N) = \tilde{\mathcal{D}}_i(N) \cap \hat{\mathcal{D}}_i(N)$, where $\tilde{\mathcal{D}}_i(N)$ captures feasibility of terminal state, while relaxing monotonicity, and $\hat{\mathcal{D}}_i(N)$ captures monotonicity while relaxing feasibility of the terminal state. These two sets are formally defined as:

$$\tilde{\mathcal{D}}_i(N) := \{(z_i^0, \dots, z_i^{N-1}) \in \mathbf{R}^N \mid (\mathcal{E}_i^{N-1}, z_i^{N-1} a_i) \in \mathcal{S}; \mathcal{E}_i^t = \mathcal{F}_{\mathcal{E}}(\mathcal{E}_i^{t-1}, z_i^{t-1} a_i), \forall t \in [N - 1]\} \quad (13)$$

$$\hat{\mathcal{D}}_i(N) := \{(z_i^0, \dots, z_i^{N-1}) \in \mathbf{R}^N \mid z_i^0 \in \text{cube } \tilde{p}_i, z_i^t \in \text{cube } z_i^{t-1}, \forall t \in [N - 1]\} \quad (14)$$

When clear from the context, we shall not show the explicit dependence of $\tilde{\mathcal{D}}_i$ and $\hat{\mathcal{D}}_i$ on N .

⁴That is, for every directed link (i, j) , we have $i > j$.

- Remark 9:* • Note that $\tilde{\mathcal{D}}_i$ includes control actions that cause loss of connectivity in \mathcal{G}_i . In this case, since we have only one supply and demand, the constraint that the terminal state $(\mathcal{E}_i^{N-1}, z_i^{N-1} a_i)$ is feasible, implies that $z_i^{N-1} = 0$. In addition, since all links have symmetrical capacities, $\tilde{\mathcal{D}}_i = -\hat{\mathcal{D}}_i$.
- $\hat{\mathcal{D}}_i$ is a polytope. Without considering the trivial case that $(\emptyset, \mathbf{0}) \in \mathcal{S}$, $\tilde{\mathcal{D}}_i$ is bounded as the link capacities are assumed to be finite. The explicit computation of $\tilde{\mathcal{D}}_i$ follows from the discussion in Section IV-C (cf. Remark 18).

The flexibility afforded by splitting the control constraints into (13) and (14) for an isolated reducible sub-network allows to translate capacity constraints from individual links in a general tree reducible network \mathcal{G} into equivalent constraints for the equivalent links in \mathcal{E}_T as follows. The control u_i^t ⁵ at node $i \in \mathcal{V}_T$ at time $t \in \{0, \dots, N-1\}$ is split as $u_i^t = z_i^t - \sum_{j \in \mathcal{C}_i} z_j^t$. For example, referring to Figure 7, $u_5^t = z_5^t - z_7^t - z_8^t$. In this case, the outflow from link i in \mathcal{E}_T , z_i^t , is interpreted as \mathcal{G}_i 's *share* of control input u_i^t . $u_i := (u_i^0, \dots, u_i^{N-1})$, $i \in \mathcal{V}_T$, is constrained to satisfy (14) for $\tilde{p}_i = p_i^0$, and $z_i := (z_i^0, \dots, z_i^{N-1})$, $i \in \mathcal{E}_T$, is constrained to satisfy (13).

Consider the following optimization problem that will inform the decomposition approach. For $i \in \mathcal{E}_T$, given $z_i \in \tilde{\mathcal{D}}_i$, let:

$$g_i(z_i) := \sup_{\substack{z_k \in \tilde{\mathcal{D}}_k \forall k \in \bar{\mathcal{C}}_i \setminus i \\ u_k \in \hat{\mathcal{D}}_k \forall k \in \bar{\mathcal{C}}_i}} \sum_{k \in \bar{\mathcal{C}}_i} d_k u_k^{N-1} \quad (15)$$

s.t. $z_k = u_k + \sum_{j \in \mathcal{C}_k} z_j, \quad \forall k \in \bar{\mathcal{C}}_i$

(15) can be interpreted as maximizing a certain *utility function* over the subtree rooted at node $i \in \mathcal{V}_T$, given that the outflow sequence from node i is $z_i \in \mathbf{R}^N$. (15) is a generalization of (9), in the sense that $g_0(\mathbf{0})$ is equal to the optimal value of (9). Since the objective function of (15) is separable and the decision variables are coupled with only equality constraints of a simple form, standard distributed algorithm, for example, ADMM [21], can be used to solve (15) if sets $\tilde{\mathcal{D}}_k$ are convex. In order to reduce the complexity of non-convexity, we decompose (15) into the following *nested form*:

$$g_i(z_i) = \sup_{\substack{z_j \in \mathcal{Z}_j \forall j \in \mathcal{C}_i \\ u_i \in \hat{\mathcal{D}}_i}} d_i u_i^{N-1} + \sum_{j \in \mathcal{C}_i} g_j(z_j) \quad (16)$$

s.t. $z_i = u_i + \sum_{j \in \mathcal{C}_i} z_j$

where $\mathcal{Z}_j := \tilde{\mathcal{D}}_j \cap \left(\hat{\mathcal{D}}_j + \sum_{k \in \mathcal{C}_j} \mathcal{Z}_k \right)$ combines both the constraints $z_j \in \tilde{\mathcal{D}}_j$ and $z_j = u_j + \sum_{k \in \mathcal{C}_j} z_k$, for all $j \in \mathcal{E}_T$. The equivalence between (15) and (16) can be seen via induction. In particular, if i is a leaf node, then $\mathcal{C}_i = \emptyset$. Both (15) and (16) reduce to $g_i(z_i) = \max_{z_i = u_i \in \hat{\mathcal{D}}_i} d_i u_i^{N-1}$. The optimal value function is $g_i(z_i) = d_i z_i^{N-1}$ if $z_i \in \tilde{\mathcal{D}}_i \cap \hat{\mathcal{D}}_i = \mathcal{Z}_i$, and is $-\infty$ otherwise due to infeasibility. If i is not a leaf node, then (16) can be interpreted as being associated with a local *star* subnetwork in \mathcal{T} . Fig. 8 shows all such local (star) sub-networks for the network shown in Fig. 7b.

The solution to (15) is obtained by solving sub-problems in (16) over two iterations:

- (I) Compute $g_i : \mathcal{Z}_i \rightarrow \mathbf{R}$ via (16) for every $i \in \mathcal{V}_T$ in the reverse topological order;

⁵With a slight abuse of notation, we use u to denote control inputs for the original network as well as the reduced network.

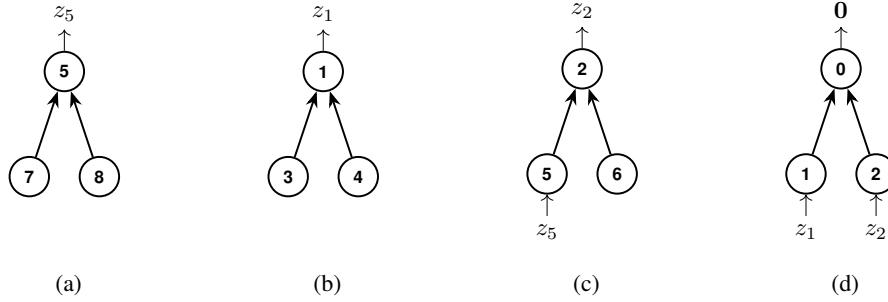


Fig. 8: The four local (star) sub-networks corresponding to Figure 7b.

(II) Set $z_0^* = \mathbf{0}$. Following the topological order, for every $i \in \mathcal{V}_T$, compute an optimal solution $(u_i^*, \{z_j^*, j \in \mathcal{C}_i\})$ to (16) corresponding to $g_i(z_i^*)$.

It is easy to check that, for all $i \in \mathcal{V}_T$, we have $\mathbf{0} \in \hat{\mathcal{D}}_i$ and $\mathbf{0} \in \tilde{\mathcal{D}}_i$, and hence $\mathbf{0} \in \mathcal{Z}_i$. Therefore, iteration (II) is well-posed.

Remark 10: The optimal solution to (9) as computed by the decomposition approach is invariant with respect to the choice of root node, directions of the links in \mathcal{E}_T , and the topological ordering used for labeling nodes in \mathcal{V}_T .

While the decomposition approach reduces complexity of solving (9) for general tree reducible networks, the bottleneck is still non-convexity of the local problems in (16). In Section III-D, we show that, for constant controls, the two iterations involving solutions to the local problems in (16) admit closed-form expressions. The required machinery is first developed in the next subsection in a general setting.

C. Input-output Properties of the Subproblem in for Constant Control

The original problem (15) and the sub-problem (16) is simplified to a great extent if only constant controls are considered: for all $i \in \mathcal{V}_T$, the decision variables z_i and u_i reduce to one dimensional real numbers; and the sets $\hat{\mathcal{D}}_i$ and $\tilde{\mathcal{D}}_i$ reduce to cube p_i^0 and the collection of multiple one dimensional line intervals, respectively. Remark 18 explains how to obtain $\tilde{\mathcal{D}}_i$ in this case. As illustrated in Example 2, the line intervals for $\tilde{\mathcal{D}}_i$ can be half open, which can make (15) unsolvable. Nevertheless, because the objective function in (15) is linear and hence continuous, we use the closure of $\tilde{\mathcal{D}}_i$ in (15) and hence closure of \mathcal{Z}_i in (16) for simplicity. An interior feasible point that is arbitrarily close to the solution to the problem over the closure can be obtained, as shown in Proposition 4. Therefore, we obtain the following problem, which generalizes (16) in the case of constant controls.

$$g^{\text{out}}(z) = \Omega\{g_j^{\text{in}}, X_j\}_{j \in [n]} := \max_{x \in \mathbf{R}^n} \sum_{j=1}^n g_j^{\text{in}}(x_j) \quad (17)$$

$$\text{s.t.} \quad \mathbf{1}^T x = z; \quad x_j \in X_j, \quad \forall j \in [n]$$

where $X_j \subset \mathbf{R}$ is the union of finite number of disjoint closed intervals for all $j \in [n]$. Operator Ω maps from n input functions g_j^{in} with restricted domain X_j to a single output function g^{out} with domain $\sum_{j=1}^n X_j$, where the domain of g^{out} is not explicit written in (17). Due to the possible disconnected feasible set, (17) is in general non-convex.

Remark 11: (17) becomes (16) with the following substitutions: $i = 1$, $\mathcal{C}_i = [n] \setminus \{1\}$, $g_1^{\text{in}}(x) = d_1 x$, $X_1 = \text{cube } p_i^0$, $g_j^{\text{in}}(x) = g_j(x)$ and $X_j = \mathcal{Z}_j$ for all $j \in [n] \setminus \{1\}$.

We now show that for a special class of input functions, Ω preserves certain function properties and has analytical characterization. This class of functions relates to the following construct. For a given point $\tau = (\tau_1, \tau_2) \in \mathbf{R}^2$, define a (continuous) piecewise linear function: $\chi_\tau : \mathbf{R} \rightarrow \mathbf{R}$ as:

$$\chi_\tau(x) := \begin{cases} x - \tau_1 + \tau_2 & x \leq \tau_1 \\ -x + \tau_1 + \tau_2 & x > \tau_1 \end{cases} \quad (18)$$

As shown in Fig 9, function χ_τ contains two rays joining at τ , which is referred as the *top point* of χ_τ . It is straightforward that χ_τ intersects the vertical axis at $(0, \tau_2 - |\tau_1|)$.

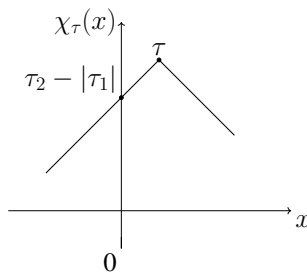


Fig. 9: Illustration of $\chi_\tau(x)$ defined in (18).

It is often useful to have a χ function defined over a restricted domain. When the restricted domain is a closed interval, Lemma 3 can be used to translate the top point, if not already, into the domain, without changing function values.

Lemma 3: Consider a point $\tau = (\tau_1, \tau_2) \in \mathbf{R}^2$ and a closed interval $[b_1, b_2] \subset \mathbf{R}$ such that $\tau_1 \notin [b_1, b_2]$, let $\tau' := (b_2, b_2 - \tau_1 + \tau_2)$ if $\tau_1 > b_2$ and $\tau' := (b_1, -b_1 + \tau_1 + \tau_2)$ if $\tau_1 < b_1$. Then $\chi_\tau(x) = \chi_{\tau'}(x)$ for all $x \in [b_1, b_2]$.

We are now ready to present the results on operator Ω . We first consider the case when every X_j contains only a single piece of interval. In this case, the feasible set of (17) is convex and hence (17) is convex if input functions g_j^{in} are concave. The next result shows that χ functions are invariant through the operator Ω if X_j is a single piece of interval for all $j \in [n]$.

Lemma 4: If g_j^{in} is a χ function (cf. (18)) with top point $\tau_j = (\tau_j^1, \tau_j^2)$ and $X_j = [q_j^l, q_j^u]$ ($q_j^l \leq \tau_j^1 \leq q_j^u$) for all $j \in [n]$, then the following hold true for Ω defined in (17):

- (i) $g^{\text{out}} = \Omega\{(g_j^{\text{in}}, X_j)\}_{j \in [n]}$ is a χ function with top point $(\mathbf{1}^T \tau^1, \mathbf{1}^T \tau^2)$ and domain $[\mathbf{1}^T q^l, \mathbf{1}^T q^u]$.
- (ii) the set of maximizers of (17) is $\{x^* \in [q^l, \tau^1] \mid \mathbf{1}^T x^* = z\}$ if $\mathbf{1}^T q^l \leq z < \mathbf{1}^T \tau^1$, $\{\tau^1\}$ if $z = \mathbf{1}^T \tau^1$, and is $\{x^* \in [\tau^1, q^u] \mid \mathbf{1}^T x^* = z\}$ if $\mathbf{1}^T \tau^1 < z \leq \mathbf{1}^T q^u$.

where $\tau^1 := \tau_{[n]}^1$, $\tau^2 := \tau_{[n]}^2$, $q^l := q_{[n]}^l$ and $q^u := q_{[n]}^u$ are n dimensional vectors.

Proof: First of all, it is clear that (17) is feasible only for $z \in [\mathbf{1}^T q^l, \mathbf{1}^T q^u]$. Secondly, since g_j is concave and X_j is convex, (17) is convex and strong duality holds. Therefore, it is sufficient to consider the dual problem

in order to solve (17). Let $\mu \in \mathbf{R}$ be the Lagrange multiplier associated with the constraint $z = \mathbf{1}^\top x$. The dual function is then given by:

$$\begin{aligned}\phi(\mu) &= -\mu z + \max_{q^l \leq x \leq q^u} \sum_{j=1}^n (\chi_{\tau_j}(x_j) + \mu x_j) = -\mu z + \sum_{j=1}^n \max_{q_j^l \leq x_j \leq q_j^u} (\chi_{\tau_j}(x_j) + \mu x_j) \\ &= \left(\sum_{j=1}^n x_j^*(\mu) - z \right) \mu + \sum_{j=1}^n \chi_j(x_j^*(\mu))\end{aligned}$$

where $x_j^*(\mu) \in \mathcal{X}_j^*(\mu) := \operatorname{argmax}_{q_j^l \leq x_j \leq q_j^u} (\chi_{\tau_j}(x_j) + \mu x_j)$, for all $j \in [n]$.

For $\mu \in [-1, 1]$, $\chi_{\tau_j}(x_j) + \mu x_j$ is piecewise linear: nondecreasing with slope $(1 + \mu)$ over $(-\infty, \tau_j^1]$ and nonincreasing with slope $(\mu - 1)$ over $(\tau_j^1, +\infty)$. Therefore, $\tau_j^1 \in \mathcal{X}_j^*(\mu)$ for all $\mu \in [-1, 1]$ and $j \in [n]$. This implies that $\phi(\mu)$ is linear over $[-1, 1]$, for every z . In particular, $\mathcal{X}_j^*(-1) = [q_j^l, \tau_j^1]$ and $\mathcal{X}_j^*(1) = [\tau_j^1, q_j^u]$ for all $j \in [n]$. For $\mu > 1$, $\chi_{\tau_j}(x_j) + \mu x_j$ is strictly increasing, and hence $\mathcal{X}_j^*(\mu) = \{q_j^u\}$. Since $z \leq \mathbf{1}^\top q^u$, $\phi(\mu)$ is linear and non-decreasing over $(1, +\infty)$. Similarly, by considering $\mu < -1$, we have $\mathcal{X}_j^*(\mu) = \{q_j^l\}$ and $\phi(\mu)$ is linear and non-increasing over $(-\infty, -1)$. Collecting these facts gives that, for every $z \in [\mathbf{1}^\top q^l, \mathbf{1}^\top q^u]$, the dual function $\phi(\mu)$ is convex and piecewise linear with possible break points at $\mu = -1$ and $\mu = 1$. Therefore, $g^{\text{out}}(z) = \min_{\mu \in \mathbf{R}} \phi(\mu) = \min\{\phi(-1), \phi(1)\}$.

As $\tau_j^1 \in \mathcal{X}_j^*(\mu)$ for $\mu \in [-1, 1]$, we have $\phi(-1) = z - \mathbf{1}^\top \tau^1 + \mathbf{1}^\top \tau^2$ and $\phi(1) = -z + \mathbf{1}^\top \tau^1 + \mathbf{1}^\top \tau^2$. $\phi(-1) \leq \phi(1)$ for $z \in [\mathbf{1}^\top q^l, \mathbf{1}^\top \tau^1]$, and $\phi(1) \leq \phi(-1)$ for $z \in [\mathbf{1}^\top \tau^1, \mathbf{1}^\top q^u]$. Therefore,

$$g^{\text{out}}(z) = \begin{cases} z - \mathbf{1}^\top \tau^2 + \mathbf{1}^\top \tau^2 & \mathbf{1}^\top q^l \leq z \leq \mathbf{1}^\top \tau^1 \\ -z + \mathbf{1}^\top \tau^1 + \mathbf{1}^\top \tau^2 & \mathbf{1}^\top \tau^1 \leq z \leq \mathbf{1}^\top q^u \end{cases}$$

Comparing with (18) establishes (i). (ii) follows from the fact that, for a given optimal dual solution μ^* , $x_j^*(\mu^*) \in \mathcal{X}_j^*(\mu^*)$, $j \in [n]$, is an optimal primal solution if and only if the constraint $z = \mathbf{1}^\top x^*$ is satisfied. \blacksquare

Remark 12:

- 1) Lemma 4 implies that the condition $\tau_j^1 \in X_j$ in Lemma 4 is without loss of generality. In addition, the top point of g^{out} is inside its domain, that is, $\mathbf{1}^\top \tau^1 \in [\mathbf{1}^\top q^l, \mathbf{1}^\top q^u]$.
- 2) Lemma 4 implies the following. If g_j^{in} , $j \in [n]$, are linear functions with the same slope 1 (and -1 , respectively), then g^{out} is linear with the same slope 1 (and -1 , respectively). If g_j^{in} is a linear function with slope 1 (and -1 , respectively) for all $j \in S \subset [n]$ (and $j \in [n] \setminus S$, respectively), then g^{out} contains two linear pieces with slope 1 over domain $[\mathbf{1}^\top q^l, \mathbf{1}^\top \tau^1]$ and slope -1 over domain $[\mathbf{1}^\top \tau^1, \mathbf{1}^\top q^u]$, and moreover, for $z \in [\mathbf{1}^\top \tau^1, \mathbf{1}^\top q^u]$: $x_j^* = q_j^u$ for all $j \in S$, and for $z \in [\mathbf{1}^\top q^l, \mathbf{1}^\top \tau^1]$: $x_j^* = q_j^l$ for all $j \in [n] \setminus S$.
- 3) It is straightforward to see from the proof of Lemma 4 that the same results hold when X_j is unbounded for some j , that is $q_j^1 = -\infty$ and/or $q_j^2 = \infty$.

We then consider the case when X_j contains multiple pieces of disjoint intervals. Without loss of generality, for all $j \in [n]$, assume X_j contains m_j pieces of intervals and denote each piece by X_j^k , then $X_j = \cup_{k=1}^{m_j} X_j^k$. Let $\Theta := \prod_{j=1}^n [m_j] \subset \mathbf{R}^n$. The way to solve the nonconvex problem (17) is to decompose it into multiple convex subproblems. Each of the subproblem is associated with a combination $\sigma \in \Theta$ of intervals $X_j^{\sigma_j}$ and is denoted by

$\Omega(\sigma) := \Omega\{(g_j^{\text{in}}, X_j^{\sigma_j})\}_{j \in [n]}$. The following is straightforward.

$$\Omega\{(g_j^{\text{in}}, X_j)\}_{j \in [n]} = \max_{\sigma \in \Theta} \Omega(\sigma) \quad (19)$$

If the restriction of every input function g_j^{in} over X_j^k is a χ function for all $k \in [m_j]$, then then Lemma 4 can be used to solve the subproblem $\Omega(\sigma)$ for all $\sigma \in \Theta$. This is illustrated by the next example.

Example 3: Consider the case shown in Fig. 10a: $n = 2$, $m_1 = m_2 = 3$, $X_1^1 = [-3, -2.5]$, $X_1^2 = [-1, 1]$, $X_1^3 = [2.5, 3]$, $X_2^1 = [-3, -2]$, $X_2^2 = [-1.5, 1.5]$, $X_2^3 = [2, 3]$. $\text{conv } X_1 = \text{conv } X_2 = [-3, 3]$. Function $g_1^{\text{in}} : [-3, 3] \rightarrow \mathbf{R}$ and $g_2^{\text{in}} : [-3, 3] \rightarrow \mathbf{R}$ are χ functions with top point $(2.5, 6)$ and $(-1.5, 5)$, respectively. Since the input functions are χ functions over the convexified domains, the output function $g_{\text{cvx}}^{\text{out}} := \Omega\{g_j^{\text{in}}, [-3, 3]\}_{j=1}^2$ from the convexified problem is a χ function with top point $(1, 11)$, as shown using dotted line in Fig 10b. For every $\sigma \in \{1, 2, 3\} \times \{1, 2, 3\}$, the output function $g_\sigma^{\text{out}} := \Omega(\sigma)$ from the subproblem is a χ function upper bounded by $g_{\text{cvx}}^{\text{out}}$, as shown using solid line in Fig 10b. More specifically, for $\sigma \in \{(1, 1), (2, 1)\}$ and $\sigma \in \{(3, 2), (3, 3)\}$, g_σ^{out} is linear and coincide with the left and right wing of $g_{\text{cvx}}^{\text{out}}$, respectively, and for $\sigma \in \{(1, 1), (2, 1)\}$, g_σ^{out} is χ function that contains two pieces and is smaller than \tilde{g} on at least one piece. As a result, the output function $g^{\text{out}} := \Omega\{(g_j^{\text{in}}, X_j)\}_{j \in [n]}$ is a two pieces function, with each piece being a χ function.

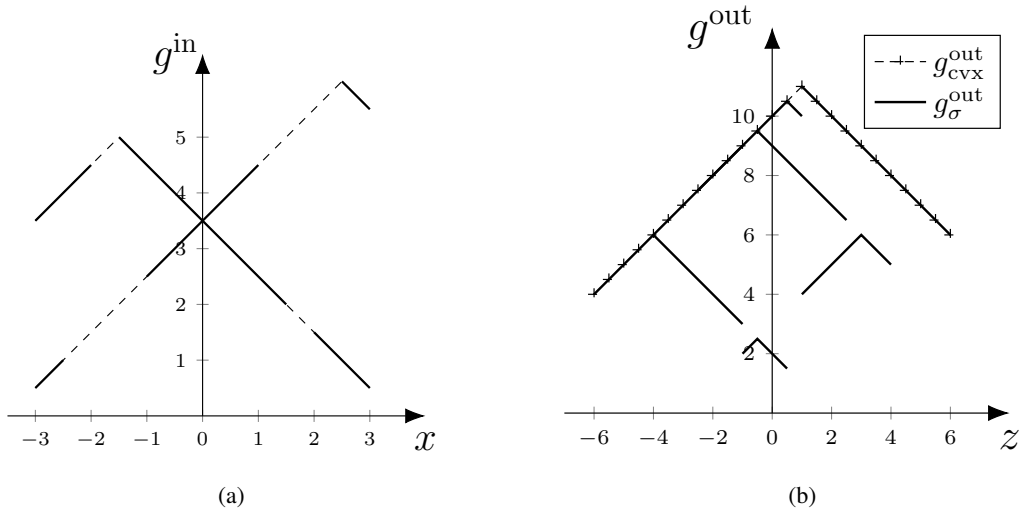


Fig. 10: (a). Input functions to Ω ; (b). Output function from each subproblem.

Formally, we call a single variable real valued function a *piecewise χ function* if it is composed of some number of segments defined over an equal number of intervals such that each segment is a χ function. Example 3 shows that the output function from Ω is a piecewise χ function if the input functions are all χ function. The next result generalizes this observation and shows that piecewise χ functions are invariant through operator Ω .

Proposition 2: If $X_j \subset \mathbf{R}$ is the union of multiple disjoint and closed intervals (including rays) and $g_j^{\text{in}} : X_j \rightarrow \mathbf{R}$ is a piecewise χ function for all $j \in [n]$, then $\Omega\{g_j^{\text{in}}, X_j\}_{j=1}^n$ is a piecewise χ function.

Proof: The proof follows straightforwardly from (19), Lemma 4, Remark 12 and the fact the point-wise maximum of multiple χ functions is a piecewise χ function. ■

On the other hand, while the point-wise maximum of multiple χ functions is not necessarily a χ function, as demonstrated by Example 3, the next result gives the necessary and sufficient conditions for the output function from Ω to be a χ function given that all input functions are χ functions. The proof is shown in Appendix B.

Proposition 3: For all $j \in [n]$, $X_j \subset \mathbf{R}$ is the union of multiple disjoint and closed intervals (including rays) and $g_j^{\text{in}} : \text{conv } X_j \rightarrow \mathbf{R}$ is a χ function with top point $\tau_j = (\tau_j^1, \tau_j^2)$. Then $\Omega\{(g_j^{\text{in}}, X_j)\}_{j \in [n]} = \Omega\{(g_j^{\text{in}}, \text{conv } X_j)\}_{j \in [n]}$ if and only if (1) $\tau_j^1 \in X_j$ for all $j \in [n]$; and (2) both $\sum_{j=1}^n X_j \cap (-\infty, \tau_j^1]$ and $\sum_{j=1}^n X_j \cap [\tau_j^1, \infty)$ are connected sets.

The second condition in Proposition 3 is related to the relative lengths of the intervals and the gaps between them, as well as the number sets in summation, as illustrated by Lemma 5 and 6.

Lemma 5: Let X_1 be a closed interval and X_j be the union of multiple disjoint and closed intervals. Let $|X_j| := \max X_j - \min X_j$ and δ_j be the maximal length of the gaps between intervals of X_j . Assume X_j is labeled such that $\delta_j \leq \delta_{j+1}$ for all j , then $\sum_j X_j$ is connected if $\delta_{j+1} \leq \sum_{k=1}^j |X_k|$ for all j .

Remark 13: Lemma 5 implies that the second condition in Proposition 3 is satisfied if $X_j = \mathbf{R}$ for some $j \in [n]$.

Lemma 6: Consider m disjoint closed intervals denoted by X_j , $j \in [m]$, and labeled in increasing order, that is, $\max X_j < \min X_{j+1}$ for all $j \in [m-1]$. Let $|X_j| := \max X_j - \min X_j$ for all $j \in [m]$, $\bar{\delta}_j = \min X_{j+1} - \max X_j$ for all $j \in [m-1]$, and $X = \cup_{j=1}^m X_j$. Then $\sum_{i=1}^n X$ is connected for $n \geq 1 + \max_{i=1}^{m-1} \bar{\delta}_j / \min\{|X_j|, |X_{j+1}|\}$.

Proof: We first prove for $m = 2$. Let $X_1 =: [x_1, x_2]$ and $X_2 =: [x_3, x_4]$. Then

$$\sum_{i=1}^n X = \cup_{k=0}^n [(n-k)x_1 + kx_3, (n-k)x_2 + kx_4]$$

The necessary and sufficient condition for $\sum_{i=1}^n X$ to be connected in this case is $(n-k)x_1 + kx_3 \leq (n-k+1)x_2 + (k-1)x_4$ for all $k \in [n]$, which is equivalent to $x_3 - x_2 \leq (n-1) \min\{x_2 - x_1, x_4 - x_3\}$. The condition can be equivalently written as $n \geq 1 + \bar{\delta}_j / \min\{|X_1|, |X_2|\}$. Then the assertion for $m > 2$ follows by considering each adjacent pair of intervals separately. ■

D. Optimal Constant Control Action for Tree Reducible Networks

Lemma 4, Proposition 2 and Proposition 3 can be used in the two iteration algorithm proposed in Section III-B to obtain an optimal load shedding control action within the class of constant control actions (cf. Definition 1) for tree reducible networks. We provide the explicit algorithm in Algorithm 1 for the case when the conditions in Proposition 3 are satisfied. The algorithm for the general case can be extrapolated from this straightforwardly. With Remark 11 showing the correspondence between (16) and (17), we use the following additional notation in Algorithm 1. let $\tau_i = (\tau_i^1, \tau_i^2)$ be the top point and $[z_i^l, z_i^u] := \mathcal{Z}_i$ be the domain of function $g_i(z)$ for all $i \in \mathcal{V}$; the top point and domain of function $d_i z_i$ are cube p_i^0 and $(p_i^0, |p_i^0|)$, respectively. For a real number x , let $[x]^+ := \max\{x, 0\}$ and $[x]^- := \min\{x, 0\}$. Hence, cube $p_i^0 \equiv [[p_i^0]^- , [p_i^0]^+]$. Furthermore, let $q_i > 0$ be the maximal value of $\tilde{\mathcal{D}}_i$ for the case of constant control for all $i \in \mathcal{E}_T$. Remark 9 implies that $-q_i$ is the minimal

value of \tilde{D}_i . Algorithm 1 shows the two iterations using two *for* loops. The first loop computes τ_i , z_i^l and z_i^u for all $i \in \mathcal{V}$ in reverse topological order, where $(p_i^0, |p_i^0|)$ on line 3 is a top point for function $d_i z_i$. The second loop extracts a particular maximizer from the solution set shown in Proposition 3.

Remark 14: The specific value of γ_i is chosen to ensure the constraint $z_i = u_i + \sum_{j \in \mathcal{C}_i} z_j$ to be satisfied. While one can choose other values of γ_i , this particular choice ensures that the resulting maximizer $(u_i, \{z_j\}_{j \in \mathcal{C}_i})$ on line 12 and 15 to lie in cube τ^1 at every iteration.

Algorithm 1: Optimal constant control for tree reducible network.

input : reduced tree $\mathcal{T} = (\mathcal{V}, \mathcal{E})$, initial supply-demand vector $p^0 \in \mathbf{R}^{\mathcal{V}}$, $q^l \in \mathbf{R}^{\mathcal{E}}$, $q^u \in \mathbf{R}^{\mathcal{E}}$

output: optimal constant load shedding control action $u \in \mathbf{R}^{\mathcal{V}}$

```

1 for  $i \in \mathcal{V}$  in reverse topological order do
2    $z_i^l = \max \{q_i^l, [p_i^0]^- + \sum_{j \in \mathcal{C}_i} z_j^l\}$ ,  $z_i^u = \min \{q_i^u, [p_i^0]^+ + \sum_{j \in \mathcal{C}_i} z_j^u\}$ 
3    $\tau_i^1 = p_i^0 + \sum_{j \in \mathcal{C}_i} \tau_j^1$ ,  $\tau_i^2 = |p_i^0| + \sum_{j \in \mathcal{C}_i} \tau_j^2$ 
4   update  $(\tau_i^1, \tau_i^2)$  according to Lemma 3 if  $\tau_i^1 \notin [q_i^l, q_i^u]$ 
5 end
6  $z_0 = 0$ 
7 for  $i \in \mathcal{V}$  in topological order do
8   if  $z_i = \tau_i^1$  then
9      $u_i = p_i^0$ ,  $z_j = \tau_j^1$  for all  $j \in \mathcal{C}_i$ 
10  else if  $0 \leq z_i < \tau_i^1$  then
11     $\gamma_i = (z_i - \sum_{j \in \mathcal{C}_i} [\tau_j^1]^- - [p_i^0]^-) / (\sum_{j \in \mathcal{C}_i} [\tau_j^1]^+ + [p_i^0]^+)$ 
12     $u_i = \min\{p_i^0, \gamma_i p_i^0\}$ ,  $z_j = \min\{\tau_j^1, \gamma_i \tau_j^1\}$  for all  $j \in \mathcal{C}_i$ 
13  else if  $\tau_i^1 < z_i < 0$  then
14     $\gamma_i = (z_i - \sum_{j \in \mathcal{C}_i} [\tau_j^1]^+ - [p_i^0]^+) / (\sum_{j \in \mathcal{C}_i} [\tau_j^1]^- + [p_i^0]^-)$ 
15     $u_i = \max\{p_i^0, \gamma_i p_i^0\}$ ,  $z_j = \max\{\tau_j^1, \gamma_i \tau_j^1\}$  for all  $j \in \mathcal{C}_i$ 
16  end
17 end
18 return  $u$ 

```

IV. AN EQUIVALENT STATE AGGREGATION APPROACH

The computational approach proposed in Section III has provable guarantees only for tree reducible networks. In this section, we return to the approach outlined in Section II-D, and (11) in particular, for a general network topology. We recall that, in its current form, (11) is not amenable to implementations because the underlying state space is uncountably infinite. In this section, we develop an equivalent finite abstraction of the state space through *state aggregation*, and correspondingly develop an aggregated version of (11).

A. A State Aggregation Approach

The key idea is to develop a finite *consistent partition* of one time step reachable sets. We recall a few standard terminologies. A *cover* of a set S is a collection of nonempty subsets $\{S_i\}_{i \in I}$ of S such that $S = \cup_{i \in I} S_i$ and a *partition* is a cover with pairwise disjoint elements. We call a cover or partition finite if it contains finitely many elements. Furthermore, for a network state (\mathcal{E}, p) , a partition $\{S_i\}_{i \in I}$ of set $S \subseteq \mathcal{B}_{\mathcal{E}}$ is said to be *consistent* if, $\mathcal{F}_{\mathcal{E}}(\mathcal{E}, u) = \mathcal{F}_{\mathcal{E}}(\mathcal{E}, \tilde{u})$ for all $u, \tilde{u} \in S_i, i \in I$. Consistency implies that it is valid to write $\mathcal{F}_{\mathcal{E}}(\mathcal{E}, u) \equiv \mathcal{F}_{\mathcal{E}}(\mathcal{E}, S_i)$ for all $u \in S_i$ and $i \in I$. Note here that the set S_i is not necessarily the set of feasible control actions $U(\mathcal{E}, p)$, and can be an arbitrary set of balanced supply-demand vectors. We extend the notion of the set of feasible control actions (6) as follows: for a link set \mathcal{E} and a set $P \subseteq \mathcal{B}_{\mathcal{E}}$,

$$U(\mathcal{E}, P) := \cup_{p \in P} U(\mathcal{E}, p) = \mathcal{B}_{\mathcal{E}} \cap \text{cube } P \quad (20)$$

where $\text{cube } P := \cup_{p \in P} \text{cube } p$.

A finite consistent partition of the set of control actions induces a natural finite cover of the state space at each stage in the cascading dynamics. At $t = 0$, the state space $\{(\mathcal{E}^0, p^0)\}$ is a singleton, and therefore $\{(\mathcal{E}^0, P^0)\}$ forms a trivial partition with $P^0 := \{p^0\}$. Let $\{U_i^0\}_{i \in I_1}$ be a finite consistent partition of $U(\mathcal{E}^0, P^0)$. Then at $t = 1$, the reachable state space $\{(\mathcal{F}_{\mathcal{E}}(\mathcal{E}^0, u), u) \mid u \in U(\mathcal{E}^0, p^0)\}$ is covered by $\{(\mathcal{E}_i^1, P_i^1)\}_{i \in I_1} = \{(\mathcal{F}_{\mathcal{E}}(\mathcal{E}^0, U_i^0), U_i^0)\}_{i \in I_1}$. Let $\{U_j^1\}_{j \in I_2^i}$ be a finite consistent partition of $U(\mathcal{E}_i^1, P_i^1)$, for all $i \in I_1$. Then at $t = 2$, the state space reachable from (\mathcal{E}_i^1, P_i^1) , $\{(\mathcal{F}_{\mathcal{E}}(\mathcal{E}_i^1, u), u) \mid u \in U(\mathcal{E}_i^1, P_i^1)\}$, is covered by $\{(\mathcal{E}_j^2, P_j^2)\}_{j \in I_2^i} = \{(\mathcal{F}_{\mathcal{E}}(\mathcal{E}_i^1, U_j^1), U_j^1)\}_{j \in I_2^i}$, for all $i \in I_1$. Repeated application of this procedure to all the subsequent stages then gives the desired finite representation. Let (\mathcal{E}^t, P^t) denote an arbitrary element of the cover at time t . A natural extension of (4) to dynamics over aggregated states is as follows:

$$(\mathcal{E}^{t+1}, P^{t+1}) = \mathcal{F}(\mathcal{E}^t, P^t, U^t), \quad U^t \in \mathbb{U}(\mathcal{E}^t, P^t) \quad (21)$$

where

$$\begin{aligned} \mathcal{F}_{\mathcal{E}}(\mathcal{E}, P, U) &\equiv \mathcal{F}_{\mathcal{E}}(\mathcal{E}, U) := \{i \in \mathcal{E} \mid -c_i \leq f_i(\mathcal{E}, u) \leq c_i \text{ for all } u \in U\} \\ \mathcal{F}_P(\mathcal{E}, P, U) &\equiv \mathcal{F}_P(U) := U \end{aligned} \quad (22)$$

$\mathbb{U}(\mathcal{E}^t, P^t)$ is defined by the particular choice of consistent partition of $U(\mathcal{E}^t, P^t)$, and serves as the set of feasible aggregated control actions at state (\mathcal{E}^t, P^t) . We associate \mathcal{E} with a vector $\beta \in \{1, 0, -1\}^{\mathcal{E}}$. β_i is used to denote whether the flow capacity constraint of link $i \in \mathcal{E}$ is satisfied or not: the flow stays within capacities for $\beta_i = 0$ and exceeds the upper and lower capacities for $\beta_i = 1$ and $\beta_i = -1$, respectively. The consistent partition used in this paper is:

$$\mathbb{U}(\mathcal{E}, P) := \{U(\mathcal{E}, P, \beta^j) \mid j \in I(\mathcal{E}, P)\} \quad (23)$$

where

$$\begin{aligned} I(\mathcal{E}, P) &:= \{j \mid U(\mathcal{E}, P, \beta^j) \neq \emptyset\} \\ U(\mathcal{E}, P, \beta) &:= \{u \in U(\mathcal{E}, P) \mid f_i(\mathcal{E}, u) < -c_i \text{ for } \beta_i = -1; -c_i \leq f_i(\mathcal{E}, u) \leq c_i \text{ for } \beta_i = 0; \\ &\quad f_i(\mathcal{E}, u) > c_i \text{ for } \beta_i = 1; \forall i \in \mathcal{E}\} \end{aligned} \quad (24)$$

It is straightforward to see that $\mathbb{U}(\mathcal{E}, P)$ defined in (23)-(24) is a consistent partition of $U(\mathcal{E}, P)$. If $U(\mathcal{E}, P)$ is a polytope, then each member of $\mathbb{U}(\mathcal{E}, P)$ is also a polytope, with possibly half open boundary due to the strict inequality in $U(\mathcal{E}, P, \beta)$. An algorithmic procedure to compute and store the partition \mathbb{U} defined in (23)-(24) will be presented in Section V.

State aggregation gives a finite tree (cf. Section II-D), whose nodes are aggregated states and arcs are aggregated control actions. The set of aggregated goal states is $\mathbb{S} := \{(\mathcal{E}, P) \mid (\mathcal{E}, p) \in \mathcal{S}, \forall p \in P\}$ and the utility associated with an aggregated state $(\mathcal{E}, P) \in \mathcal{S}$ is $\sup_{p \in P} s^T p = \max_{p \in \text{cl}(P)} s^T p$, where $\text{cl}(P)$ denotes the closure of P . The optimal search over the aggregated tree can be performed through the following calculations, which are adaptations of (11):

$$\mathbb{J}_1(\mathcal{E}, P) = \max_{u \in U(\mathcal{E}, \text{cl}(P))} s^T u \quad \text{s.t.} \quad -c_{\mathcal{E}} \leq f(\mathcal{E}, u) \leq c_{\mathcal{E}} \quad (25a)$$

$$\mathbb{J}_t(\mathcal{E}, P) = \max_{U \in \mathbb{U}(\mathcal{E}, P)} \mathbb{J}_{t-1}(\mathcal{F}_{\mathcal{E}}(\mathcal{E}, U), U), \quad t = 2, \dots, N \quad (25b)$$

where $\mathbb{J}_t(\mathcal{E}, P)$ is the maximum among values of all the aggregated states that can be reached in at most t time steps starting from (\mathcal{E}, P) . Similar to (11a), the flow constraint is imposed in (25a) to ensure the additional constraint on u^{N-1} (cf. Remark 2). This implies that the unique (and optimal) aggregated control action associated with $\mathbb{J}_1(\mathcal{E}, P)$ is $U^{N-1,*} = U(\mathcal{E}, P, \mathbf{0})$. This is to be contrasted with (25b) for $t \geq 2$ that the optimal aggregated control action $U^{t,*}$ is not trivial to obtain. (25a) maximize a linear function over a bounded closed set and (25b) maximizes over the finite set $\mathbb{U}(\mathcal{E}, P)$. Therefore, the optimal value is achievable on every iteration in (25). The next result shows that the iterations in (25) give the same value as that in (11).

Theorem 1: Consider a network with initial state (\mathcal{E}^0, p^0) , link weights $w \in \mathbf{R}_{\geq 0}^{\mathcal{E}^0}$ and link capacities $c \in \mathbf{R}_{\geq 0}^{\mathcal{E}^0}$. For every aggregated state (\mathcal{E}, P) obtained from the consistent partition in (23)-(24), the computations in (11) and (25) satisfy the following for every $p \in P$ and $t \in [N]$:

$$\mathbb{J}_t(\mathcal{E}, P) = \sup_{p \in P} J_t(\mathcal{E}, p)$$

Proof: We prove by induction. For $t = 1$:

$$\sup_{p \in P} J_1(\mathcal{E}, p) = \sup_{p \in P} \max_{u \in U(\mathcal{E}, p)} s^T u \quad \text{s.t.} \quad -c_{\mathcal{E}} \leq f(\mathcal{E}, u) \leq c_{\mathcal{E}}$$

which is equal to $\mathbb{J}_1(\mathcal{E}, P)$ as shown in (25a). Suppose the claim is true for $t \in [k]$.

$$\begin{aligned} \mathbb{J}_{k+1}(\mathcal{E}, P) &= \max_{U \in \mathbb{U}(\mathcal{E}, P)} \mathbb{J}_k(\mathcal{F}_{\mathcal{E}}(\mathcal{E}, U), U) = \max_{U \in \mathbb{U}(\mathcal{E}, P)} \sup_{u \in U} J_k(\mathcal{F}_{\mathcal{E}}(\mathcal{E}, u), u) \\ &= \sup_{u \in U(\mathcal{E}, P)} J_k(\mathcal{F}_{\mathcal{E}}(\mathcal{E}, u), u) = \sup_{p \in P} \sup_{u \in U(\mathcal{E}, p)} J_k(\mathcal{F}_{\mathcal{E}}(\mathcal{E}, u), u) \\ &= \sup_{p \in P} J_{k+1}(\mathcal{E}, p) \end{aligned}$$

where the first equality is due to (25b); the second equality is due to the induction assumption; the third and fourth equalities are due to $\cup_{U \in \mathbb{U}(\mathcal{E}, P)} U = U(\mathcal{E}, P) = \cup_{p \in P} U(\mathcal{E}, p)$, as implied by the definitions of $\mathbb{U}(\mathcal{E}, P)$ and $U(\mathcal{E}, P)$; and the last equality is due to (11). \blacksquare

We make the following remarks on the state aggregation and aggregated tree search.

Remark 15:

- 1) Every path of length N in the aggregated search tree corresponds to a, possible different, topology sequence that can occur in the cascading dynamics. The state aggregation provides a way to quantify the complexity of a general posed optimal control problem. Details can be found in Section VI-A.
- 2) The aggregated tree search based on (25) can be interpreted as a systematic way to decompose the nonconvex feasible set $\mathcal{D} \subset \mathbf{R}^{N \times |\mathcal{V}|}$ in (9)-(10) into a finite number of subsets. Each subset is a polytope and corresponds to an topology sequence and aggregated control action sequence. For example, the subset corresponding to (U^0, \dots, U^{N-1}) is $\Pi_{t=0}^{N-1} U^t$. Similar to (19), the optimal value of (9) is equal to the maximum among the optimal values of multiple subproblems associated with the subsets. Each subproblem is a linear program of the form $\sup_{u \in \Pi_{t=0}^{N-1} U^t} s^T u^{N-1}$ and indeed coincides with (25a).
- 3) The state aggregation approach allows to include include running cost into the problem formulation. In that case, instead of a linear program, a dynamic program with constraint

$$u \in \{(u^0, \dots, u^{N-1}) \in \Pi_{t=0}^{N-1} U^t \mid u^t \in \text{cube } u^{t-1}, 1 \leq t \leq N-1\}$$

is required to be solved for the path (U^0, \dots, U^{N-1}) .

B. Optimal Control Synthesis: From Aggregated to the Original State Space

The numerical implementation of (25) is shown in Section V. Given such a procedure to compute $U^* = (U^{0,*}, \dots, U^{N-1,*})$, we next present a result to derive $u^* = (u^{0,*}, \dots, u^{N-1,*})$, i.e., control actions for the cascading failure dynamics in (4)-(5) over the unaggregated state space. However, since the set of feasible control action sequences \mathcal{D} is not necessarily closed (cf. Remark 2(ii)), finding u^* whose cost is *exactly* the same as that of U^* may not be possible. It is however possible to find u^* whose cost is arbitrarily close to that of U^* .

Proposition 4: For a network with initial state (\mathcal{E}^0, p^0) , link weights $w \in \mathbf{R}_{\geq 0}^{\mathcal{E}^0}$, and link capacities $c \in \mathbf{R}_{\geq 0}^{\mathcal{E}^0}$, consider $\mathbb{J}_N(\mathcal{E}^0, \{p^0\})$ computed by (25). For every $\epsilon > 0$, there exists $\tilde{u} \in \mathcal{D}$ such that $\mathbb{J}_N(\mathcal{E}^0, \{p^0\}) \geq s^T \tilde{u}^{N-1} \geq \mathbb{J}_N(\mathcal{E}^0, \{p^0\}) - \epsilon$.

Proof: For brevity, in this proof, we let $\mathbb{J}_N(\mathcal{E}^0, \{p^0\}) \equiv \mathbb{J}_N(\mathcal{E}^0, p^0)$. Theorem 1 implies that $\mathbb{J}_N(\mathcal{E}^0, p^0) = J_N(\mathcal{E}^0, p^0) \geq s^T u^{N-1}$ for all $u \in \mathcal{D}$. Therefore, we only prove the second inequality.

Let U^* be an optimal aggregated control sequence associated with computing $\mathbb{J}_N(\mathcal{E}^0, p^0)$ in (25), and let \mathcal{E}^* be the induced active link set sequence (recall $U^{N-1,*} = U(\mathcal{E}^{N-1,*}, U^{N-2,*}, \mathbf{0})$). Let $u^{N-1,*}$ be a maximizer to (25a) for $\mathbb{J}_1(\mathcal{E}^{N-1,*}, U^{N-2,*})$. Then, $u^{N-1,*} \in \text{cl}(U^{N-1,*})$ and $\mathbb{J}_N(\mathcal{E}^0, p^0) = s^T u^{N-1,*}$. We now show that, for arbitrary $\epsilon > 0$, there exists $\tilde{u} \in \mathcal{D}$ such that $s^T \tilde{u}^{N-1} \geq s^T u^{N-1,*} - \epsilon$.

Let $M(u, \epsilon)$ be the open ball centered at $u \in \mathbf{R}^{\mathcal{V}}$ with radius ϵ . Since $u^{N-1,*} \in \text{cl}(U^{N-1,*})$, $U^{N-1,*} \cap M(u^{N-1,*}, \epsilon/|\mathcal{V}_l|) \neq \emptyset$ for every $\epsilon > 0$. It is then possible to pick $\tilde{u}^{N-1} \in U^{N-1,*} \cap M(u^{N-1,*}, \epsilon/|\mathcal{V}_l|)$ such that $\tilde{u}^{N-1} \neq u^{N-1,*}$ and $s^T \tilde{u}^{N-1} > s^T u^{N-1,*} - \epsilon$. It is now sufficient to show that there exist $\tilde{u}^0, \tilde{u}^1, \dots, \tilde{u}^{N-2}$ such that $\tilde{u}^{t+1} \in \text{cube } \tilde{u}^t$ and $\tilde{u}^t \in U^{t,*}$ for all $0 \leq t \leq N-2$. We provide details for \tilde{u}^{N-2} ; the reasoning for $\tilde{u}^{N-3}, \dots, \tilde{u}^0$ follows along the same lines.

Since $u^{N-1,*} \in U(\mathcal{E}^{N-1,*}, \text{cl}(U^{N-2,*}))$, there exists $u^{N-2,*} \in \text{cl}(U^{N-2,*})$ such that $u^{N-1,*} \in \text{cube } u^{N-2,*}$. Hence, we can pick $\tilde{u}^{N-2} \in U^{N-2,*} \cap M(u^{N-2,*}, \|u^{N-1,*} - \tilde{u}^{N-1}\|_2)$ so that $\tilde{u}^{N-2} \neq u^{N-2,*}$ and $\tilde{u}^{N-1} \in \text{cube } \tilde{u}^{N-2}$, where the special choice of $\tilde{u}^{N-1} \neq u^{N-1,*}$ ensures that $M(u^{N-2,*}, \|u^{N-1,*} - \tilde{u}^{N-1}\|_2)$ has positive radius. ■

Proposition 4 implies that, in order to find u^* , it is sufficient to solve for U^* and $u^{N-1,*}$ from (25). Because the value of $\mathbb{J}_1(\mathcal{E}, P)$ depends only on $\text{cl}(P)$ in (25a), the value of $J_t(\mathcal{E}, P)$ depends only on $\text{cl}(U)$ and $\text{cl}(P)$ in (25b) for every $t \geq 2$. Therefore, in order to find U^* , for sake of numerical implementation, we use $(\mathcal{E}, \text{cl}(P))$ and $\text{cl}(U)$ in place of (\mathcal{E}, P) and U , without introducing error in computation of U^* . Equivalently, we use the following variant of (24):

$$\begin{aligned} U(\mathcal{E}, P, \beta) := \{u \in U(\mathcal{E}, P) \mid f_i(\mathcal{E}, u) \leq -c_i \text{ if } \beta_i = -1; -c_i \leq f_i(\mathcal{E}, u) \leq c_i \text{ if } \beta_i = 0; \\ f_i(\mathcal{E}, u) \geq c_i \text{ if } \beta_i = 1; \forall i \in \mathcal{E}\} \end{aligned} \quad (26)$$

Therefore, without stating explicitly, hereafter we use (26) in place of (24). In order to find $u^{N-1,*}$, the next result implies that (25a) is a linear program by showing that, for every (\mathcal{E}, P) , the set $U(\mathcal{E}, P)$ is a polytope.

Lemma 7: Consider a network with initial state (\mathcal{E}^0, p^0) , link weights $w \in \mathbf{R}_{\geq 0}^{\mathcal{E}^0}$ and link capacities $c \in \mathbf{R}_{\geq 0}^{\mathcal{E}^0}$. For every aggregated state (\mathcal{E}^t, P^t) , $t \in [N] \cup \{0\}$, induced by the consistent partition in (23) and (26), both P^t and $U(\mathcal{E}^t, P^t)$ are polytopes.

Proof: The claim is proved by induction. It is easy to see that $P^0 = \{p^0\}$ and $U(\mathcal{E}^0, P^0) = U(\mathcal{E}^0, p^0)$ are polytopes. Suppose P^t and $U(\mathcal{E}^t, P^t)$ are polytopes for some $t \in [N-1] \cup \{0\}$. It is sufficient to show that, for arbitrary aggregated control action $U \in \mathbb{U}(\mathcal{E}^t, P^t)$, the resulting P^{t+1} and $U(\mathcal{E}^{t+1}, P^{t+1})$ are polytopes. $P^{t+1} = U^t = U(\mathcal{E}^t, P^t, \beta)$ for some $\beta \in \{-1, 0, +1\}^{\mathcal{E}^t}$ (cf. (23)-(24)). Combining this with the induction assumption that $U(\mathcal{E}^t, P^t)$ is a polytope, we get that P^{t+1} is a polytope. It follows from the definition in (20) that $U(\mathcal{E}^{t+1}, P^{t+1})$ is a polytope as well. ■

Remark 16: Combined with the definition of cube P , the proof of Lemma 7 also implies that both P and $U(\mathcal{E}, P)$ are contained in a closed orthant of $\mathbf{R}^{\mathcal{V}_l}$ for every (\mathcal{E}, P) .

C. Efficient Aggregated Tree Search

With (21) and (23) specifying how to expand nodes of aggregated network state and (25) directing the goal of search, one can then employ any classical tree search algorithm, e.g., the ones in [18, Chap 3], to solve the problem. However, we would like to make the following remarks. Firstly, the following relationship can be used for tree pruning in a standard branch and bound algorithm framework.

$$J_1(\mathcal{E}, P) \leq J_t(\mathcal{E}, P) \leq \max_{p \in \text{cl}(P)} s^T p \quad \forall (\mathcal{E}, P), \forall t \in [N]$$

Secondly, iterative deepening depth-first search algorithm presents several advantages for the optimal control problem. On one hand, it achieve a good balance between running time and memory consumption. This is of particular importance because, as would shown in Section VI-A, the number of aggregated states in the optimal

control problem can be enormous. On the other hand, the search can be stopped anytime in the process of computation while producing a feasible control action with reasonable performance. In fact, the search over the first $t < N$ layer provides an optimal t -stage load shedding scheme. At the same time, the upper bound provides an estimate of performance gap from the optimal value when search is terminated early.

Finally, while the detailed search algorithm including pruning is standard and omitted here, its implementation with set objects, that are, the aggregated control action $U \in \mathbb{U}(\mathcal{E}, P)$ and the set $U(\mathcal{E}, P)$, required additional tools. Section V is devoted to address the problem.

V. COMPUTING AGGREGATION THROUGH ARRANGEMENT OF HYPERPLANES

The numerical implementation of (25) relies critically on proper representation of the set of feasible aggregated control actions $U(\mathcal{E}, P)$ and its partition $\mathbb{U}(\mathcal{E}, P)$. While Lemma 7 characterizes an important property of these objects, in this section, we provide an algorithmic procedure for their representation. Our machinery relies on and extends tools from the domain of *arrangement of hyperplanes* e.g., see [9] [10, Chapter 24], and *convex polytopes*, e.g., see [11] [12].

A. Arrangement of Hyperplanes, Polytope and Incidence Graph

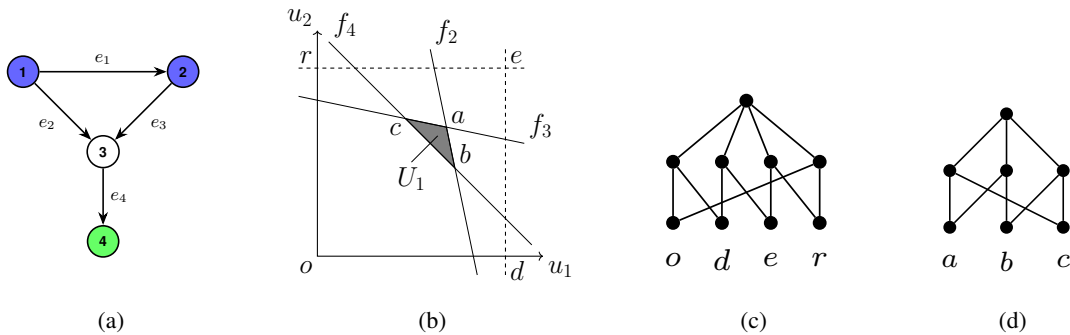


Fig. 11: (a) A network $(\mathcal{V}, \mathcal{E}^0)$ with $\mathcal{V}_s = \{1, 2\}$, $\mathcal{V}_d = \{4\}$, $w = \mathbf{1}$, $c = [10, 2, 2, 3]^T$, $p^0 = [-4, -4, 0, 8]^T$; (b) Projection of $U(\mathcal{E}^0, p^0)$ and $\{u \in \mathcal{B}_{\mathcal{E}} \mid f_i(\mathcal{E}^0, u) = c_i\}$, $i \in \{2, 3, 4\}$, on $u_1 - u_2$ plane; (c) Incidence graph of $U(\mathcal{E}^0, p^0)$; (d) incidence graph of U_1 .

We start with the simple illustrative example shown in Fig. 11a. Referring to (7), there are three non-trivial components of p^0 . Taking into account the additional constraint imposed by $\mathcal{B}_{\mathcal{E}}$, referring to (6), the set of feasible control actions $U(\mathcal{E}^0, p^0)$ can be completely understood in terms of its two dimensional projection, say on the $u_1 - u_2$ plane. In Fig. 11b, the box $oder$ and the point e corresponding to the projections of $U(\mathcal{E}^0, p^0)$ and p^0 respectively. The solid lines labeled by f_2, f_3, f_4 , or (projections of) hyperplanes, correspond to the capacity constraints associated with the three links. The flow capacity constraint for e_1 is ignored here because it is satisfied by all $u \in U(\mathcal{E}^0, p^0)$ and hence irrelevant for the problem. Line f_2, f_3 and f_4 dissect the box $oder$ into seven

pieces. These seven pieces constitute the partition $\mathbb{U}(\mathcal{E}^0, \{p^0\})$. Each piece, e.g., the triangle abc denoted by U_1 , is an aggregated control action, e.g., $U_1 = U(\mathcal{E}^0, p^0, [0, 0, 0, 1]^T)$.

In general, a finite collection \mathcal{H} of hyperplanes in \mathbf{R}^d dissects \mathbf{R}^d into finitely many connected pieces of various dimensions. The collection of these pieces is called the *arrangement*, denoted by $\mathcal{A}(\mathcal{H})$, induced by \mathcal{H} , and each piece is called a *face*, denoted by Γ , of the arrangement⁶. The dimension of a face is the dimension of its affine hull; a k dimensional face is called a k -face, denoted by Γ^k . For convenience, 0-face, 1-face, $(d-2)$ -face, $(d-1)$ -face and d -face are, respectively, referred to as *vertex*, *edge*, *ridge*, *facet* and *cell*. We call two faces *incident* if one is contained in the boundary of the other and if the difference in their dimensions is one. In a pair of incident faces, the lower (or higher) dimensional face is called the *subface* (or *superface*) of the other. In Fig. 11b, the three solid lines (i.e., hyperplanes) dissect box *oder* into seven cells, nine edges (or facets) and three vertices (or ridges). As indicated by this example, in the setting of this paper, for every state (\mathcal{E}, P) , the capacity constraints, balanced condition (captured by $\mathcal{B}_{\mathcal{E}}$), and load shedding requirement (captured by $\text{cube}(P)$) form the collection of hyperplanes. We are interested in the substructure of the arrangement of these hyperplanes inside $U(\mathcal{E}, P)$, since the closure of each facet in this arrangement corresponds to an aggregated control action, and $\mathbb{U}(\mathcal{E}, P)$ corresponds to the collection of these facets⁷.

The closure of a bounded face in the arrangement is a convex polytope, or polytope for short. We use the same letter P , as in the aggregated state, to denote a general polytope for simplicity, because every aggregated state is a polytope, as shown in Lemma 7. Formally, a *polytope* is a point set $P \subset \mathbf{R}^d$ that can be presented either as a convex hull of a finite number of points in \mathbf{R}^d or the bounded intersection of finite number of closed half spaces in \mathbf{R}^d [11]. The same notion of face, as in an arrangement, is used for a polytope $P \subset \mathbf{R}^d$ ⁸ and furthermore, a face of P is can be described as $\Gamma = P \cap \{x \in \mathbf{R}^d \mid \pi^T x = \pi_0\}$, where the linear inequality $\pi^T x \leq \pi_0$ must be satisfied for all $x \in P$, that is, the hyperplane $\{x \in \mathbf{R}^d \mid \pi^T x = \pi_0\}$ must contain P on one of its closed sides. We call $P \subset \mathbf{R}^d$ full dimensional if its dimension is d . For a full dimensional polytope, the affine hull of its facet Γ_i^{d-1} is a hyperplane, denoted by $H_i = \{x \in \mathbf{R}^d \mid (\pi^i)^T x = \pi_0^i\}$ and referred as the *defining hyperplane* of facet Γ_i^{d-1} . As a convention, the direction of π^i for H_i is chosen to point outwards from P . Every k -face Γ^k of P ($k < \dim P$) is the convex hull of exactly $k+1$ vertices and every ridge Γ^{d-2} is contained in exactly two facets [12, Chapter 3].

The geometry of the arrangement of hyperplanes and polytopes is difficult to comprehend, especially in high dimensions. Because of this, they are represented using the *incidence graph* (sometimes called the *facial lattice* or *face lattice*). The incidence graph of an arrangement or a polytope contains the incidence relationship between various faces. It is a layered (undirected) graph whose nodes have a one-to-one correspondence with faces of the

⁶In some literature, *cells* are used to refer to the connected pieces. In that context, *face* is used exclusively for the 2-face. In this paper, we adopt the terminology convention in [9] and use *cell* to denote d -face exclusively in \mathbf{R}^d .

⁷Fig. 11b shows the projection of the arrangement in \mathbf{R}^3 onto the $u_1 - u_2$ plane. Each cell in Fig. 11b is the projection of a facet of the arrangement.

⁸The notion of *face* is slightly different for an arrangement and a polytope. While the former considers a face as an open set, the latter treat a face as as a closed set. This difference does not affect the results in this section and ignored.

arrangement or polytope, and an (undirected) edge exists between two nodes if and only if the corresponding faces are incident. All the nodes corresponding to faces of the same dimension constitute a layer. We place the layer corresponding to vertices at the bottom, and the layer corresponding to cells on the top.

For example, Fig. 11c shows the incidence graph of the polytope *oder* (or action set $U(\mathcal{E}^0, p^0)$). The single node at the top layer corresponds to *oder* itself, the four nodes in the middle layer correspond to the four edges *or*, *re*, *ed* and *do*, and the four nodes in the bottom layer correspond to the four vertices *o*, *r*, *e* and *d*. The edges between these layers correspond to the incidence relation between the faces, as shown in Figure 11b. Similarly, 11d shows the incidence graph of the polytope *acb* (or aggregated control action U_1).

Furthermore, we have the following remark on the auxiliary information required for storing the incidence graph of an arrangement or a polytope.

Remark 17: When implemented, the incidence graph is usually associated with some auxiliary information that enables numerical algorithms with geometric operations such as determining if a hyperplane intersecting with a face and finding the intersection of hyperplane and edge. Details of this can be found in textbooks, e.g., [22] and [9]. While other choice of auxiliary information is possible, what we use in this paper includes the following: the analytical expression of hyperplanes, coordinate of vertices and the mean of the coordinates of all contained vertices of a face. We shall not explicitly mention these auxiliary information hereafter.

B. On Construction of the Incidence Graph of $U(\mathcal{E}, P)$ and $\mathbb{U}(\mathcal{E}, P)$

We recall from Section IV-C that the implementation of (25) relies on an efficient procedure to construct representation of the one-time aggregated reachable set from an arbitrary aggregated state (\mathcal{E}, P) . It is sufficient to get such a representation for $U(\mathcal{E}, P)$, and its partition $\mathbb{U}(\mathcal{E}, P)$ consisting of aggregated control actions. Ideally, such a representation for $U(\mathcal{E}, P)$ and $\mathbb{U}(\mathcal{E}, P)$ should build upon the representation for P . With regards to $U(\mathcal{E}, P)$, it is sufficient to focus on cube P , since $U(\mathcal{E}, P)$ is the intersection of cube P with hyperplanes corresponding to $\mathcal{B}_{\mathcal{E}}$ (cf. (20)). Upon constructing the incidence graph of cube P , one can add hyperplanes corresponding to balance conditions to get the arrangement for $U(\mathcal{E}, P)$. The incidence graph of the arrangement, associated with $\mathbb{U}(\mathcal{E}, P)$, is then obtained by adding to the incidence graph of $U(\mathcal{E}, P)$, one by one, the hyperplanes corresponding to the flow capacity constraints while maintaining the representation of arrangement of the objects added so far. The key step for updating the incidence graph after adding a hyperplane is adopted from the well-known algorithm in [23] and [9, Chapter 7] for constructing arrangement of an arbitrary set \mathcal{H} of hyperplanes in \mathbf{R}^d . Therefore, in this paper, we focus our efforts on constructing the incidence graph of cube P , given the incidence graph of P , and implicitly assume that one can adopt the standard algorithm to complete the construction of incidence graph of $U(\mathcal{E}, P)$, and then the arrangement associated with $\mathbb{U}(\mathcal{E}, P)$. Thereafter, the aggregated tree search in Section IV-C can be implemented by constructing alternatively the incidence graphs of $U(\mathcal{E}, P)$ and $\mathbb{U}(\mathcal{E}, P)$ throughout the search process.

Remark 18:

- (1) This algorithm in [23] and [9, Chapter 7] has optimal time complexity $\Theta(|\mathcal{H}|^d)$ for constructing a general positioned arrangement in \mathbf{R}^d . If the arrangement is contained in a k dimensional affine space, the time complexity is $O(|\mathcal{H}|^{d-k})$. Note for a connected network with active link set \mathcal{E} , $U(\mathcal{E}, P)$ is contained in the $|\mathcal{V}_l| - 1$ dimensional affine space $\mathcal{B}_{\mathcal{E}} \cap \{p \in \mathbf{R}^{\mathcal{V}} \mid p_i = 0, \forall i \in \mathcal{V} \setminus \mathcal{V}_l\}$.
- (2) For a network with single supply and single demand, the hyperplanes are single points and control actions are associated with line intervals that can be represented using two real numbers. The relevant incidence graph at a state (\mathcal{E}, P) can be computed in linear time with respect to the number of infeasible links. Furthermore, in this case $\text{cube}(P)$ can be computed in constant time: for $P = (p^l, p^u)$, $\text{cube}(P) = [0, p^u]$ if $p^u \geq 0$ and $\text{cube}(P) = [p^l, 0]$ if $p^l \leq 0$.
- (3) The set $\tilde{\mathcal{D}}_i$ used in (15) and (16) can be obtained similarly except that $U(\mathcal{E}, P)$ needs to be replaced with the interval from origin to the minimum cut capacity of subnetwork \mathcal{G}_i , at the step of constructing the incidence graph of $U(\mathcal{E}, P)$ (also see Remark 9).
- (4) The restricted set of $\tilde{\mathcal{D}}_i$ for constant control used in Section III-C is obtained in the same way as that for $\tilde{\mathcal{D}}_i$. The difference is that $U(\mathcal{E}, P)$ is to be replaced with interval P .

C. Constructing the Incidence Graph of $\text{cube } P$ from the Incidence Graph of P

Remark 16 implies that it is sufficient to focus on $P \in \mathbf{R}_{\geq 0}^d$. We first consider $\text{cube } p^0$ for $p^0 \in \mathbf{R}_{\geq 0}^d$. Since the dimensions corresponding to $p_i^0 = 0$ can be ignored, we assume $p^0 \in \mathbf{R}_{> 0}^d$ without loss of generality. In this case, $\text{cube } p^0 \subset \mathbf{R}_{\geq 0}^d$ is a hypercube and its incidence graph can be obtained straightforwardly by Lemma 8, whose proof is omitted. Fig. 11c shows an example in \mathbf{R}^2 .

Lemma 8: For $p^0 \in \mathbf{R}_{> 0}^d$, let $\alpha : \text{cube } p^0 \rightarrow \{-1, 0, 1\}^d$ be defined as: $\alpha_i(x) = -1$ if $x_i = 0$, $\alpha_i(x) = 0$ if $x_i \in (0, p_i^0)$, and $\alpha_i(x) = 1$ if $x_i = p_i^0$. Then,

- (i) every $\tilde{\alpha} \in \{-1, 0, 1\}^d$ is associated with a $(d - |\tilde{\alpha}|_1)$ -face $\Gamma(\tilde{\alpha}) := \text{cl}(\{x \in \text{cube } p^0 \mid \alpha(x) = \tilde{\alpha}\})$ of $\text{cube } p^0$;
- (ii) two faces $\Gamma(\alpha^1)$ and $\Gamma(\alpha^2)$ of $\text{cube } p^0$ are incident if α^1 and α^2 are equal except for one component which equals zero in one among α^1 and α^2 .

Remark 19: Lemma 8 (i) describes a procedure to enumerate all the nodes in the incidence graph of $\text{cube } p^0$, in terms of all vectors in $\{-1, 0, 1\}^d$, whereas (ii) specifies how to add edges to the incidence graph.

For a general polytope $P \subset \mathbf{R}_{\geq 0}^d$, we present a sequential procedure to construct the incidence graph of $\text{cube } P$ from that of P . For this purpose, we define the *projection* and *sweep* of a polytope $P \subset \mathbf{R}_{\geq 0}^d$ in direction \mathbf{e}_k , $k \in [d]$:

$$\text{proj}_k(P) := \{p - p_k \mathbf{e}_k \mid p \in P\} \quad (27)$$

$$\text{sweep}_k(P) := \{p - \theta_k p_k \mathbf{e}_k \mid p \in P, \theta_k \in [0, 1]\} \quad (28)$$

It is straightforward that $P \subseteq \text{sweep}_k(P)$ and $\text{proj}_k P \subseteq \text{sweep}_k(P)$. In fact, $\text{sweep}_k(P)$ is the trace of P projecting to $\text{proj}_k P$ in the direction of \mathbf{e}_k and therefore, it is also a polytope in $\mathbf{R}_{\geq 0}^d$. One can again apply sweep on $\text{sweep}_k(P)$

along \mathbf{e}_i for some $i \neq k$ and get $\text{sweep}_i(\text{sweep}_k(P)) = \{p - \theta_1 p_k \mathbf{e}_k - \theta_2 p_i \mathbf{e}_i \mid p \in P, (\theta_1, \theta_2) \in [0, 1]^2\}$. This motivates us to define sweep for an index set $I \subseteq [d]$ as

$$\text{sweep}_I(P) := \left\{ p - \sum_{k \in I} \theta_k p_k \mathbf{e}_k \mid p \in P, \theta_k \in [0, 1] \forall k \in I \right\}$$

Similarly, $\text{proj}_I(P) := \{p - \sum_{k \in I} p_k \mathbf{e}_k \mid p \in P\}$. With this definition, $\text{sweep}_{\emptyset}(P) = P$ and $\text{sweep}_{[d]}(P) = \text{cube } P$. $\text{sweep}_{[d]}(P)$ can be obtained by recursively applying sweep on P , e.g.,

$$\text{sweep}_{[d]}(P) = \text{sweep}_1(\text{sweep}_2(\dots \text{sweep}_d(P)))$$

Therefore, in order to obtain cube P , it is sufficient to focus on constructing $\text{sweep}_k(P)$ from P for a given $k \in [d]$.

Let $\bar{H} := \{x \in \mathbf{R}^d \mid x_k = 0\}$ and $\bar{H}^+ := \{x \in \mathbf{R}^d \mid x_k \geq 0\}$.⁹ For a given polytope $P \subset \bar{H}^+$ and $k \in [d]$, $\text{sweep}_k(P)$ relates to projection between two affine spaces: $\text{aff } P \subset \mathbf{R}^d$ and $\text{aff } \text{proj}_k P \subset \bar{H}$. We differentiate between the following two scenarios based on the difference in dimensions of these two affines spaces: (I) $\dim P = \dim(\text{proj}_k P)$; and (II) $\dim P = \dim(\text{proj}_k P) + 1$. Scenario I occurs when $P \subset H := \{x \in \mathbf{R}^d \mid \pi^\top x = \pi_0\}$ with $\pi_k \neq 0$, i.e., when H is not perpendicular to \bar{H} . In this case, there is a one-to-one correspondence between the points in P and $\text{proj}_k P$. On the other hand, scenario II occurs when either $\dim P = d$, or every hyperplane containing P is orthogonal to \bar{H} . The two scenarios are illustrated in Figure 12 for \mathbf{R}^2 and $k = 1$.

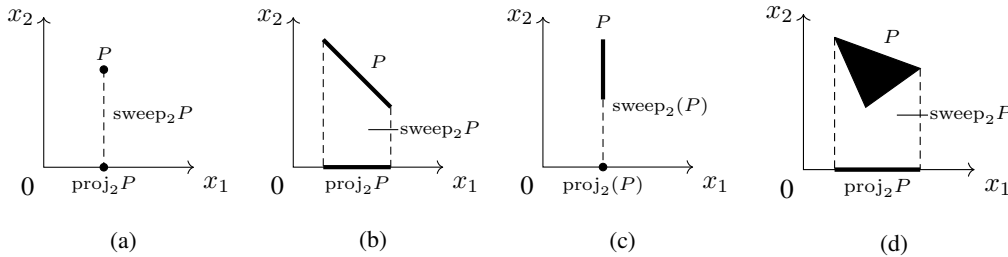


Fig. 12: Two possible scenarios for projection: (a) and (b) show the projection onto a space of the same dimension; and (c) and (d) show projection onto a space of lower dimension.

Scenario I

In this scenario, $\text{proj}_k(P)$ is *affinely isomorphic*¹⁰ to P . Therefore, its the incidence graph is identical to that of P . The following results relates the incidence graph of $\text{sweep}_k(P)$ to that of P and $\text{proj}_k(P)$.

Proposition 5: Consider an n dimensional polytope $P \subset \{x \in \mathbf{R}^d \mid x_k > 0\}$, $0 \leq n \leq d - 1$. If there exists a hyperplane containing P which is not perpendicular to \bar{H} , then: (i) $\text{sweep}_k(P)$ is an $(n + 1)$ dimensional polytope; (ii) an l -face of $\text{sweep}_k(P)$ is either a l -face of P or of $\text{proj}_k P$, or it is $\text{sweep}_k \Gamma^{l-1}$ for some $(l - 1)$ -face Γ^{l-1}

⁹We do not show subscript k for brevity in notation.

¹⁰Two polytopes $P_1 \subseteq \mathbf{R}^{d_1}$ and $P_2 \subseteq \mathbf{R}^{d_2}$ are *affinely isomorphic* to each other if there exists an affine and bijection map between them.

of P ; and (iii) each face of P and of $\text{proj}_k P$ is a face of $\text{sweep}_k(P)$, and $\text{sweep}_k \Gamma$ is a face of $\text{sweep}_k P$ for every face Γ of P .

Proof: Let $\hat{\gamma} := 1.2 \max_{x \in P} x_k$. Since P is contained in a hyperplane that is not perpendicular to \bar{H} , the line segment $[0, \hat{\gamma} \mathbf{e}_k]$ is not parallel to $\text{aff } P$. Let $\hat{P} := P - [0, \hat{\gamma} \mathbf{e}_k]$. We have the following facts on \hat{P} [12, Chapter 4.4]: \hat{P} is an $(n + 1)$ dimensional polytope; an l -face of \hat{P} is either a l -face of P or of $P - \{\hat{\gamma} \mathbf{e}_k\}$, or it is the vector-sum of $-\{\hat{\gamma} \mathbf{e}_k\}$ with some $(l - 1)$ -face of P ; each face of P and of $P - \{\hat{\gamma} \mathbf{e}_k\}$ is a face of \hat{P} and the vector-sum of $-\{\hat{\gamma} \mathbf{e}_k\}$ with any face of P is a face of \hat{P} .

It is then sufficient to show that $\text{sweep}_k P$ and \hat{P} are combinatorial isomorphic¹¹. By definition, $\text{sweep}_k(P) = \hat{P} \cap \bar{H}^+$. The facets of \hat{P} include $P \subset \bar{H}^+$, $P - [0, \hat{\gamma} \mathbf{e}_k] \subset \bar{H}^- := \{x \in \mathbf{R}^d \mid x_k < 0\}$ and $\Gamma^{n-1} - [0, \hat{\gamma} \mathbf{e}_k]$ for all ridge Γ^{n-1} of P . The facet $\Gamma^{n-1} - [0, \hat{\gamma} \mathbf{e}_k]$ is orthogonal to and intersects with \bar{H} on $\text{proj}_k \Gamma^{n-1}$ for every ridge Γ^{n-1} of P . It is then straightforward to see that $\text{sweep}_k(P)$ and \hat{P} are combinatorial isomorphic, with facet P of $\text{sweep}_k P$ corresponding to facet P of \hat{P} , facet $P - \{\hat{\gamma} \mathbf{e}_k\}$ corresponding to $\text{proj}_k(P)$, and $\Gamma^{l-1} - \{\hat{\gamma} \mathbf{e}_k\}$ corresponding to $\text{proj}_k(\Gamma^{n-1})$ for all ridges Γ^{n-1} of P . ■

Remark 20: For $P \subset \bar{H}$, it is straightforward that $\text{sweep}_k(P) = P = \text{proj}_k(P)$. For $P \not\subset \bar{H}$ and $P \subset \bar{H}^+$, one can consider a disturbed version \tilde{P} of P such that $\tilde{P} \subset \{x \in \mathbf{R}^d \mid x_k > 0\}$ and employ Proposition 5 to obtain the incidence graph of \tilde{P} . The incidence graph of P can then be obtained by merging the “close” faces (within disturbances) of \tilde{P} while keeping their incidence relationships.

Example 4 illustrates how to use Proposition 5 to obtain the incidence graph of $\text{sweep}_k(P)$ in \mathbf{R}^2 .

Example 4: Consider the polytope P corresponding to the line segment between points a and b in Figure 13a. The figure also shows the corresponding \hat{P} , $\text{proj}_2(P)$ and $\text{sweep}_2(P)$. The subgraph shown in solid black in Figure 13b is the incidence graph of P , whereas the subgraph shown in gray, which is identical to the solid black one, is the incidence graph of \hat{P} , where $a' = \text{proj}_2(a)$, $b' = \text{proj}_2(b)$. The incidence graph of $\text{sweep}_2(P)$ is constructed from Proposition 5 as follows:

- 1) $\text{sweep}_2(P)$ is a two dimensional polytope;
- 2) The vertices (0-faces) of $\text{sweep}_2(P)$ contain only the vertices of P , that are a and b , and the vertices of $\text{proj}_2(P)$, that are a' and b' ;
- 3) The edges (1-faces) of P contain both the edge of P , that is ab , the edge of $\text{proj}_2(P)$, that is $a'b'$, and the edges formed by sweep of vertices, that are aa' and bb' ;
- 4) Edges aa' and bb' are incident to a , a' and b , b' , respectively, because the edges, as a results of sweeping, contain the corresponding vertices and their dimensions differ by 1;
- 5) $\text{sweep}_2(P)$ contains itself as a 2-face and is incident to all the edges, due to the same reason.

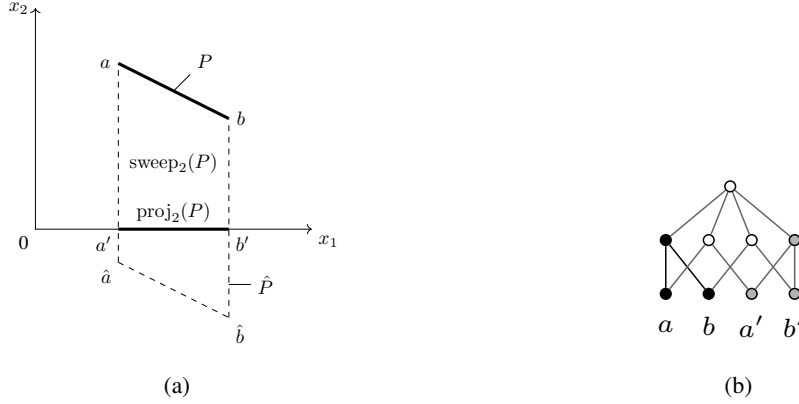


Fig. 13: Illustration of sweep in scenario I: (a) the geometrical graph; and (b) the incidence graph.

Scenario II

For the second scenario, we first identify the faces of P that do play roles in the projection and then resort to Proposition 5 for construction of $\text{sweep}_k(P)$. It is sufficient to consider $P \subset \mathbf{R}_{\geq 0}^d$ to be full dimensional, that is, $\dim P = d$. One can work in the affine space aff P otherwise and the same results hold. Let Γ_i^{d-1} be a facet of $P \subset \bar{H}^+$ and $H_i = \{x \in \mathbf{R}^d \mid (\pi^i)^\top x = \pi_0^i\}$ be its defining hyperplane; recall that the direction of π^i is pointed outwards the polytope. A direction vector $\mu \in \mathbf{R}^d$ classifies the facets of P into three types [24] according to the value of $\mu^\top \pi^i$: μ -facet for $\mu^\top \pi^i = 0$, μ -bottom for $\mu^\top \pi^i < 0$ and μ -top for $\mu^\top \pi^i > 0$. With this definition, a facet Γ^i belongs to \mathbf{e}_k -top if $\pi_k^i > 0$, \mathbf{e}_k -facet if $\pi_k^i = 0$ and \mathbf{e}_k -bottom if $\pi_k^i < 0$. This is illustrated in Figure 14.

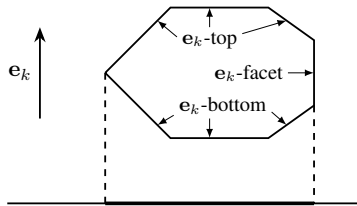


Fig. 14: Different facets according to the direction \mathbf{e}_k

The \mathbf{e}_k -top and \mathbf{e}_k -bottom facets can be described as the facets that are “visible from the direction $-\mathbf{e}_k$ ” and “visible from the direction \mathbf{e}_k ”, respectively. For the projection concerned in $\text{sweep}_k(P)$, only points in \mathbf{e}_k -top play a role. This is straightforward to see in \mathbf{R}^2 and \mathbf{R}^3 . For example, in Fig. 12c and 12c, the top vertex of the vertical edge and the top edge of the triangular face shade all other points and fully determines the sweeps. In general, Proposition 6 shows the same is true for \mathbf{R}^d , where we say point $x \in \mathbf{R}^d$ is shaded by point $\hat{x} \in \mathbf{R}^d$ in direction

¹¹Two polytopes P_1 and P_2 are *combinatorial isomorphic* to each other if there exists a one-to-one correspondence φ between the set of faces in P_1 and the set of faces in P_2 , such that φ is inclusion-preserving, i.e., for two faces Γ_1 and Γ_2 of P_1 , $\Gamma_1 \subset \Gamma_2$ if and only if $\varphi(\Gamma_1) \subset \varphi(\Gamma_2)$.

\mathbf{e}_k if $\hat{x}_k \geq x_k$ and $\hat{x}_i = x_i$ for all $i \in [d] \setminus \{k\}$. It is clear from the definition that a point plays no role in the projection along \mathbf{e}_k if it is shaded by another point of P in \mathbf{e}_k . The ridges in \mathbf{e}_k -top of P falls into two types: one in the intersection between a \mathbf{e}_k -top facet and a \mathbf{e}_k -bottom facet or \mathbf{e}_k -facet and one in the intersection between two \mathbf{e}_k -top facets. Proposition 6 implies that the first type of ridges determines the boundary of $\text{sweep}_k(P)$. They are hence called *boundary ridges* of P in direction \mathbf{e}_k .

The following lemma, which is also referred to as the geometric version of Farkas Lemma [25], will be used in the next result.

Lemma 9 ([11, Sect. 1.4]): Consider a full dimensional polytope $P \subset \mathbf{R}^d$ with facets Γ_i^{d-1} whose defining hyperplanes are $H_i := \{x \in \mathbf{R}^d \mid (\pi^i)^\top x = \pi_0^i\}$, and let $\Gamma \subset \cap_{i \in S} \Gamma_i^{d-1}$ be a nonempty face of P for some index set S . Then, $\Gamma = \text{argmax}_{x \in P} \mu^\top x$ for some $\mu \in \mathbf{R}^d$ if and only there exists $\theta \in \mathbf{R}_{>0}^S$ such that $\mu = \sum_{i \in S} \theta_i \pi^i$.

Proposition 6: For a full dimensional polytope $P \subset \bar{H}^+$ and $k \in [d]$, the following are true:

- (i) every point in P is shaded in direction \mathbf{e}_k by a point in a \mathbf{e}_k -top facet of P ;
- (ii) every \mathbf{e}_k -top facet is a facet of $\text{sweep}_k(P)$; and
- (iii) for a ridge Γ^{d-2} of P , $\text{sweep}_k(\Gamma^{d-2})$ is a facet of $\text{sweep}_k(P)$ if and only if Γ^{d-2} is a boundary ridge and $\Gamma^{d-2} \not\subseteq \bar{H}$.

Proof: For each point $x \in P$, let $\tau(x) := \text{argmax}_{\hat{x}} \{\hat{x}_k \mid \hat{x}_j = x_j, \forall j \neq k; \hat{x} \in P\}$, and let $P^t := \cup_{x \in P} \{\tau(x)\}$. It follows from the definition that every $x \in P$ is shaded by $\tau(x) \in P^t$ in direction \mathbf{e}_k . We now show that P^t is included in the \mathbf{e}_k -top facets of P . For each point $\tilde{x} \in P^t$, $P \cap (\{\tilde{x}\} + (0, +\infty)\mathbf{e}_k) = \emptyset$, where the set $\{\tilde{x}\} + (0, +\infty)\mathbf{e}_k$ is the half open ray starting from \tilde{x} and pointing in the \mathbf{e}_k direction. The separating hyperplane theorem, e.g., see [26], then implies that there exist $\mu \in \mathbf{R}^d$ and $\mu_0 \in \mathbf{R}$ such that $\mu^\top x \leq \mu_0$ for all $x \in P$ and $\mu^\top x > \mu_0$ for all $x \in \{\tilde{x}\} + (0, +\infty)\mathbf{e}_k$. In order for the latter to hold, it must hold that $\mu_k = \mu^\top \mathbf{e}_k > 0$.

We now show that \tilde{x} is included in a \mathbf{e}_k -top facet of P . If \tilde{x} is in the interior of some facet Γ_i^{d-1} , then, since H_i is the unique separating hyperplane, we get $\pi_k^i > 0$. Hence Γ_i^{d-1} is a \mathbf{e}_k -top facet. If x is in a lower dimensional face, then consider a non-empty set \mathcal{J} such that $x \in \cap_{i \in \mathcal{J}} \Gamma_i$. By contradiction, from Lemma 9, there exists a $j \in \mathcal{J}$ such that $\pi_k^j > 0$. This implies that \tilde{x} belongs to the facet Γ_j^{d-1} , a \mathbf{e}_k -top facet. This establishes (i).

For (ii), pick an arbitrary point \hat{x} from an arbitrary \mathbf{e}_k -top facet Γ_i^{d-1} . By definition of a facet, $\hat{x} \in \text{argmax}_{x \in P} (\pi^i)^\top x$. This implies that $\tau(\hat{x}) = \hat{x}$, i.e., $\hat{x} \in P^t$. It is then straightforward to see that Γ_i^{d-1} remains to be a facet in $\text{sweep}_k(P)$, since the hyperplane H_i contains $\text{sweep}_k(P)$ on one side.

We now prove (iii). Let $\Gamma^{d-2} \not\subseteq \bar{H}$ be an arbitrary ridge of P and Γ_i^{d-1} and Γ_j^{d-1} be the two incident facets of Γ^{d-2} . We first prove the conditions to be necessary by considering the following cases:

- (a) If $\Gamma^{d-2} \subset \bar{H}$, then $\text{sweep}_k(\Gamma^{d-2}) = \Gamma^{d-2}$ is of dimension $(d-2)$ and it is trivial that $\text{sweep}_k(\Gamma^{d-2})$ is not a facet of $\text{sweep}_k(P)$.
- (b) If neither Γ_i^{d-1} and Γ_j^{d-1} are \mathbf{e}_k -top facets, all points in Γ^{d-2} are shaded by some other points in P and $\text{sweep}_k(\Gamma^{d-2})$ is not a facet of $\text{sweep}_k(P)$.

(c) If both Γ_i^{d-1} and Γ_j^{d-1} are \mathbf{e}_k -top facets. As shown in previous paragraph, both Γ_i^{d-1} and Γ_j^{d-1} remains to be facets of $\text{sweep}_k(P)$. Because a ridge is contained in exactly two facets, $\text{sweep}_k(\Gamma^{d-2})$ can not be a facet of $\text{sweep}_k(P)$.

We then prove the condition is sufficient. Let Γ^{d-2} be a boundary ridge and, without loss of generality, Γ_i^{d-1} be the \mathbf{e}_k -top facet and Γ_j^{d-1} be either a \mathbf{e}_k -facet or a \mathbf{e}_k -bottom facet. Hence $\pi_k^i > 0$ and $\pi_k^j \leq 0$. Proposition 5 implies that $\text{sweep}_k(\Gamma^{d-2})$ is of dimension $(d-1)$. Therefore, $\text{sweep}_k(\Gamma^{d-2})$ is a facet if it is a face of $\text{sweep}_k(P)$. We now construct the defining hyperplane H of $\text{sweep}_k(\Gamma^{d-2})$. Let $\theta := \pi_k^i / (\pi_k^i - \pi_k^j) \in (0, 1]$, $\pi := (1-\theta)\pi^i + \theta\pi^j$ and $\pi_0 := (1-\theta)\pi_0^i + \theta\pi_0^j$. It is straightforward that $\pi_k = 0$. Define $H := \{x \in \mathbf{R}^d \mid \pi^\top x = \pi_0\}$. It is sufficient to show that $\text{sweep}_k(\Gamma^{d-2}) \subset H$ and H contains $\text{sweep}_k(P)$ on one side. Since $\pi_k = 0$, $\Gamma^{d-2} \subset H$ if and only if $\text{sweep}_k(\Gamma^{d-2}) \subset H$. The latter is straightforward from the definition of H . In order to show that H contains $\text{sweep}_k(P)$ on one side, we consider the following two cases. In the first case, $u_k^j < 0$ and hence $\theta \in (0, 1)$. Lemma 9 implies the claim. In the second case, $u_k^j = 0$ and hence $\theta = 1$. $H = H_j$, that is, the defining hyperplane of Γ_j^{d-1} . The claim follows trivially. ■

With Proposition 5 and Proposition 6, cube P of a full dimensional polytope $P \subset \mathbf{R}_{\geq 0}^d$ can be constructed as follows: set $k = 1$; while $k \leq d$, do the following:

- (I) find \mathbf{e}_k -top facets of P and remove all faces of P that are not contained in any one of them;
- (II) find the boundary ridges and construct their sweep along \mathbf{e}_k according to Proposition 5 and Remark 20;
- (III) add a facet in \bar{H} that is incident to the projections of all boundary ridges along \mathbf{e}_k and a cell, corresponding to $\text{sweep}_k(P)$, that is incident to all the facets;
- (IV) set $P = \text{sweep}_k(P)$, $k = k + 1$, and repeat;

where the second step is possible because every boundary ridge belongs to a \mathbf{e}_k -top facet that is not perpendicular to \bar{H} . The above four-step procedure is illustrated in Example 5.

Example 5: Consider $P = U_1 \subset \mathbf{R}_{\geq 0}^2$ shown in Fig. 11b, in this case cube $U_1 = \text{sweep}_1(\text{sweep}_2(U_1))$. These two sweep operations are shown in Fig. 15a and 15a, respectively. In particular, Fig. 15b shows the incidence graph of $\text{sweep}_2(U_1)$, where the black substructure is inherited from the incidence graph of U_1 . As can be seen, the \mathbf{e}_2 -top facets, edges ac and ab , and the boundary ridges, vertices b and c , play critical role in construction of $\text{sweep}_2(U_1)$. The \mathbf{e}_2 -bottom facet cb is removed and the projection b' and c' and sweep bb' and cc' of boundary ridges are added as ridges and facets of $\text{sweep}_2(U_1)$.

Finally, we consider the case when the network gets disconnected. In this case, each connected network component is associated with a subspace of balanced supply-demand vectors that are supported on the network component. One first needs to compute for each of the connected network components the projection of P onto the associated subspace, and then perform the sweep operation within the subspace. The additional step of computing the projection of P can be achieved recursively in the same fashion as that for sweep of P , that is, $\text{proj}_{\{i,j\}} P = \text{proj}_i(\text{proj}_j P)$. The implementation of the projection is straightforward by using Proposition 5 and 6.

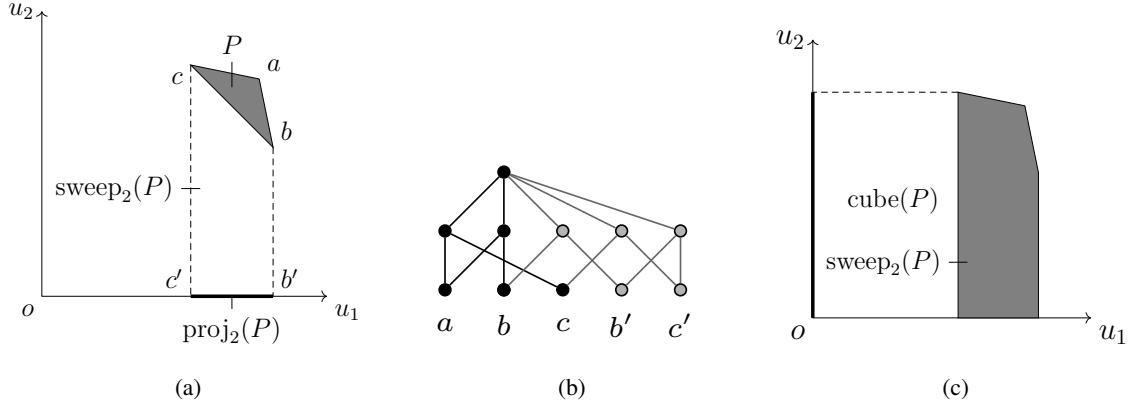


Fig. 15: Illustration of sweep: (a) sweep of U_1 ; (b) the incidence graph of $\text{sweep}_2(U_1)$; and (c) cube U_1 as sweep of $\text{sweep}_2(U_1)$.

VI. COMPLEXITY ANALYSIS

This section includes discussion on the complexity of the optimal control problem and the relevant algorithms, as well as the extension to more general problem settings. A connected network $\mathcal{G} = (\mathcal{V}, \mathcal{E})$ is considered without loss of generality. If the network consists of multiple connected components, the same analysis can be done on every component. In addition, we assume $d := |\mathcal{V}_i| - 1$ to be a constant.

A. Complexity of Optimal Control of Cascading Failure

For a connected network $\mathcal{G} = (\mathcal{V}, \mathcal{E})$, an initial supply demand vector p and a time constant N , we define the *complexity*, denoted by $\kappa(\mathcal{E}, p, N)$, of the optimal control problem (9) to be the number of possible topology sequences that can occur in (4) under all possible controls $u \in \mathcal{D}(\mathcal{E}, p, N)$ (cf. (10)). The rationale of the definition is as follows. On one hand, Remark 15 implies in order to solve (9), it is sufficient to solve $\kappa(\mathcal{E}, p, N)$ number of linear programs. On the other hand, for a general network, due to non-monotonicity of power flow [16], [20], the only way to determine an ordering, in terms of residual load, between two topology sequences is through direct computation. Therefore, in principle all the $\kappa(\mathcal{E}, p, N)$ topology sequences need to be considered in order to solve (9) exactly.

Consider the optimal control problem for a tuple (\mathcal{E}, p, N) . For an arbitrary aggregated state (\mathcal{E}', P') (cf. (21)-(23)) and a link $i \in \mathcal{E}'$, if $\{u \in \mathbf{R}^{\mathcal{V}} \mid f_i(\mathcal{E}', u) < -c_i\} \cap U(\mathcal{E}', P') \neq \emptyset$ (or $\{u \in \mathbf{R}^{\mathcal{V}} \mid f_i(\mathcal{E}', u) > c_i\} \cap U(\mathcal{E}', P') \neq \emptyset$, respectively), then we call the constraint $f_i(\mathcal{E}, u) \geq -c_i$ (or $f_i(\mathcal{E}, u) \leq c_i$, respectively) an *intersecting constraint* and link i an *infeasible link* (in both case). Let $n(\mathcal{E}, p, N)$ be the maximal number of intersecting constraints over all aggregated states. It is clear that $n(\mathcal{E}, p, N)$ is upper bounded by the maximal number of infeasible links over all aggregated states. We then have the following result on $\kappa(\mathcal{E}, p, N)$.

Proposition 7: For a connected network $\mathcal{G} = (\mathcal{V}, \mathcal{E})$, an initial supply demand vector p and a time constant N , $\kappa(\mathcal{E}, p, N) = O(n^{d(N-1)})$, where $n := n(\mathcal{E}, p, N)$ is the maximal number of intersecting constraints, $d :=$

$|\mathcal{V}_i(p)| - 1$, $|\mathcal{V}_i(p)|$ is the number of non-transmission nodes in \mathcal{G} . Furthermore, there exists a choice of $\mathcal{G} = (\mathcal{V}, \mathcal{E})$, p and N such that the bound is tight, that is, $\kappa(\mathcal{E}, p, N) = \Theta(n^{d(N-1)})$. In these bounds the constant of proportionality depends on d .

Proof: We first show that $\kappa(\mathcal{E}, p, N) = O(n^{d(N-1)})$. It is clear that from the definition in (23), at an aggregated state (\mathcal{E}', P) , the number of possible topologies at the next stage is no larger than $|\mathbb{U}(\mathcal{E}, P)|$. From Section V-B, we know that $\mathbb{U}(\mathcal{E}, P)$ contains a subset of cells, the ones within $U(\mathcal{E}, P)$, of the associated arrangement, that is, the arrangement of the hyperplanes associated with the \hat{n} intersecting capacity constraints at (\mathcal{E}, P) . According to [10, Chapter 24], $|\mathbb{U}(\mathcal{E}, P)|$ is upper bounded by $\sum_{i=0}^d \binom{\hat{n}}{i}$. For $d \leq \hat{n}/2$, $\sum_{i=0}^d \binom{\hat{n}}{i} \leq \frac{\hat{n}-d}{\hat{n}-2d} \binom{\hat{n}}{d} = O(\hat{n}^d)$. For $d > \hat{n}/2$, $\sum_{i=0}^d \binom{\hat{n}}{i} \leq 2^{\hat{n}} = O(2^d)$ ¹². Considering the nontrivial case that $\hat{n} \geq 2$, it is then clear that $|\mathbb{U}(\mathcal{E}, P)| = O(n^d)$ for all aggregated state (\mathcal{E}, P) . In other words, the branching factor of the aggregated search tree is $O(n^d)$. Nevertheless, the additional constraints on the control at $t = N - 1$, as commented in Remark 2, implies that $|U(\mathcal{E}, P)| = 1$ for all aggregated state (\mathcal{E}, P) at $t = N - 1$. It is equivalent to consider the depth of the search tree to be $N - 1$. Therefore, the total number of topology sequences is $\kappa(\mathcal{E}, p, N) = O(n^{d(N-1)})$.

Furthermore, the network in Fig. 11a, with $N = 2$, provides an example to show that the bound can be tight. In this example, $n = 3$, $d = 3$ and the number of topology sequences is $\sum_{i=0}^3 \binom{3}{i} = 7$. ■

B. Time complexity of the solution methods

TABLE I: Comparison of time complexity of several algorithms.

Method	Time Complexity
Value iteration	$O(N2^{ \mathcal{E} }n_0^{2dT})$
Search with discretization	$O(n_0^{dNT})$
Aggregated search with arrangement	$O(n^{dN} + n^{d(N-1)} \mathcal{V} ^2)$
Two iterations algorithm	$O(\mathcal{V} ^2\tilde{n}^{N-1} + \mathcal{V}_T n_0^{dN})$

n_0 : number of discretized grid points along one dimension;

$n = n(\mathcal{E}, p^0, N)$;

T : time complexity for evaluating $f(\mathcal{E}', p')$ at a given state (\mathcal{E}', p') ;

\hat{d} is the maximal degree in the reduced tree;

$\tilde{n} = \max_{i \in \mathcal{E}_T} n(\mathcal{E}_i, a_i, N)$.

Table I shows the time complexities of solving the optimal control problem for a connected network $\mathcal{G} = (\mathcal{V}, \mathcal{E})$ with initial supply-demand vector p^0 by using different methods. In all these methods, discretization, whenever used, is assumed to produce same number, denoted by n_0 , of grid points on every dimension, and T is used to denote the time to evaluate the value of $f(\mathcal{E}', p')$ at a given state (\mathcal{E}', p') . The algorithms considered are as follows:

- (I) Value iteration: The state space is considered to be $2^{\mathcal{E}} \times \mathcal{B}_{\mathcal{E}}$. As $\mathcal{B}_{\mathcal{E}}$ is a linear subspace of dimension d , the number of grid points for the state space is $2^{|\mathcal{E}|}n_0^d$. At each grid point (\mathcal{E}', p') , computing the state transition

¹² $\binom{n}{k}$ is defined to be 0 for $n < k$.

requires evaluating function value $f(\mathcal{E}', u)$ for all $u \in U(\mathcal{E}', p')$. It takes $O(n_0^d T)$. Therefore, the overall time for N time steps is $O(N 2^{|\mathcal{E}|} n_0^{2d} T)$.

- (II) Search with discretization: The control space $U(\mathcal{E}', p')$ for state (\mathcal{E}', p') at each time step is discretized by n_0^d number of grid points. It is the branching factor of the search tree of depth equal to N . Hence the total number of nodes in the tree is $O(n_0^{dN})$. In addition, computing flow and hence time T is required for state transition to each node. Therefore, the overall time complexity is $O(n_0^{dN} T)$. It can be seen that the search method is more efficient than the value iteration if $|\mathcal{E}| \geq dN \lg_2 n_0$.
- (III) Aggregated search with arrangement: the proof of proposition 7 implies that the number of nodes in the aggregated tree is $O(n^{d(N-1)})$. At an aggregated state (\mathcal{E}', P') , Remark 18 implies that $\mathbb{U}(\mathcal{E}, P)$ can be computed in time $O(n^d)$ through constructing the associated arrangements by using the incremental algorithm in Section V-B. The overall time for constructing the aggregated search tree is $O(n^{d(N-1)})$. In addition, every node (\mathcal{E}', P') needs to conduct two computational tasks. The first task is to update the pseudo-inverse of Laplacian matrix according to (33) and (34). This takes $O(|\mathcal{V}|^2)$. The second task is to compute cube P' by using Proposition 5 and Proposition 6. Its time complexity is determined by the time complexity of a single sweep operation. The latter is bounded by the number of faces in P' and hence is $O(n^d)$. Therefore, the overall time complexity for the aggregated tree search is $O(n^{dN} + n^{d(N-1)} |\mathcal{V}|^2)$.
- (IV) Two iteration algorithm: it works only for tree reducible network. Let the reduced tree be $\mathcal{T} = (\mathcal{V}_T, \mathcal{E}_T)$. The time complexity of the algorithm consists of two parts: computing \tilde{D}_i for all $i \in \mathcal{E}_T$ and solving (16) through discretization for all $i \in \mathcal{V}_T$. This first part amount to constructing the aggregated search tree for a network that contains a single supply demand pair. Since the sweep operation in one dimensional space takes constant time, the above analysis implies that it takes time $O(|\mathcal{V}_i| \tilde{n}^{N-1})$ to compute \tilde{D}_i for $\mathcal{G}_i = (\mathcal{V}_i, \mathcal{E}_i)$, where $\tilde{n} = \max_{i \in \mathcal{E}_T} n(\mathcal{E}_i, a_i, N)$ as defined in Section VI-A and a_i is as shown in (13). It is straightforward to see that $n(\mathcal{E}_i, a_i, N)$ is much smaller than $n(\mathcal{E}, p, N)$ for all $i \in \mathcal{E}_T$. Hence the total time for computing \tilde{D}_i all $i \in \mathcal{E}_T$ is $O(|\mathcal{V}|^2 \tilde{n}^{N-1})$, since in most cases $\sum_{i \in \mathcal{E}_T} |\mathcal{V}_i|^2$ is smaller than $|\mathcal{V}|^2$. The second part is to solve sub-problems (16) of a dimension no larger than $N \hat{d}$, where \hat{d} is the maximal node degree of the reduced tree. Using the same discretization parameter n_0 , a single subproblem takes time $O(n_0^{\hat{d}N})$ and the total time complexity of the recursive procedure is the summation of these subproblems over all nodes in \mathcal{T} , that is, $O(|\mathcal{V}_T| n_0^{\hat{d}N})$. Therefore, the overall time complexity for the algorithm is $O(|\mathcal{V}|^2 \tilde{n}^{N-1} + |\mathcal{V}_T| n_0^{\hat{d}N})$.

Remark 21: The time complexity for aggregated tree search may not be tight due to several reasons:

- The arrangement problem at a network state could be highly degenerated, that is, two hyperplanes do not necessarily intersect and more than d hyperplanes can intersect at a vertex, in which case the corresponding branching factor is much smaller than n^d .
- When the network gets disconnected due to link failures, the arrangement problem is solved for each connected component independently. Therefore, an accurate estimate of d is related to the number of non-transmission nodes in a component, as opposed to the entire network. Since the number of connected components is non-

decreasing along a path in the search tree, the pertinent value of d may be much less than $|\mathcal{V}_l| - 1$ away from the initial state $(\mathcal{E}^0, \{p^0\})$.

- As shown in Section V, lower and upper bounds at each aggregated state can be used to prune the aggregated search tree. This avoids searching through the entire aggregated state space without compromising the performance, and therefore improves the efficiency of the aggregated tree search algorithm.

VII. APPROXIMATION ALGORITHM AND SIMULATIONS

A. Approximation Algorithm via Projection

The exponential dependence of the time complexity on $d = |\mathcal{V}_l| - 1$, as discussed in Section VI, may be prohibitive for networks that contains large number of non-transmission nodes. We now outline a strategy to project the (aggregated) supply-demand vectors onto a lower dimensional space. Aggregation and search in the lower dimensional space then gives an approximation.

For a network $\mathcal{G} = (\mathcal{V}, \mathcal{E})$ with supply-demand vector p . For the sake of presentation in this section, assume, without loss of generality that $\mathcal{V} = \mathcal{V}_l$, i.e., every node is a non-transmission node; if this is not the case, then one can focus only on the subspace of control actions corresponding to the non-transmission nodes. Let $\Phi = [\Phi_1, \dots, \Phi_{|\mathcal{V}_l|}] \in \mathbf{R}^{|\mathcal{V}_l| \times |\mathcal{V}_l|}$ be an orthonormal (transformation) matrix, and let $B \subset [|\mathcal{V}_l|]$ be an index set. The approximation strategy, which is parametrized by (Φ, B) , considers aggregated set of feasible control actions in the sub-space $U(\mathcal{E}, P) \cap \mathcal{R}(\Phi_B) = \{u \in U(\mathcal{E}, P) \mid \Phi_i^T u = 0, i \notin B\}$, i.e., in the subspace of control actions which can be expressed as a linear combination of $\Phi_i, i \in B$. Remark 18 implies that this reduces the dimension, and hence correspondingly the time complexity, from $|\mathcal{V}_l|$ to B . Moreover, since the constraints $\Phi_i^T u = 0, i \notin B$, are hyperplanes, they can be easily integrated into the construction of arrangements to get $U(\mathcal{E}, P) \cap \mathcal{R}(\Phi_B)$. In fact, by setting $\Phi_i = \frac{1}{\sqrt{|\mathcal{V}_l|}}$ for some $i \notin B$, the constraint $\Phi_i^T u = 0$ is the balance constraint for a connected network (cf. (2)).

Example 6: Consider a network with initial supply-demand vector p^0 . By choosing $B = \{1\}$ and $\Phi_1 = p^0 / \|p^0\|_2$, we get *proportional control policies* [8, Section 6.1.1], i.e., a class of control policies whose action set at state (\mathcal{E}, p) is $\{\lambda p \mid 0 \leq \lambda \leq 1\}$.

The one-dimensional search space resulting from proportional control policy, as shown in Example 6, is favorable for computational purposes. However, the projection-based approximation strategy implies that one could possibly find better control actions, using the comparable computational budget, by using different projections. This is illustrated using simulations on IEEE 39 benchmark system in Section VII-B.

B. Simulations

We conducted numerical experiments on the IEEE 39 bus system illustrated in Figure 16. Node 39 is selected to the only supply; nodes 4 and 16 are selected as loads; all the other nodes are transmission nodes. This particular choice of supply-demand nodes is consistent with the fact that the actual supply and demand on these nodes, as reported in [27], have relatively large values. p^0 was chosen to be proportional to the actual values reported in

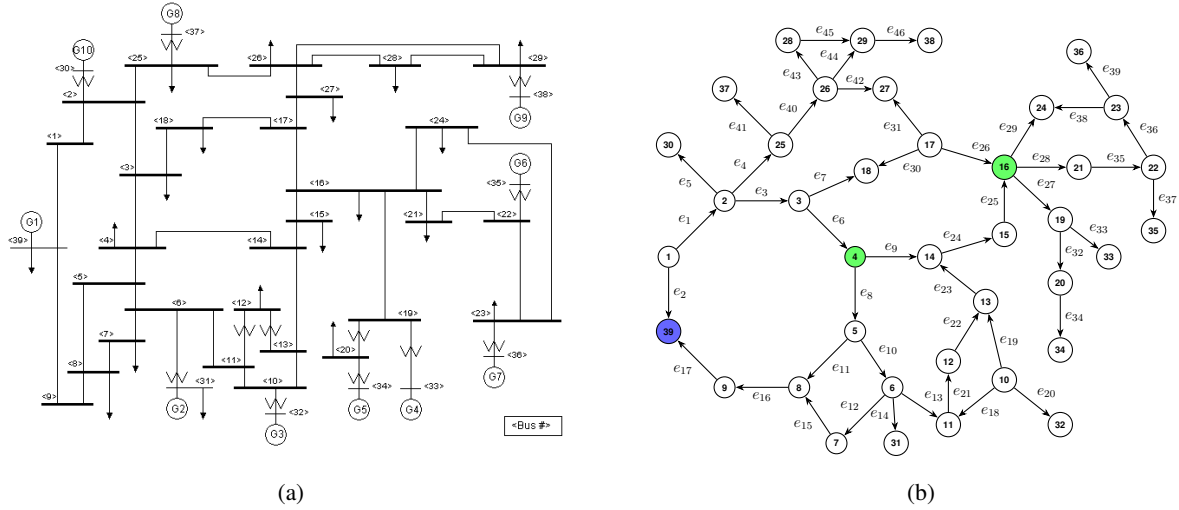


Fig. 16: The IEEE 39 bus network.

[27] for nodes 4, 16 and 39: $p_4^0 = p_{16}^0 = -5$, $p_{39}^0 = 10$ and $p_i^0 = 0$ for all $i \notin \{4, 16, 39\}$. Link susceptances w are from [27]. The link capacities were selected as follows: $c_8 = 0.5$, $c_9 = 1$, $c_i = 2.5$ for $i \in \{13, 21, 22, 23\}$; $c_i = 3.0$ for $i \in \{3, 28, 29, 35, 36, 38\}$; $c_i = 3.5$ for $i \in \{16, 17\}$; $c_i = 4.0$ for $i \in \{7, 26, 30\}$; $c_i = 4.5$ for $i \in \{1, 2, 4, 24, 25, 31, 39, 40, 42\}$ and $c_i = 2.0$ for the remaining links, with respect to link labels in [27].

TABLE II: Optimal residual load under (9) and under the projection-based approximations in (29)

$N \backslash \eta$	0	0.1	0.2	0.3	0.4	0.5	0.6	0.7	0.8	0.9	1	Optimal Control
1	3.716	3.502	3.310	3.140	2.984	2.844	2.718	2.600	2.494	2.396	2.304	3.716
2	9.860	9.806	9.750	9.696	8.974	9.000	7.334	6.742	4.578	4.078	4.000	9.860
3	10.000	11.112	11.090	11.028	10.000	9.000	7.334	6.742	5.000	4.444	4.000	11.150
4	10.000	11.112	11.090	11.028	10.000	9.000	7.334	6.742	5.000	4.444	4.000	11.150
5	10.000	11.112	11.090	11.028	10.000	9.000	7.334	6.742	5.000	4.444	4.000	11.150

For the above network parameters, (\mathcal{E}^0, p^0) is infeasible. Furthermore, under no load shedding control action, i.e., $u^T \equiv p^0$ for all t , the only supply node 39 would get disconnected at $t = 1$ from the load nodes 4 and 16. However, using the control formulation of this paper, such a scenario can be prevented while minimizing the amount of load to be shed. Table II (last column) shows the values of residual load, i.e., the optimal solution to (9), computed by the techniques in Section V, for different control horizons N . The residual load is expectedly is nondecreasing with N . This confirms that multi-round control does lead to increase in the residual load, or equivalently decrease in cumulative load shed, in comparison to the single round ($N = 1$) control underlying power re-dispatch. However, there are no gains in residual load beyond $N \geq 3$. This is because the network in Figure 16 contains a very few

cycles; and once the active link set becomes a tree, the optimal load shedding action is to ensure feasibility of all the links in this case.

Table II also shows optimal residual load within the class of control policies obtained by projection onto a one-dimensional space, as described in Section VII-A. Specifically, we chose

$$B = \{1\}, \quad \Phi_1 = \eta \bar{p}^1 + (1 - \eta) \bar{p}^2, \quad \eta \in [0, 1] \quad (29)$$

where $\bar{p}^1 \in \mathbf{R}^{39}$ has 1 and -1 on node 39 and 4, respectively, and 0 elsewhere; $\bar{p}^2 \in \mathbf{R}^{39}$ has 1 and -1 on node 39 and 16, respectively, and 0 elsewhere. Recalling Example 6, it is easy to see that the set of proportional control policies [8, Section 6.1.1] corresponds to $\eta = 0.5$. Table II contains values for optimal residual load under such an approximation for different values of η and N . These values show that, similar to the optimal control actions, for every η , the optimal residual load is nondecreasing in N and stays constant for $N \geq 3$. While there is no general monotone relationship in η (uniformly for all N), the best control actions for $N \geq 3$ correspond to $\eta = 0.1$. The control actions corresponding to $\eta = 0.1$ perform uniformly better than the proportional control policy ($\eta = 0.5$) which requires comparable computational cost, and give fairly similar performance as the optimal control actions which are obtained under considerable computational costs (Section V).

VIII. CONCLUSIONS AND FUTURE WORK

The phenomenon of cascading failure in physical networks has attracted a lot of interest, and yet formal approaches for its control are relatively very few. This paper builds upon a previously proposed formulation for optimal control of cascading failure in power networks under DC approximation, and provides approaches for computing optimal control within this setting. The cascading dynamic model can be readily extended to other large scale dynamical systems whose constituent components are allowed to fail and underlying physical dynamics are on a considerable faster time scale than the cascades of failure. The connections to network optimization and computational geometry underlying these approaches are novel, and are suggestive of several avenues for future work.

We plan to extend the network decomposition approach beyond the specific settings of this paper. Specifically, we are interested in conditions for non tree-reducible networks under which there exists a decomposition into coupled local problems which can be solved to optimality asymptotically through distributed optimization techniques. With regards to the search-based approach, we plan to explore approximation techniques beyond the projection approach in this paper. In particular, we are interested in techniques for pruning the search tree while giving provable approximation guarantees. Finally, the equivalent finite representation paradigm in this paper is reminiscent of the literature on finite abstractions for hybrid systems, which has been done primarily for stability analysis. We plan to explore connections between setting of this paper, possibly extended to continuous time domain, and recent work on symbolic optimal control, e.g., see [28]

APPENDIX

A. Flow redistribution under link failure

We first provide a procedure to incrementally compute pseudo-inverse of Laplacian under failure of links, which is then used for efficient computation of flow redistribution under failure of links. Recall we consider undirected network. Furthermore, we assume the network under consideration is connected before link failure. If it is disconnected, the same results can be used on every connected component.

1) *Incremental Computation of Pseudo-inverse of Laplacian under Link Failure:* For a network $\mathcal{G} = (\mathcal{V}, \mathcal{E})$ with weight $W \in \mathbf{R}_{>0}^{\mathcal{E} \times \mathcal{E}}$ and node-link incidence matrix $A \in \mathbf{R}^{\mathcal{V} \times \mathcal{E}}$, define the sensitivity matrix $K := WA^T L^\dagger A^T \in \mathbf{R}^{\mathcal{E} \times \mathcal{E}}$. K has the following physical interpretation: K_{ij} is the flow on link i when a unit supply and a unit demand are imposed on the tail and head node of link j , respectively, i.e., when the supply-demand vector is A_j . We further define the normalized sensitivity matrix $K^{\text{sym}} := W^{1/2} A^T L^\dagger A^T W^{1/2} = W^{-1/2} K W^{1/2}$. Note that K is similar to K^{sym} . Let $\bar{A} = AW^{1/2}$ be the weighted node-link incidence matrix. Then $K^{\text{sym}} = \bar{A}^T L^\dagger \bar{A} = \bar{A}^T (\bar{A} \bar{A}^T)^\dagger \bar{A}$ is the orthogonal projection matrix onto the row space of \bar{A} . Hence it only has eigenvalues of 0 and 1. In addition, for a set $\mathcal{I} \subset \mathcal{E}$, let $\bar{\mathcal{I}} := \mathcal{E} \setminus \mathcal{I}$.

Lemma 10: Consider a connected network $\mathcal{G} = (\mathcal{V}, \mathcal{E})$ with link weights $W \in \mathbf{R}_{>0}^{\mathcal{E} \times \mathcal{E}}$. Then, for every $\mathcal{I} \subset \mathcal{E}$, $K_{\bar{\mathcal{I}}\bar{\mathcal{I}}}^{\text{sym}}$ is positive semi-definite and

$$\rho^2(K_{\bar{\mathcal{I}}\bar{\mathcal{I}}}^{\text{sym}}) = \max_{x \in \mathbf{R}^{\bar{\mathcal{I}}}} \frac{\|x'_{\bar{\mathcal{I}}}\|_2^2}{\|x'_{\bar{\mathcal{I}}}\|_2^2 + 2\|x'_{\bar{\mathcal{I}}}\|_2^2 + \|x - x'_{\bar{\mathcal{I}}}\|_2^2} \leq 1 \quad (30)$$

where $\rho(K_{\bar{\mathcal{I}}\bar{\mathcal{I}}}^{\text{sym}})$ is the spectral radius of $K_{\bar{\mathcal{I}}\bar{\mathcal{I}}}^{\text{sym}}$, and $x' := K_{\bar{\mathcal{I}}\bar{\mathcal{I}}}^{\text{sym}} x$. Moreover, (30) holds true with equality if and only if $(\mathcal{V}, \mathcal{E} \setminus \mathcal{I})$ is disconnected.

Proof: It is straightforward that $K_{\bar{\mathcal{I}}\bar{\mathcal{I}}}^{\text{sym}} = \bar{A}_{\bar{\mathcal{I}}}^T L^\dagger \bar{A}_{\bar{\mathcal{I}}}$ is positive semi-definite, where $\bar{A}_{\bar{\mathcal{I}}}$ is the $\mathcal{E} \times \bar{\mathcal{I}}$ submatrix of \bar{A} . For arbitrary $x \in \mathbf{R}^{\bar{\mathcal{I}}}$, let $\hat{x} = [x^T \ 0^T]^T \in \mathbf{R}^{\mathcal{E}}$. Then, $\|x\|_2 = \|\hat{x}\|_2$, and $x' = K_{\bar{\mathcal{I}}\bar{\mathcal{I}}}^{\text{sym}} x = K^{\text{sym}} \hat{x}$. Since $K^{\text{sym}} = \bar{A}^T (\bar{A} \bar{A}^T)^\dagger \bar{A}$ is an orthogonal projection matrix,

$$\|\hat{x}\|_2^2 = \|K^{\text{sym}} \hat{x}\|_2^2 + \|\hat{x} - K^{\text{sym}} \hat{x}\|_2^2 = \|x'\|_2^2 + \|x - x'_{\bar{\mathcal{I}}}\|_2^2 + \|x'_{\bar{\mathcal{I}}}\|_2^2 = \|x'_{\bar{\mathcal{I}}}\|_2^2 + 2\|x'_{\bar{\mathcal{I}}}\|_2^2 + \|x - x'_{\bar{\mathcal{I}}}\|_2^2 \quad (31)$$

Since $K_{\bar{\mathcal{I}}\bar{\mathcal{I}}}^{\text{sym}}$ is symmetric,

$$\rho(K_{\bar{\mathcal{I}}\bar{\mathcal{I}}}^{\text{sym}}) = \max_{x \in \mathbf{R}^{\bar{\mathcal{I}}}} \frac{\|K_{\bar{\mathcal{I}}\bar{\mathcal{I}}}^{\text{sym}} x\|_2}{\|x\|_2} = \max_{x \in \mathbf{R}^{\bar{\mathcal{I}}}} \frac{\|x'_{\bar{\mathcal{I}}}\|_2}{\|\hat{x}\|_2}$$

Substituting $\|\hat{x}\|_2^2$ from (31) gives (30).

(30) holds true with equality if and only if $K_{\bar{\mathcal{I}}\bar{\mathcal{I}}}^{\text{sym}} x = x$ for some $x \neq 0$, or equivalently, $K_{\bar{\mathcal{I}}\bar{\mathcal{I}}} y = y$ for some $y \neq 0$. In other words, this happens when one imposes y_i unit supply and demand on the tail and head node of link $i \in \bar{\mathcal{I}}$, respectively, the resulting flow would be y_i for all $i \in \bar{\mathcal{I}}$ and 0 for all $i \in \mathcal{E} \setminus \bar{\mathcal{I}}$. If network $(\mathcal{V}, \mathcal{E} \setminus \bar{\mathcal{I}})$ remained to be connected, pick a link $i \in \bar{\mathcal{I}}$ with $y_i \neq 0$, there exist another path connecting the end nodes of i but containing 0 flow on all its links. This contradict with the ‘‘Ohm’s law’’. On the other hand, if $(\mathcal{V}, \mathcal{E} \setminus \bar{\mathcal{I}})$ is disconnected, let $\mathcal{I}' \subseteq \bar{\mathcal{I}}$ be the set of links connecting two components of $(\mathcal{V}, \mathcal{E} \setminus \bar{\mathcal{I}})$, and $y'_i = w_i$ for all $i \in \mathcal{I}'$ and $y'_i = 0$ for all $i \in \bar{\mathcal{I}} \setminus \mathcal{I}'$, then it is straightforward to check $K_{\bar{\mathcal{I}}\bar{\mathcal{I}}} y' = y'$. ■

We now provide formula to incrementally compute pseudo-inverse of Laplacian under link failures. We consider two scenarios where the network remains to be connected or gets disconnected. The first scenario is addressed by the next proposition, which is a combined result of Lemma 10 and [29, Lemma 3], and was considered in [14].

Proposition 8: Consider a connected network $\mathcal{G} = (\mathcal{V}, \mathcal{E})$ with link weights $W \in \mathbf{R}_{>0}^{\mathcal{E} \times \mathcal{E}}$. Let $\hat{\mathcal{G}} = (\mathcal{V}, \mathcal{E} \setminus \mathcal{I})$ be a sub-graph of \mathcal{G} obtained by removing $\mathcal{I} \subset \mathcal{E}$ links. Let L and \hat{L} denote the weighted Laplacian matrices for \mathcal{G} and $\hat{\mathcal{G}}$, respectively. If $\hat{\mathcal{G}}$ is connected, then:

$$\hat{L}^\dagger = L^\dagger + L^\dagger A_{\mathcal{I}} (I - K_{\mathcal{I}\mathcal{I}})^{-1} W_{\mathcal{I}\mathcal{I}} A_{\mathcal{I}}^\top L^\dagger \quad (32)$$

where $K_{\mathcal{I}\mathcal{I}} = W_{\mathcal{I}\mathcal{I}} A_{\mathcal{I}}^\top L^\dagger A_{\mathcal{I}} \in \mathbf{R}^{\mathcal{I} \times \mathcal{I}}$.

Corollary 2 is a special case of Proposition 8 when $|\mathcal{I}| = 1$. It appeared previously in [20], where it was proven using a standard rank one perturbation method [30].

Corollary 2: Consider a connected network $\mathcal{G} = (\mathcal{V}, \mathcal{E})$ with link weights $W \in \mathbf{R}_{>0}^{\mathcal{E} \times \mathcal{E}}$. Let $\hat{\mathcal{G}} := (\mathcal{V}, \mathcal{E} \setminus \{j\})$ be a sub-network of \mathcal{G} obtained by removing link $j \in \mathcal{E}$. Let L and \hat{L} denote the weighted Laplacian matrices for \mathcal{G} and $\hat{\mathcal{G}}$, respectively. If $\hat{\mathcal{G}}$ is connected, then:

$$\hat{L}^\dagger = L^\dagger + \frac{1}{1 - K_{jj}} L^\dagger A_j w_j A_j^\top L^\dagger \quad (33)$$

The next result addresses the scenario when removal of a single link j disconnects \mathcal{G} . Repeated application of this result allows to consider this scenario when multiple links are removed. Lemma 10 implies that, in this case, $K_{jj} = 1$, and hence (33) can not be applied. Nevertheless, standard rank one perturbation method [30] can be used to get the following result.

Proposition 9: Consider a connected network $\mathcal{G} = (\mathcal{V}, \mathcal{E})$ with link weights $W \in \mathbf{R}_{>0}^{\mathcal{E} \times \mathcal{E}}$. Let $\hat{\mathcal{G}} := (\mathcal{V}, \mathcal{E} \setminus \{j\})$ be a sub-network of \mathcal{G} obtained by removing link $j \in \mathcal{E}$. Let L and \hat{L} denote the weighted Laplacian matrices for \mathcal{G} and $\hat{\mathcal{G}}$, respectively. If $\hat{\mathcal{G}}$ is disconnected, then

$$\hat{L}^\dagger = L^\dagger - h h^\top L^\dagger - L^\dagger h h^\top + (h^\top L^\dagger h) h h^\top \quad (34)$$

where $h := L^\dagger A_j / \|L^\dagger A_j\|_2$.

Proof: The lemma follows directly from [30, Theorem 6]. One only needs to show that A_j is in the range space of L , which is straightforward. ■

Remark 22: In Proposition 9, if the nodes of the two connected components are labeled as $[n_1]$ and $[n_2] + \{n_1\}$, then

$$h = L^\dagger A_j / \|L^\dagger A_j\|_2 = \frac{1}{\sqrt{n_1 n_2 (n_1 + n_2)}} \begin{bmatrix} n_2 \mathbf{1}_{n_1} \\ -n_1 \mathbf{1}_{n_2} \end{bmatrix}$$

and furthermore, \hat{L}^\dagger is a block diagonal matrix in which the diagonal elements are two matrices of size $n_1 \times n_1$ and $n_2 \times n_2$.

2) *Incremental Computation of Flow Redistribution under Link Failure:* We now use Proposition 8 and Proposition 9 to study flow redistribution under failure of links in $\mathcal{I} \subset \mathcal{E}$. Analogous to Section A.1, we separately treat the two scenarios where failure of links would not or would disconnects the network. When the network remains

connected, one can use (32) to calculate the flow redistribution due to removal of links in $\mathcal{I} \subset \mathcal{E}$ from the active link set \mathcal{E} , under a given balanced supply-demand vector p . We have the following relationship:

$$\begin{aligned} f(\bar{\mathcal{I}}, p) &= W_{\bar{\mathcal{I}}\bar{\mathcal{I}}} A_{\bar{\mathcal{I}}}^T \hat{L}^\dagger p = W_{\bar{\mathcal{I}}\bar{\mathcal{I}}} A_{\bar{\mathcal{I}}}^T (L^\dagger + L^\dagger A_{\mathcal{I}} (I - K_{\mathcal{I}\mathcal{I}})^{-1} W_{\mathcal{I}\mathcal{I}} A_{\bar{\mathcal{I}}}^T L^\dagger) p \\ &= f_{\bar{\mathcal{I}}}(\mathcal{E}, p) + W_{\bar{\mathcal{I}}\bar{\mathcal{I}}} A_{\bar{\mathcal{I}}}^T L^\dagger A_{\mathcal{I}} (I - K_{\mathcal{I}\mathcal{I}})^{-1} W_{\mathcal{I}\mathcal{I}} A_{\bar{\mathcal{I}}}^T L^\dagger p \\ &= f_{\bar{\mathcal{I}}}(\mathcal{E}, p) + f_{\bar{\mathcal{I}}}(\mathcal{E}, A_{\mathcal{I}} (I - K_{\mathcal{I}\mathcal{I}})^{-1} f_{\mathcal{I}}(\mathcal{E}, p)) \end{aligned} \quad (35)$$

Letting

$$\theta := (I - K_{\mathcal{I}\mathcal{I}})^{-1} f_{\mathcal{I}}(\mathcal{E}, p), \quad (36)$$

and substituting into (35), we get the following:

$$\Delta f_{\bar{\mathcal{I}}} = f(\bar{\mathcal{I}}, p) - f_{\bar{\mathcal{I}}}(\mathcal{E}, p) = f_{\bar{\mathcal{I}}}(\mathcal{E}, A_{\mathcal{I}} \theta) = K_{\bar{\mathcal{I}}\mathcal{I}} \theta \quad (37)$$

(37) implies that the flow change due to failure of links in \mathcal{I} is equal to that induced by the additional supply-demand vector $A_{\mathcal{I}} \theta$ added to the original network. Since $A_{\mathcal{I}} \theta = \sum_{i \in \mathcal{I}} A_i \theta_i$, adding $A_{\mathcal{I}} \theta$ is equivalent to adding θ_i unit of supply (demand) on the tail (head) node of link i , for every $i \in \mathcal{I}$. In other words, θ acts the source that leads to the flow change due to link failure, for which we make the following remark.

Remark 23: Lemma 8 implies the following:

$$\theta = (I - K_{\mathcal{I}\mathcal{I}})^{-1} f_{\mathcal{I}} = f_{\mathcal{I}} + K_{\mathcal{I}\mathcal{I}} f_{\mathcal{I}} + K_{\mathcal{I}\mathcal{I}}^2 f_{\mathcal{I}} + \dots$$

where θ can be interpreted as a result from an *echo effect* of $f_{\mathcal{I}}$ that intensifies itself and $K_{\mathcal{I}\mathcal{I}}^n f_{\mathcal{I}}$ can be seen as the gain at the n -th *reflection*.

Furthermore, (36) can be re-written as

$$\theta = f_{\mathcal{I}}(\mathcal{E}, p) + K_{\mathcal{I}\mathcal{I}} \theta = f_{\mathcal{I}}(\mathcal{E}, p + A_{\mathcal{I}} \theta) \quad (38)$$

(38) means that for the network under the original supply-demand vector p and the additional supply-demand vector $A_{\mathcal{I}} \theta$, the flow on every link $i \in \mathcal{I}$ is equal to the additional supply and demand added on the incident nodes of i . This motivates the following alternate approach for finding flow change due to link failure.

Proposition 10: Consider a connected network $\mathcal{G} = (\mathcal{V}, \mathcal{E})$ with link weights $W \in \mathbf{R}_{>0}^{\mathcal{E} \times \mathcal{E}}$ and balanced supply demand vector $p \in \mathbf{R}^{\mathcal{V}}$. If there exists $\theta \in \mathbf{R}^{\mathcal{I}}$, $\mathcal{I} \subset \mathcal{E}$, satisfying (38), then the flow changes on the residual network due to the failure of links in \mathcal{I} is $\Delta f_{\bar{\mathcal{I}}} = f(\bar{\mathcal{I}}, p) - f_{\bar{\mathcal{I}}}(\mathcal{E}, p) = K_{\bar{\mathcal{I}}\mathcal{I}} \theta$.

Proof: It is sufficient to prove that $f(\bar{\mathcal{I}}, p) = f_{\bar{\mathcal{I}}}(\mathcal{E}, p + A_{\mathcal{I}} \theta)$ for θ satisfying (1). Consider a network $(\mathcal{V}, \mathcal{E})$ with supply-demand vector $p + A_{\mathcal{I}} \theta$ and let $f \in \mathbf{R}^{\mathcal{E}}$ and $\phi \in \mathbf{R}^{\mathcal{V}}$ be the flow and phase angle satisfying (1). Combination of the first equality in (1) and (38) implies that $A_{\bar{\mathcal{I}}} f_{\bar{\mathcal{I}}} = p$, which can be seen as the flow conservation constraint for network $(\mathcal{V}, \bar{\mathcal{I}})$ with supply-demand vector p . It straightforward to see that $f_{\bar{\mathcal{I}}}$ and ϕ satisfy the ‘‘ohm’s law’’ (the second equality in (1)) as well. This is to say, $f_{\bar{\mathcal{I}}} = f(\bar{\mathcal{I}}, p)$. ■

Remark 24: The proof of Proposition 10 does not require that the residual network $(\mathcal{V}, \bar{\mathcal{I}})$ to be connected. However, if the network gets disconnected, then such θ satisfying (38) exist if and only if $f_{\mathcal{I}}(\mathcal{E}, p) = \mathbf{0}$. On the other hand, if $(\mathcal{V}, \bar{\mathcal{I}})$ is connected, then such θ satisfying (38) is unique, as shown in (36).

Flow redistribution in the scenario where link failure disconnects the network is not necessarily well-posed, and requires additional specifications. In order to illustrate this point, for simplicity, consider the case when only one link $j \in \mathcal{E}$ fails, due to which $\hat{\mathcal{G}} = (\mathcal{V}, \mathcal{E} \setminus \{j\})$ has two connected components. If j does not carry flow before failure, then trivially there is no redistribution of flow upon failure of link j . However, if j carries flow, then the demand-supply vector p is not balanced with respect to the two connected components in $\hat{\mathcal{G}}$. One needs to specify a protocol for inducing such a balance, which will then determine new flows in the two components. One such protocol is to proportionally reduce supply or demand at nodes, depending on whether there is excessive supply or demand respectively. If \hat{p} is the balanced supply-demand rendered by such a balancing protocol, then the new flow can be computed using (3) and (34).

B. Proof of Proposition 3

Proof: We first show that the conditions are sufficient. We start by showing that the output functions from $\Omega\{(g_j^{\text{in}}, X_j)\}_{j \in [n]}$ and $\Omega\{(g_j^{\text{in}}, \text{conv } X_j)\}_{j \in [n]}$ have the same domain under the given conditions. Since $\tau_j^1 \in X_j$ for all $j \in [n]$ and $\sum_{j=1}^n X_j \cap (-\infty, \tau_j^1]$ is connected, $\sum_{j=1}^n X_j \cap (-\infty, \tau_j^1] = [\sum_{j=1}^n \min X_j, \sum_{j=1}^n \tau_j^1]$. Similarly, $\sum_{j=1}^n X_j \cap [\tau_j^1, \infty) = [\sum_{j=1}^n \tau_j^1, \sum_{j=1}^n \max X_j]$. Therefore, $\sum_{j=1}^n X_j = [\sum_{j=1}^n \min X_j, \sum_{j=1}^n \max X_j] = \sum_{j=1}^n \text{conv } X_j$.

It is straightforward that $\Omega\{(g_j^{\text{in}}, X_j)\}_{j \in [n]} \leq \Omega\{(g_j^{\text{in}}, \text{conv } X_j)\}_{j \in [n]}$. Hence it is sufficient to prove the other direction. By Lemma 4, $\Omega\{(g_j^{\text{in}}, \text{conv } X_j)\}_{j \in [n]}$ is a χ function with top point $\tilde{\tau} := (\sum_{j=1}^n \tau_j^1, \sum_{j=1}^n \tau_j^2)$. We need to show that $(\Omega\{(g_j^{\text{in}}, X_j)\}_{j \in [n]})(z) \geq \chi_{\tilde{\tau}}(z)$ for all $z \in [\sum_{j=1}^n \min X_j, \sum_{j=1}^n \max X_j]$.

We first consider $z \in [\sum_{j=1}^n \min X_j, \sum_{j=1}^n \tau_j^1]$. Let X_j contain m_j pieces of intervals. Plus that $\tau_j^1 \in X_j$ separates an interval of X_j into two pieces, with possibly one of the two containing the single point τ_j , there are $m_j + 1$ pieces in total. Without loss of generality, label the $m_j + 1$ intervals X_j^k in increasing order, that is, X_j^k such that $\max X_j^{k-1} \leq \min X_j^k$ for all $k \in [m_j + 1]$. In particular, let $l_j \in [m_j + 1]$ be such that $\tau_j^1 = \max X_j^{l_j} = \min X_j^{l_j+1}$ for all $j \in [n]$. Furthermore, let $\tilde{\Theta} := \prod_{j=1}^n [m_j + 1]$ and $\tilde{\Theta}_{\leq \sigma'} := \{\sigma \in \tilde{\Theta} \mid \sigma \leq \sigma'\}$ for all $\sigma' \in \tilde{\Theta}$. The notation $\tilde{\Theta}_{> \sigma'}$ has similar meaning. With these notations, $X_j \cap (-\infty, \tau_j^1] = \cup_{\sigma_j \leq l_j} X_j^{\sigma_j}$. Then $\cup_{\sigma \in \tilde{\Theta}_{\leq l}} \sum_{j=1}^n X_j^{\sigma_j} = \sum_{j=1}^n \cup_{\sigma_j \leq l_j} X_j^{\sigma_j} = \sum_{j=1}^n X_j \cap (-\infty, \tau_j^1] = [\sum_{j=1}^n \min X_j, \sum_{j=1}^n \tau_j^1]$. It is then sufficient to prove that for all $\sigma \in \tilde{\Theta}_{\leq l}$, $\Omega(\sigma) = \chi_{\tilde{\tau}}$ over the domain $\sum_{j=1}^n X_j^{\sigma_j}$.

Pick arbitrary $\sigma \in \tilde{\Theta}_{\leq l}$, without loss of generality, let $[q_j^l, q_j^u] := X_j^{\sigma_j}$. Restricted in this domain, g_j^{in} is a linear function with slope 1. Lemma 3 implies that $(q_j^u, q_j^u - \tau_j^1 + \tau_j^2)$ can be treated as the top point of g_j^{in} over domain $[q_j^l, q_j^u]$. Lemma 4 and Remark 12 then implies that $\Omega(\sigma)$ is a linear function with top point $(\sum_{j=1}^n q_j^u, \sum_{j=1}^n q_j^u - \sum_{j=1}^n \tau_j^1 + \sum_{j=1}^n \tau_j^2)$. It is straightforward to check that this top point lies on $\chi_{\tilde{\tau}}$. As a result, $\Omega(\sigma) = \chi_{\tilde{\tau}}$ when evaluated in the domain $\sum_{j=1}^n X_j^{\sigma_j}$. Due to symmetry, the same result can be shown for the case $z \in [\sum_{j=1}^n \tau_j^1, \sum_{j=1}^n \max X_j]$ by considering $\sigma \in \tilde{\Theta}_{> l}$.

We then show that the conditions are necessary. Lemma 4 implies that the problem $(\Omega\{(g_j^{\text{in}}, \text{conv } X_j)\}_{j \in [n]})(z)$ corresponding to $z = \sum_{j=1}^n \tau_j^1$ is unique and $x_j^* = \tau_j^1$ for all $j \in [n]$. In order for $\Omega\{(g_j^{\text{in}}, X_j)\}_{j \in [n]} = \chi_{\tilde{\tau}}$ to be true, it must be that $\tau_j^1 \in X_j$ for all $j \in [n]$. Previous arguments imply that it is sufficient to prove

that for all $\sigma \in \tilde{\Theta} \setminus (\tilde{\Theta}_{\leq l} \cup \tilde{\Theta}_{> l})$, either $\Omega(\sigma) < \chi_{\tilde{\tau}}$ or $\Omega(\sigma) = \Omega(\sigma')$ for some $\sigma' \in \tilde{\Theta}_{\leq l} \cup \tilde{\Theta}_{> l}$. Pick arbitrary $\sigma \in \tilde{\Theta} \setminus (\tilde{\Theta}_{\leq l} \cup \tilde{\Theta}_{> l})$, both $\{j : \sigma_j \leq l_j\}$ and $\{j : \sigma_j \geq l_j + 1\}$ are nonempty. Similarly as that in previous paragraphs, let $[q_j^l, q_j^u] := X_j^{\sigma_j}$, then Lemma 3 and Lemma 4 imply that $\Omega(\sigma)$ is a χ function with top point $(\hat{\tau}_1, \hat{\tau}_2) := \left(\sum_{\{j: \sigma_j \leq l_j\}} q_j^u + \sum_{\{j: \sigma_j \geq l_j + 1\}} q_j^l, \sum_{\{j: \sigma_j \leq l_j\}} (q_j^u - \tau_j^1) + \sum_{\{j: \sigma_j \geq l_j + 1\}} (\tau_j^1 - q_j^l) + \sum_{j=1}^n \tau_j^2 \right)$ and domain $[\sum_{j=1}^n q_j^l, \sum_{j=1}^n q_j^u]$. It is simple algebra to check the following:

$$\chi_{\tilde{\tau}}(\hat{\tau}_1) - \hat{\tau}_2 = \min \left\{ \sum_{\{j: \sigma_j \leq l_j\}} (\tau_j^1 - q_j^u), \sum_{\{j: \sigma_j \geq l_j + 1\}} (q_j^l - \tau_j^1) \right\} \geq 0$$

If both $\{j : \sigma_j \leq l_j - 1\}$ and $\{j : \sigma_j \geq l_j + 2\}$ are nonempty, then the above inequality is strict. $(\hat{\tau}_1, \hat{\tau}_2)$ is below $\chi_{\tilde{\tau}}$ and hence $\Omega(\sigma) < \chi_{\tilde{\tau}}$. Otherwise, if either $\{j : \sigma_j \leq l_j\} = \{j : \sigma_j = l_j\}$ or $\{j : \sigma_j \geq l_j + 1\} = \{j : \sigma_j = l_j + 1\}$, the above inequality becomes equality and $(\hat{\tau}_1, \hat{\tau}_2)$ lies on $\chi_{\tilde{\tau}}$. We consider the first case and show that $(\Omega(\sigma))(z) < \chi_{\tilde{\tau}}(z)$ for $z \in [\sum_{j=1}^n q_j^l, \hat{\tau}_1)$ and $(\Omega(\sigma))(z) = \Omega(\sigma')$ for some $\sigma' \in \tilde{\Theta}_{\leq l} \cup \tilde{\Theta}_{> l}$ for $z \in [\hat{\tau}_1, \sum_{j=1}^n q_j^u]$. Similar result can be obtained for the second case from the same argument.

In this case, $q_k^u = \tau_k^1$ for all $k \in \{j : \sigma_j = l_j\}$ and $q_k^u \geq \tau_k^1$ for all $k \in \{j : \sigma_j \geq l_j + 1\}$. Then $\hat{\tau}_1 \geq \sum_{j=1}^n \tau_j^1 = \tilde{\tau}_1$. Remark 12 implies that for $z \in [\sum_{j=1}^n q_j^l, \hat{\tau}_1)$, $\Omega(\sigma)$ is a linear function with slope -1 over and hence $(\Omega(\sigma))(z) < \chi_{\tilde{\tau}}(z)$, and for $z \in [\hat{\tau}_1, \sum_{j=1}^n q_j^u]$, $x_k^* = \tau_k^1$ for all $k \in \{j : \sigma_j = l_j\}$. Let $\sigma' \in \tilde{\Theta}_{> l}$ be such that $\sigma'_k = l_j + 1$ for all $k \in \{j : \sigma_j = l_j\}$ and $\sigma'_k = \sigma_k$ for all $k \in \{j : \sigma_j \geq l_j + 1\}$. Since by definition $x_k^* = \tau_k^1 \in X_k^{l_k+1}$ for all $k \in \{j : \sigma_j = l_j\}$ and by construction $x_k^* \in X_k^{l_k+1}$ for all $k \in \{j : \sigma_j \geq l_j + 1\}$, we have $\Omega(\sigma) = \Omega(\sigma')$. ■

REFERENCES

- [1] R. Cohen, K. Erez, D. Ben-Avraham, and S. Havlin, "Resilience of the internet to random breakdowns," *Physical review letters*, vol. 85, no. 21, p. 4626, 2000.
- [2] D. J. Watts, "A simple model of global cascades on random networks," *PNAS*, vol. 99, no. 9, pp. 5766–5771, 2002.
- [3] A. Motter, "Cascade-based attacks on complex networks," *Phys. Rev. E; Physical Review E*, vol. 66, no. 6, 2002.
- [4] P. Crucitti, V. Latora, and M. Marchiori, "Model for cascading failures in complex networks," *Physical Review E*, vol. 69, no. 4, 2004.
- [5] A. Barrat, M. Barthelemy, and A. Vespignani, *Dynamical Processes on Complex Networks*. Cambridge University Press, 2008.
- [6] D. Bienstock, "Optimal control of cascading power grid failures," in *Decision and Control and European Control Conference (CDC-ECC), 2011 50th IEEE Conference on*, pp. 2166–2173, IEEE, 2011.
- [7] K. Savla, G. Como, and M. A. Dahleh, "Robust network routing under cascading failures," *IEEE Transactions on Network Science and Engineering*, vol. 1, no. 1, pp. 53–66, 2014.
- [8] D. Bienstock, *Electrical Transmission System Cascades and Vulnerability: An Operations Research Viewpoint*, vol. 22. SIAM, 2016.
- [9] H. Edelsbrunner, "Algorithms in combinatorial geometry, volume 10 of eacts monographs on theoretical computer science," 1987.
- [10] C. D. Toth, J. O'Rourke, and J. E. Goodman, *Handbook of discrete and computational geometry*. CRC press, 2004.
- [11] G. M. Ziegler, *Lectures on polytopes*, vol. 152. Springer Science & Business Media, 2012.
- [12] B. Grünbaum, V. Klee, M. A. Perles, and G. C. Shephard, *Convex polytopes*, vol. 16. Springer, 1967.
- [13] C. Lai and S. H. Low, "The redistribution of power flow in cascading failures," in *51st Annual Allerton Conference on Communication, Control, and Computing*, pp. 1037–1044, 2013.
- [14] S. Soltan, A. Loh, and G. Zussman, "Analyzing and quantifying the effect of k -line failures in power grids," *IEEE Transactions on Control of Network Systems*, 2017. In press.
- [15] D. Halperin and M. Sharir, "Arrangements and their applications in robotics: recent developments," in *Proceedings of the workshop on Algorithmic foundations of robotics*, pp. 495–511, AK Peters, Ltd., 1995.

- [16] Q. Ba and K. Savla, "Robustness of DC networks under controllable link weights," *IEEE Transactions on Control of Network Systems*, 2017. In Press. Available at <http://arxiv.org/abs/1609.02179>.
- [17] A. Bernstein, D. Bienstock, D. Hay, M. Uzunoglu, and G. Zussman, "Power grid vulnerability to geographically correlated failures-analysis and control implications," *arXiv preprint arXiv:1206.1099*, 2012.
- [18] S. J. Russell and P. Norvig, "Artificial intelligence: a modern approach (3rd edition)," 2009.
- [19] J. Chen, J. S. Thorp, and I. Dobson, "Cascading dynamics and mitigation assessment in power system disturbances via a hidden failure model," *International Journal of Electrical Power and Energy Systems*, vol. 27, no. 4, pp. 318–326, 2005.
- [20] Q. Ba and K. Savla, "A dynamic programming approach to optimal load shedding control of cascading failure in DC power networks," in *IEEE Conference on Decision and Control*, (Las Vegas, NV), 2016.
- [21] S. Boyd, N. Parikh, E. Chu, B. Peleato, and J. Eckstein, "Distributed optimization and statistical learning via the alternating direction method of multipliers," *Foundations and Trends in Machine Learning*, vol. 3, no. 1, pp. 1–122, 2011.
- [22] M. De Berg, O. Cheong, M. Van Kreveld, and M. Overmars, *Computational Geometry: Introduction*. Springer, 2008.
- [23] H. Edelsbrunner, J. ORourke, and R. Seidel, "Constructing arrangements of lines and hyperplanes with applications," *SIAM Journal on Computing*, vol. 15, no. 2, pp. 341–363, 1986.
- [24] T. Burger, P. Gritzmann, and V. Klee, "Polytope projection and projection polytopes," *The American mathematical monthly*, vol. 103, no. 9, pp. 742–755, 1996.
- [25] R. Sanyal and G. M. Ziegler, "Construction and analysis of projected deformed products," *Discrete & Computational Geometry*, vol. 43, no. 2, pp. 412–435, 2010.
- [26] S. Boyd and L. Vandenberghe, *Convex optimization*. Cambridge university press, 2004.
- [27] R. D. Zimmerman, C. E. Murillo-Sánchez, and R. J. Thomas, "Matpower: Steady-state operations, planning, and analysis tools for power systems research and education," *Power Systems, IEEE Transactions on*, vol. 26, no. 1, pp. 12–19, 2011.
- [28] M. Rungger and G. Reissig, "Arbitrarily precise abstractions for optimal controller synthesis," in *IEEE Conf. on Decision and Control*, (Melbourne, Australia), 2017. To appear.
- [29] G. Ranjan, Z.-L. Zhang, and D. Boley, "Incremental computation of pseudo-inverse of Laplacian," in *Combinatorial Optimization and Applications*, pp. 729–749, Springer, 2014.
- [30] C. D. Meyer, Jr, "Generalized inversion of modified matrices," *SIAM Journal on Applied Mathematics*, vol. 24, no. 3, pp. 315–323, 1973.